HEAT TRANSFER ENHANCEMENT IN CYLINDRICAL TUBES BY A TURBULATOR WITH SLITS GENERATING MULTI-LONGITUDINAL VORTICES

ERIC MUGAMBI KINYUA

DOCTOR OF PHILOSOPHY
(Applied Mathematics)

JOMO KENYATTA UNIVERSITY OF AGRICULTURE AND TECHNOLOGY

2018

Heat transfer enhancement in a cylindrical tube by a turbulator with slits generating multi-longitudinal vortices.

Eric Mugambi Kinyua

A thesis submitted in fulfillment for the degree of Doctor of philosophy in applied mathematics in the Jomo Kenyatta University of agriculture and technology.

2018

DECLARATION

This thesis is my original work and has not been presented for a degree in any other university.

Signature : ..... Date : .....

Eric Mugambi Kinyua

This thesis has been submitted for examination with our approval as the University supervisors.

Signature: ..... Date: .....

Prof. Mathew Kinyanjui, (PhD)

JKUAT, Kenya

Signature: ..... Date: .....

Prof. Surindar M. Uppal, (PhD)

JKUAT, Kenya

DEDICATION

I dedicate this thesis to my extended family, with special recognition to my dear wife Lucy together with my children Sharon and Ian for enduring moments during the period of this research. Let this work also be a motivation to all those who always strive to accomplish their aspirations.

ACKNOWLEDGEMENT

My sincere thanks to the almighty God for enabling me make it this far with good health and energy to complete this work. I take this humble opportunity to thank and appreciate my supervisors Prof. Mathew Kinyanjui and Prof. Surindar M. Uppal for their guidance and encouragement during the course of this research study. I also thank the Technical University of Mombasa for the financial support that has made this research work possible. Equally thankful to Mr. Henry Murray Humphreys who offered positive criticism by editing some of the documents I prepared in this research work. Am also grateful to Mr Charles Gathua who provided expertise on operations of a computational fluid dynamics simulation software Solid works and Mr Isaac Kemoi who assisted in developing Matlab algorithms. My deepest gratitude to all those who offered support in many other different ways including social and moral support that has enabled successful completion of this thesis.

TABLE OF CONTENT

LIST OF TABLES

LIST OF FIGURES

LIST OF APPENDICES

NOMECLATURE

ROMAN SYMBOL	QUANTITY
A	Tube inner cross sectional area, m^2
a	Acceleration, m/s^2
C_P	Specific heat capacity at constant pressure, J/KgK
C_f	Coefficient of skin friction
D	Inner diameter of tube, m
d	Inlet diameter of the diverging conical insert, m
f	Friction factor
F	Force, $kgms^{-2}$
Fc	Field synergy number
g	Gravitational force, ms^{-2}
H	Head loss
h	Heat transfer coefficient, W/m^2k
$\hat{i}, \hat{j}, \hat{k}$	Directional vectors along x, y, z axis respectively
$..i-1, i, i+1...$	Counters of discrete points
K	Diffuser loss coefficient
k	Thermal conductivity, W/mk
L	Axial pitch length, m
m	Mass, kg
$\overset{\circ}{m}$	Mass flow rate, Kg/s
Nu	Nusselt number
P	Pressure, Pa (Nm^{-2})
Pc	Pressure coefficient
P_o	Pressure at the inlet, Pa (Nm^{-2})
Pr	Prandtl number
Q	Rate of heat transfer, J/s
Re	Reynolds number

r	Radial distance in the tube , m.
r, θ, z	Cylindrical coordinates
S	Slit
T	Temperature, K
t	Time, s
U	Mean velocity of flow, ms^{-1}
u, v, w	Dimensionless velocities along x,y,z axis respectively
u_r	Radial fluid velocity, m/s
u_z	Axial fluid velocity, m/s
u_θ	Angular fluid velocity, m/s
v	Fluid velocity, m/s
x, y, z	Cartesian coordinates
u^*, p^*, v^*, r^*, z^*	Non dimensional variables

GREEK SYMBOLS	QUANTITY
∇	Gradient operator
Δ	Small change
α	Angle between two planes, radians
β	Angle of rotation
ε	Rate of dissipation of kinetic energy, J
η	Thermal performance factor
Θ	Dimensional temperature, K
θ	Angular coordinate
κ	Kinetic energy
μ	Coefficient of dynamic fluid viscosity kg/ms
μ_t	Eddy viscosity
ν	Thermal diffusivity
ξ	Diffuser efficiency
π	Pi $\cong$ 3.1415926
ρ	Fluid density, kg/m^3
τ	Shear stress N/m^2
υ_t	Effective thermal conductivity
ϕ	Viscous dissipation function, W/m^3
ψ	Stream function, m^3/s
ω	Vorticity vector
ϑ	Coefficient of kinetic viscosity $m^2 s^{-1}$
∞	Infinity

LIST OF ABBREVIATIONS

DCR Diverging conical ring

HTE Heat transfer enhancement

JH Jeffery Hamel

PT Plane tube

RNG Re -normalization Group

RSM Reynolds stress model

ABSTRACT

This study analyses the effect of number of slits on a diverging conical ring insert when symmetrically cut out on the curved surface to generate multi longitudinal vortices in an incompressible fluid flow on a cylindrical tube. This is a passive augmentation technique aimed at achieving heat transfer enhancement. The insert disrupts flow creating a mixture between core and near wall fluid into a swirl flow with a pressure drop and friction characteristic generating higher heat transfer enhancement than that attained by either laminar or turbulent fluid flows achieved in a tube of equal diameter using other augmentation techniques. In this research work hot water is used as the test fluid in a simulation to establish the pressure drop and temperature variation along a tube of inner diameter 0.05 m and 8 m long with a diverging conical ring insert placed at a fixed distance from the entrance where uniform fluid velocity is attained to avoid the pipe entrance effect. Using a conical ring insert with inlet diameter of 0.036 m and an outlet diameter of 0.05 m giving a pitch ratio of 0.72, when the fluid flows into the pipe inlet region at a pressure P_0=110,000 Pa and temperature T_0 = 370 K. Analysis of the results shows a positive coefficient of heat transfer and thermal performance factor when comparing an insert with no slit and those with one, two and three slits. The highest rate of heat transfer enhancement is 423.38 attained when two multi – longitudinal vortex pairs are formed by a diverging conical ring insert with two slits on opposite sides of the curved surface. Comparison is done of simulated multi longitudinal vortices generated and analytical vortices that can provide perfect synergy of temperature field and the fluid velocity vector to provide maximum heat transfer enhancement. Also governing equations of the fluid flow are non- dimensionalized then discretized to determine pressure and temperature profiles at various Reynolds number with the fluid considered to be a laminar flows.

CHAPTER ONE

INTRODUCTION TO THE STUDY

1.1 Introduction

In this chapter the main terms in the research work are defined. An introduction to heat transfer enhancement techniques is provided. A background of the research study is described to relate it with scientific knowledge necessary to understand the research. There after a statement indicating the research problem, the objectives and justification of the research work.

1.2 Fluid

A fluid is a substance that continuously deforms under a shear force. Fluid mechanics is therefore the study of fluid motion and the forces that cause this motion. Fluids can be classified into compressible or incompressible fluids. A fluid is said to be compressible if its volume changes significantly when subjected to change in pressure. While density of compressible fluids varies with temperature and pressure. If there are no significant changes in the density of a fluid then the fluid is assumed to be incompressible.

1.3 Vortex

A vortex is a spinning flow or any spiral motion with closed streamlines, where the fluid rotates rapidly around a central axis. It is a flow involving rotation about an axis vertical or horizontal with a circular flow that possesses vorticity which is the circulation per unit area at a point in the flow field and is a vector quantity whose direction is along the axis of the flow.

In fluid mechanics a distinction is often made between two limiting vortex cases, the free (irrotational) vortex and the forced (rotational) vortex. A free (irrotational) vortex has a tangential velocity that varies inversely as distance from the centre of

rotation and angular momentum is a constant. A forced (rotational) vortex has the fluid essentially rotating as a body with no shear force.

1.4 Multi- longitudinal vortex

They are multiple vortices with a swirling axis parallel to the main flow direction and move downstream swirling around an axis with a velocity component referred to as azimuthal, transverse or tangential which results in helical winding of the streamlines.

1.5 Heat transfer enhancement

Is an improvement in performance of a thermal system by change of surface geometry to obtain higher energy efficiency, also referred to as heat transfer augmentation or intensification. The conventional heat exchangers are improved by means of various enhancement techniques with emphasis on augmented surfaces that create one or more combinations. The following conditions are favourable for an increase in heat transfer rate with an undesirable rise of friction by either disruption in the development of boundary layer. Increase in contact surface area between fluid and the tube wall provides heat transfer area and generation of swirling or secondary flow. The main aim of researchers in this field is to study of heat transfer enhancement aiming at reducing the size and cost of heat exchangers.

1.6 Convection heat transfer

Convection is the mechanism of heat transfer by a fluid in the presence of bulk fluid motion. Convection is classified as natural or forced depending on how the fluid motion is initiated. In natural convection it occurs by natural process such as buoyancy effect, i.e. rise of warmer fluid or fall to lower altitude of cooler fluid. In forced convection the fluid is forced to flow by external means such as a pump.

1.7 Boundary layer

A boundary layer is a thin fluid region adjacent to the surface of a body or solid wall in which viscous forces exist. The fluid particles in contact with the solid body surface attain the velocity of the body. The region outside this layer is called free stream region where the flow is unaffected by viscous forces. Boundary layer thickness theory is important in analyzing fluid flow problems involving convective transport. When particles of a real fluid are in contact with a surface their velocities are retarded gradually, which in turn acts to retard the motion of particles in the next layer. This process continues until the effect becomes negligible, in cases of a pipe's internal flow. A velocity boundary layer thickness is defined as the distance away from a surface where the velocity reaches 0.99 that of the free-stream velocity.

1.8 Background of the study

Conventional sources of energy are being depleted at an alarming rate, which makes future sustainable development of energy use very difficult. Heat transfer enhancement technology has been developed and widely applied to heat exchanger applications over the past decades; for example in refrigeration, automotives, process industry and solar water heater technology, because the reduction in overall thermal resistance can lead to a smaller heat exchanger. To date there have been a large number of attempts to reduce the size and costs of heat exchangers. The development of high performance thermal systems has stimulated interest in methods to improve heat transfer. The performance of a conventional heat exchanger can be substantially improved by a number of enhancement techniques. A great deal of research effort has been devoted to developing apparatus and performing experiments to define the conditions under which an enhancement technique will improve heat transfer. The goal of enhanced heat transfer is to encourage or accommodate high heat fluxes. This results in reduction of the size of

heat exchanger, which leads to lower capital cost. Another advantage is the reduction of temperature driving force, which reduces the entropy generation and increases efficiency. In addition, the heat transfer enhancement enables heat exchangers to operate at a lower velocity, so as to achieve the same or even higher heat transfer coefficient. Therefore a reduction of pressure drop corresponds to less operating cost, achieved in reduction of pumping energy and strength of pipes used. All these advantages have made heat transfer enhancement technology attractive in heat exchanger applications with the tube insert technology being one of the most effective heat transfer enhancement technologies, particularly for the retrofit situation. With tube insert technology additional exchangers can often be avoided and thus significant cost saving becomes possible. Furthermore as a heat exchanger becomes older the resistance to heat transfer increases owing to fouling or scaling. In this case the heat transfer rate can be improved by introducing a disturbance in the fluid flow by different enhancement technologies, breaking the viscous and thermal boundary layer. Augmentation techniques are broadly classified into three different categories: passive, active and compound techniques. Passive techniques are those that do not require any direct input of external power, rather they use it from the system itself which ultimately leads to an increase in fluid pressure drop. They generally use surface or geometrical modifications to the flow channel by incorporating inserts or additional devices. They promote higher heat transfer coefficients by disturbing or altering the existing flow behaviour except for extended surfaces. Heat transfer augmentation by these techniques can be achieved by using different techniques some of which include displacement enhancement devices. These include inserts that are used primarily in confined forced convection and to improve energy transport indirectly at the heat exchange surface by displacing the fluid from the heated or cooled surface of the duct with bulk fluid from the core flow.

Swirl flow devices produce superimposed swirl flow or secondary recirculation on the axial flow in a channel. These include helical strip or coiled screw type tube

inserts. Twisted tapes in Figure 1.1 show an isometric view which illustrates swirl flow along the tube which is used for single phase and two-phase flows, to provide heat transfer enhancement in a cylindrical pipe.

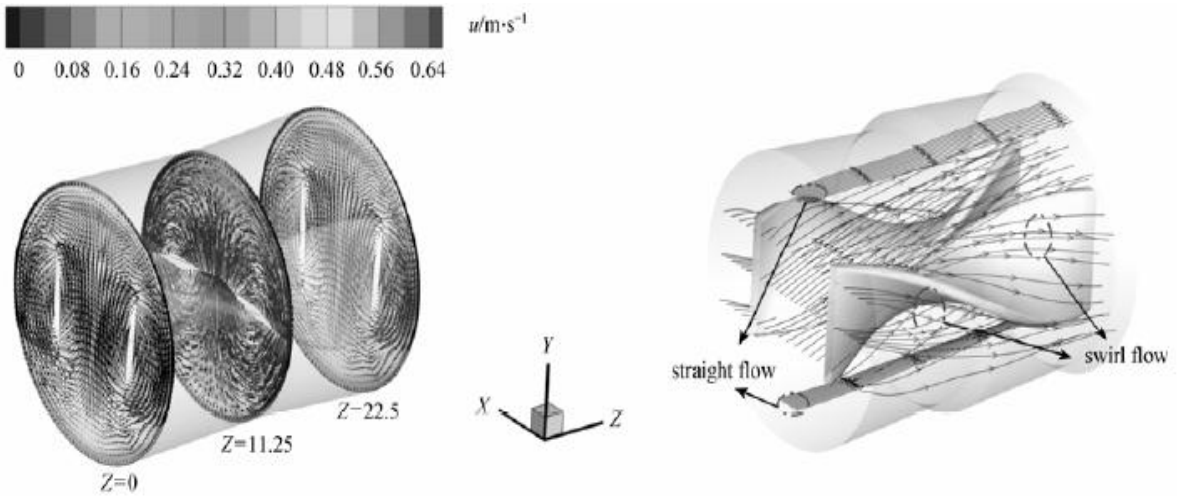

Figure 1.1: Double twisted tape inserts generating multi longitudinal vortices,

Source: **Hong *et al*,. (2012).**

Active techniques are those that have external power used to facilitate the desired flow modification and improvement in the rate of heat transfer. Augmentation of heat transfer by this method can be achieved in different ways such as; Mechanical aids: instruments stir the fluid by mechanical means or by rotating the surface. These include rotating tube heat exchangers, scrapped surface heat and mass exchangers. Other ways include surface vibration, injection and suction. Compound techniques occur when any two or more of these techniques are employed simultaneously to obtain enhancement in heat transfer that is greater than when produced by either of them if used individually. This technique involves complex design and hence has limited applications.

The swirl flow devices can be classified into two, continuous and decaying swirl flow. In continuous swirl flow the swirling motion persists over the whole length of the tube for example twisted-tape inserts, coiled wires and helical grooves. In decaying swirl flow it is generated at the entrance of the tube and decays along the

flow path for example the radial guide vane swirl generator and the tangential flow injection device.

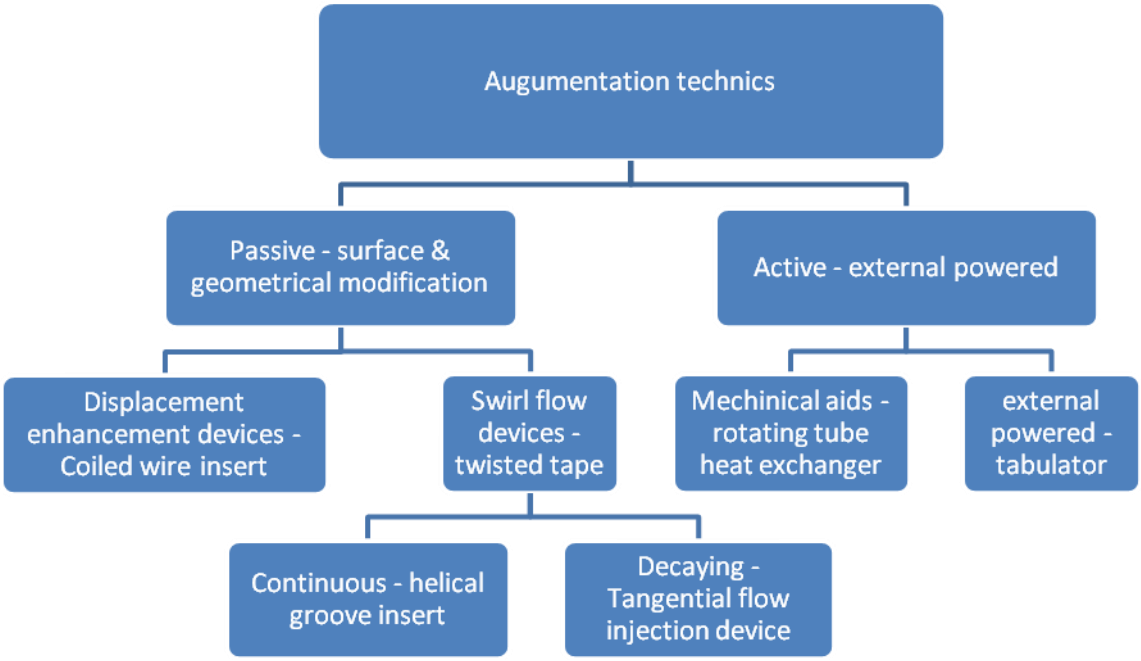

Figure 1.2**: Relationship of various heat transfer techniques used in cylindrical tubes.**

In decaying swirl flow the heat transfer coefficient and the pressure drop in the pipe decreases with axial distance while for continuous swirl flow the heat transfer coefficient and the pressure drop are kept constant. The distinction between different heat transfer augumentation techniques is illustrated in Figure 1.2 below indicating the nature of a decay swirl flows, which in this study is achived by presence of a diverging conical ring (DCR) insert with slits in symmetrical positions to generate multi longitudinal vortices in a cylindrical pipe.

It is necessary to understand heat transfer potential capacity and dissipation function as well as their physical meaning in the overall heat transfer capability and

dissipation rate of the heat transfer capacity respectively in a give set up. Dissipation function for the heat transfer potential capacity is a payout on heat transport, the laminar convection in a tube with constant thermo physical properties and without internal heat source. The dissipation of heat transfer potential capacity corresponds to the heat transfer performances. Unlike the steady heat conduction, convection heat transfer cannot be optimized only by the minimal dissipation of heat transfer potential capacity because the velocity field influences the heat transfer enormously. The field synergy equation for convective heat transfer is similar to but not the usual momentum conservation equation in the Navier–Stokes equation because it contains a virtual additional force. Synergy force on the field synergy equation is derived by conditional variation calculus based on the least flow dissipation of heat transport potential capacity. The numerical simulation of laminar convection heat transfer in a straight circular tube shows that multi-longitudinal vortex flow in a tube is the flow pattern that enhances heat transfer enormously. Therefore optimum velocity field indicates basic characteristics of a flow pattern that benefit heat transfer most for laminar flow in a tube as between 2 to 4 multi-longitudinal vortex pairs. The most direct application of the synergy equation is to offer guidance when selecting and designing an appropriate enhancement technique. The optimum velocity field for laminar convection heat transfer in a tube can be obtained through solving the field synergy equation under a specific flow and its thermal boundary conditions.

1.9 Statement of the problem

Vortex flows have higher heat transfer enhancement associated with a pressure drop and lower friction characteristic compared with both laminar and turbulent fluid flow. The interest to study effects caused by number of slits on a diverging conical ring insert when cut out in symmetrical positions on the curved surface to generate multi- longitudinal vortices in fluid flow was inspired by a need to attain field synergy. To enhance heat transfer on an incompressible fluid flow in a

cylindrical tube by designing an enhancement element that can achieve an optimum performance on both heat transfer enhancement and flow resistance.

1.10 Justification of the study

The convection heat transfer enhancement in cylindrical tubes is an essential problem with wide engineering applications as they are commonly used for fluid transmission. In addition the swirl flow generator is also used in augmenting heat transfer. Swirl flow is extensively used in several industries to enhance the rate of heat transfer in equipment such as heat exchangers, fuel combustion and fluid mixing tabulators where specific temperature is necessary for optimum results yet heat is lost during transportation in pipes and can be regained without using any other external energy.

Conical ring inserts are cheaper than twisted tapes, fins or ribs to manufacture and have a lower maintenance cost. When replacing inserts in case of fouling, scaling or wearing out you only need to detach the pipes then fix a new conical ring insert without replacing the whole piping system.

1.11 Objectives

1.11.1 General objective:

To determine the rate of heat transfer enhancement on fluid flowing in a cylindrical tube when inserted in a diverging conical ring with symmetrically cut out slits to generate multi- longitudinal vortices in the flow which disrupts thermal boundary layer.

1.11.2 Specific objectives:

i. To generate multi- longitudinal vortex pairs using diverging conical ring insert with slit cut out at symmetrical positions on the slant edges.

ii. To determine characteristic pressure variations along the flow tube in presence of a diverging conical ring insert.

iii. To investigate the rate of heat transfer in relation to the number of slits on a diverging conical ring insert.

iv. To evaluate the coefficient of skin friction in a tube with a diverging conical ring insert.

CHAPTER TWO

LITERATURE REVIEW

2.1 Introduction

A review of related literature with emphasis on recent works in the area of heat transfer enhancement and other research studies in areas of heat transfer enhancement using other different types of inserts to compare the efficiency of different passive augmentation techniques.

2.2 Literature relevant to the study

Passive and active methods of heat transfer augmentation techniques have been discussed in detail by Webb *et al.* (2005) and Dewan *et al.* (2004) who expressed that passive techniques, particularly twisted tape and wire coil insert are economical heat transfer augmentation tools. Most of the early work concerned with the effect of a conical turbulator on turbulent flow conditions was done by Yakut and Sahin (2004) who studied the effect of conical-ring turbulators on the turbulent heat transfer, pressure drop and flow-induced vibrations. Durmus (2004) investigated the effect of cutting out conical turbulators on heat transfer with different types of turbulators and different conical-angles of 5^0, 10^0, 15^0 and 20^0 establishing that heat transfer rate as well as friction coefficients increased with the angles. Chokphoemphun *et al.* (2015) found that Nusselt number values for all cases of using augmentations are higher than that of plain tube case with 115.9% for a spacing ratio of 4.2 and 97% for 6.4 this behavior is attributed to the fact that using turbulators increase turbulence intensity and reduce thickness of thermal boundary layer leading to raise convection heat transfer. Hossain *et al.* (2015) analyzed heat transfer enhancement in circular tube with and without inserts for laminar flow in the range of Re 1600 to 2400 by using COMSOL Multi physics to perform CFD simulation. A non-isothermal flow model was considered in which water was taken in the model and copper was considered as material of circular

pipe under constant heat flux of 32.087 KW/h. using governing equation of non-isothermal flow together with continuity equation the dynamic behavior of the flow was described which transport heat. In the simulation four, six and eight inserts were used on a pipe of length 800 mm and they got highest output temperature 319.28 K for four inserts while the output temperature was 307.85 K when there was no insert in the tube also noting that not just increasing the number of inserts will increase the heat transfer but determining specific distance between the inserts need to be considered. These kinds of flow have been studied by many other authors; Sadri (1997) studied asymptotic boundary conditions to examine the steady two dimensional flow of a viscous fluid in a channel and solved the nonlinear equations using numerical techniques. The instability and bifurcation of Jeffery- Hamel (JH) flow is studied as flux driven steadily along the channel is increased. This stability of flow through a diverging pipe was examined by Sahu *et al.* (2005) and the velocity profiles at threshold instability were obtained using non parallel analysis for very small angles less than four degrees. Putkaradze *et al.* (2006) studied experimentally the velocity profile and related instabilities of the flow through diverging channels and concluded in a heuristic manner that the solution revealed absolute instability. Pradip and Dinesh (2013) described heat transfer intensifiers and reviewed surface roughness, perforated baffle and twisted tape inserts applications in tubes and established that if area changes the rate of heat transfer also changes. Swaminathan *et al.* (2011) studied the spatially developing global linear stability analysis problem to reveal that disturbance modes are not the wave like perturbations assumed by local parallel or weakly non parallel analyses and question the relation between critical Reynolds number and angle at the vertex. The reverse flow with high turbulent flow can improve convection of the tube wall by increasing effective axial Reynolds number decreasing the cross-section flow area and increasing the mean velocity as well as temperature gradient. Ayhan *et al.* (1999) studied the effect of truncated hollow cone inserts on heat transfer and friction in a tube. Eiamsa-ard and Promvonge (2006) reported the effect of V-

nozzle turbulators on heat transfer and flow friction in a tube. They also studied the effect of combined conical-nozzle and snail entrance on heat transfer and friction characteristics in a uniform heat flux tube and reported a substantial increase in heat transfer obtained from the use of both enhancement devices. Curnia *et al.* (2012) carried out a parametric study of laminar flow and heat transfer characteristics of coils made of tubes of different cross- section area with an aim to determine geometrical effect on heat transfer performance. Nagarajan *et al.* (2015) found in double pipe heat exchanger of diameter 0.015 m and length of 2.5 m with variable twisted type insert in ANSYS fluent that a trend of increase in heat transfer with the provision of insert on the heat exchanger. The heat transfer was found to increase as the Reynolds number was varied over the range. The result shows that effect of insert on the enhancement of heat transfer depends on both the pattern of insert and Re of the flow. Promvonge (2007) conducted experiments by inserting several conical rings as turbulators over a test tube as shown in Figure 1.3. Conical rings with three different diameter ratios of the ring to diameter (d/D = 0.5, 0.6, 0.7) were introduced in the tests and for each ratio the rings were placed with three different arrangements: converging conical ring, diverging conical ring, diverging converging conical ring in which cold air at ambient temperature was passed through the tube.

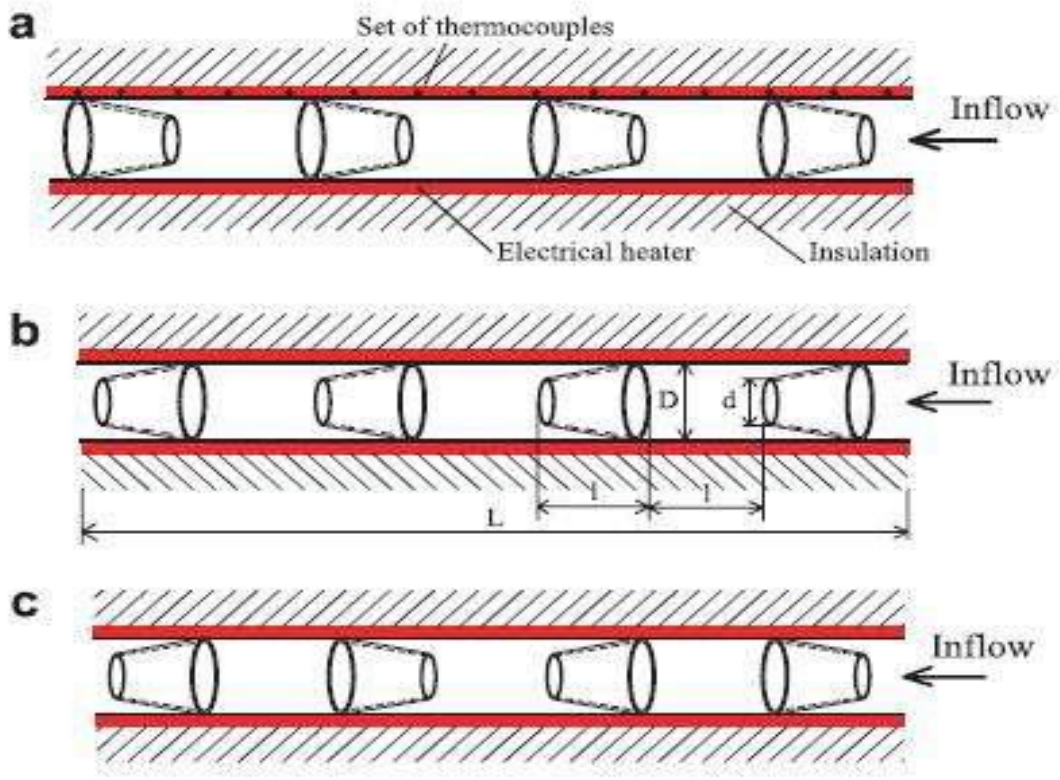

Figure 2.1: Conical ring inserts (a) diverging, (b) converging, (c) diverging-converging. **Source: Promvonge (2007)**

Yakut and Sahin (2004) used conical-ring turbulators placed inside a tube to produce reverse flow or turbulent flow for each module of the conical rings in which heat transfer was improved along the tube wall. In their experimental study the level of reverse flow (re-circulation flow) was generated from separation and reattachment of a boundary layer from different pitch lengths between the modules. Fan *et al.* (2011) numerically investigated turbulent flow and heat transfer in a circular tube fitted with conical strip inserts using k-ε turbulence model. The role of conical rings in heat transfer enhancement (HTE) and pressure drop change on a pipe with constant heat flux boundary condition was investigated by Anvari *et al.* (2011) using water as a working fluid and they found that insertion of turbulators has significant effect on the enhancement of heat especially for diverging ring

arrangement. These turbulators can be used in pipes where the compact size is more significant than pumping power. Shivalingaswamy and Narahari (2014) studied HTE in a tube fitted with circular ring turbulator as passive heat transfer augmentation techniques for different diameter ratios d/D at 0.5, 0.6 and 0.7 with Reynolds number ranging from 4,000 to 20,000. They found HTE of 57% up to 195% compared with a plain tube.

Muhammad *et al.* (2015) investigated the effects of porous twisted plate as insert to enhance heat transfer rate and flow characteristic for a single fitted tube. The porous twisted plate was designed with 3 different numbers of holes; 1, 2 and 3 with 4mm diameter on each segment. The tube was used with plain and porous twisted plates inserted. These results compared with the plain tube which showed that creation of holes changed the flow profile by generating secondary flow and caused turbulence flow. With velocity of the flow was increased and allowing more fluid mixing inside the tube it provide more heat transfer across the tube. Therefore porous twisted plate with larger numbers of holes enhance better heat transfer rate compared to plain tube and plain twisted plate. Eiasma-ard *et al.* (2008) experimentally investigated the heat transfer and friction factor characteristics in a double pipe heat exchanger fitted with full length tape and spaced twisted tape in forward and backward arrangement of louvered strips, helical screw tape with and without core rod to develop the correlations for practical applications. Mohammed *et al.* (2014) conducted experiments in enhancement of forced convection heat transfer by means of passive techniques for turbulent air flow through an aluminum tube with Reynolds number ranging from 6000 to 13500 on boundary conditions of constant heat flux. This showed that divergent nozzle turbulators without perforation provide a heat transfer rate of 317% and a friction factor 17 times over a plain tube. Kongkaitpaiboon *et al.* (2010) studied perforated conical–rings with different pitch ratios and different numbers of perforated holes, found that it leads to a heat transfer rate up to 137% over that of a plain tube. The perforated conical-rings enhanced heat transfer more than typical conical-rings on the basis of thermal

performance factor of around 0.92 at the same pumping power which was found at the smallest pitch ratio and maximum number of holes.

Bankar and Pathare (2010) examined V-nozzle inserts with pitch ratio 5.0 in a circular tube with length to diameter ratio $\frac{L}{D} = 28$ and Reynolds number ranged from 21500 to 48500 and found that heat transfer rate increased by 140% over the plain tube with a maximum gain of enhancement efficiency of 1.19. Karakaya and Durmus (2013) devised the conical spring turbulators for three different cone angles 30^o, 45^o and 60^o with Reynolds number ranging from 10000 to 34000 and they found that the best results in terms of direction of flow are diverging, converging – diverging and converging respectively while the turbulator as best results when cone angle is 30^o, 45^o and 60^o respectively. Heat transfer characteristics studies by Naphon (2006) for a twisted tape insert by varying the mass flow rate and inlet temperature of hot water. Wang and Sunden (2002) found that twisted tape is more efficient than wire coil insert if no pressure drop penalty is considered. Chang *et al*. (2007) experimentally compared the heat transfer and friction factor characteristics of smooth twisted tape with broken and separated twisted tape inserts. Promvonge and Eiamsa-ard (2007) reported the effect of combined conical-ring and twisted tape insert fitted in a tube on heat transfer enhancement and flow friction. Bilen *et al*. (2009) studied the effect of heat transfer and friction characteristics of a fully developed turbulent air flow in different grooved tubes compared with plain tube. Sivashanmugam and Suresh (2006) also studied the laminar heat transfer and friction factor characteristics in a circular tube fitted with full-length helical screw tapes with different twist ratios. Hasim *et al.* (2003) used compound enhancement i.e. twisted tape with helically ribbed tube for heat transfer enhancement based on non-dimensional clearance. Al-Fahed *et al.* (1999) experimentally compared the heat transfer and pressure drop characteristics for plain tube, micro fin and twisted tape insert tubes. Chou *et al.* (2012) worked with square cut circular ring insert in tube to promote turbulence which enhances convective heat transfer. Abdullah (2012) studied the heat transfer and pressure

drop characteristics in an eccentric converging – diverging tube with twisted tape inserts, the Nusselt number for eccentric converging diverging conical ring was found to range from 15% to 45% higher than that of the plain tube and when combined with a twisted tape insert it was found to range from 52% to 280% higher and a pressure drop 6.8 times that of the plain tube. Yongsiri *et al.* (2006) studied augmentation of heat transfer using nozzle turbulators and swirl generator in uniform heat flux tube as the conventional passive enhancement method with a pitch ratio of 2, 4 and 7, the Nusselt number being 374%, 342% and 309% respectively in comparison with the plain tube. Rashid *et al.* (2014) focused on experimental as well as numerical investigation in a horizontal circular tube by the effect of conical ring wire insert on turbulent flow heat transfer.

The swirl flow devices have been investigated by many researchers and methods of generating swirl have been classified into three main categories as done by Gupta *et al.* (1984). The first is tangential flow injection in which the idea is to introduce a tangential flow and then induce a swirling fluid motion down the tube. The second is guide vanes swirl generators which Yilmaz *et al.* (2002) grouped in two types: radial guide vanes and axial guide vanes. Another swirl generator type is direct rotation of the tube. Swirling flow in burners are common because of the stabilization of lean flames with minimum head losses, ultra low emissions and fuel saving as indicated by Parra *et al.* (2013). This issue has important environment implications since the fuel slip due to incomplete combustion is a harmful greenhouse gas. Guo *et al.* (2015) carried out a theoretical study about the effect of a secondary flow on the laminar convection heat transfer, while Saqr and Wahid (2014) proposed an empirical correlation for predicting the entropy augmentation as a function of the swirl number. Nuntadusit *et al.* (2012) studied the effect on Nusselt number for different set ups of multiple swirling jets. As for the design of swirl generators Zohir *et al.* (2013) evaluated the increase of heat transfer rate when modifying the location and pitch angle of the swirl generator upwind the test chamber. A heat transfer enhancement concept in which swirl was introduced in the

flow was proposed by Kreith and Margolis (1959) while Gambill and Bundy (1963) claimed that twisted-tapes are also effective in high Prandtl number fluids because such fluids provide high heat transfer rate with less pressure drop compared with other inserts. Zozulya and Shkuratov (1974) reported that a smooth decrease in pitch of a twisted-tape results in an improved heat transfer rate. Van Rooyen and Kroeger (1978) found that for laminar swirl flow heat transfer in a smooth tube subjected to axially constant tube wall temperature, the heat transfer rate increases considerably for a moderate increase in pressure drop. Bergles *et al.* (1985) considered all these effects and developed laminar flow correlations for the friction factor and Nusselt number including the swirl parameter which defines the interaction between viscous, convective inertia and centrifugal forces. Dewan *et al.* (2015) showed that heat transfer enhancement can be enhanced by use of passive techniques by modifying a pipe's geometrical shape or insertion of twisted tapes, inclined or porous baffle, corrugated duct, discontinuous crossed ribs and grooves but at a cost of increase in pressure drop. Saha and Dutta (2001) observed that on the basis of constant pumping power and constant heat flux boundary condition short length twisted-tapes are found to perform better than full-length twisted tapes for tighter twists. Al-Fahed and Chakroun (1996) found that there is an optimum tape width depending on the twist ratio and Reynolds number for the best thermo-hydraulic characteristics and the tight-fit tape yields a better performance over the loose-fit one. Suresh *et al.* (2004) presented the thermo-hydraulic performance of twisted-tape inserts in a large hydraulic diameter annulus. Manglik and Bergles (1994) investigated numerically the laminar convection heat transfer in circular-segment, uniform wall temperature ducts with a straight tape insert. Holit and Ozceyhan (2012) studied flow friction and heat transfer behavior of a twisted tape swirl generator inserted in a tube considered in the range of Reynolds number 5,132 to 24,989 noting that HTE tends to decrease with an increase of Reynolds number to be nearly constant at Re greater than 15,000 for twist ratios lower than three. Wisam (2012) conducted an experimental study on the effect of vortex

generators in circular and square tubes on the flow and heat transfer at variable locations ahead of a heat exchanger with Reynolds number ranging from 62000 < Re < 125000 and heat flux from 3000 to 8000W/m^2. The results showed that there is an effect when using vortex generators on heat transfer and the circular tube was found to be best shape for enhancing heat transfer. Mirzaei *et al.* (2013) numerically studied the augmentation of heat transfer by using vortex generators on flat and round tube heat exchangers, simulations performed with the steady three dimensional incompressible conditions and a renormalization group (RNG) k-ε turbulence model used. The Reynolds number based on bulk velocity and height of the channel, comparing the effectiveness of vortex generator on a round and flat tube for tube fin heat exchanger investigating the average Nusselt number, friction factor and performance factor found that the flat tube has a better thermal performance than a round tube at lower Reynolds number. Vijay *et al.* (2014) found in an experiment carried out for three heater input and different flow rates of air, the effect on heat flow rate and outlet temperature observed respectively in a threaded pipe and compared to a plain pipe. The threads increased swirl flow formation which improves the contact surface of air with the heated pipe resulting in heat transfer enhancement. Nakate *et al* (2015) performed experiments for heat exchanger by inserting twisted tape turbulators with baffle for same twist ratio comparing with baffled reduced width twisted tape with holes. Baffled reduced width twisted tape shows higher heat transfer coefficient and friction factor increase because of higher degree of turbulence created it also gives higher heat transfer coefficient than the reduced width twisted tapes. Experimental examinations were expressed by Changzhong (2016) to display the influences of a rotation of counter-clock wise and clockwise twisted tape compared to normal twisted tape inserted in the internal tube, where the maximum value of performance valuation criteria of 1.42 was found with the utilization of full length and counter-clockwise twisted tape embed at Reynolds number of 3800 while the Nusselt number intensification was 2.42 times of that of the heated tube. Avinash (2015)

studied numerically the effect of twisted tape inserts in a heated tube on heat transfer mixing and found that in the case of a tube embedded with twisted tape alongside longitudinal movement there was movement of fluid particles in transversal direction because of the helical rotational fluid flow. Liu *et al.* (2012) explained physical quantity synergy principle from field synergy by reflecting the physical mechanism of convective heat transfer in the laminar and turbulence flows and explained physical essentials on reducing flow resistance by revealing how heat transfer performance is influenced by physical quantity synergy relation on temperature, velocity and pressure. Chen *et al.* (2013) proposed the entransy dissipation based thermal resistance method for heat exchanger performance design and optimization. Jia *et al.* (2014) used computational fluid dynamics software ANSYS Fluent 6.3 to solve coupled governing equations and the SIMPLEC algorithm used for coupling pressure and velocity fields. The QUICK discrete scheme is applied in the momentum and energy equations to solve the constraint scalars and a user defined function in the ANSYS Fluent software was used. Different values of Reynolds number and power consumption on a straight circular tube 1.7 m long and a diameter 0.02 m model with an inlet temperature of 300 K and tube wall temperature 310 K in an optimization section at 1.35m were analyzed to determine the temperature and flow field in the cross section as indicated in figures 2.2: a and b to show a relation between the temperature and velocity vectors.

By setting entransy dissipation as an optimization objective and viscous dissipation as a constraint condition, the optimization flow field equation for convective heat transfer is expressed by Meng *et al.* (2005). The entransy dissipation can be regarded as an expression of the irreversibility of heat transfer process, which is similar to the entropy generation like that of a thermodynamic process. Entransy always decreases in heat transfer process, while entropy always increases. The smaller the entransy dissipation the smaller the temperature difference in the fluid is and thereby the smaller the irreversibility of heat transfer process.

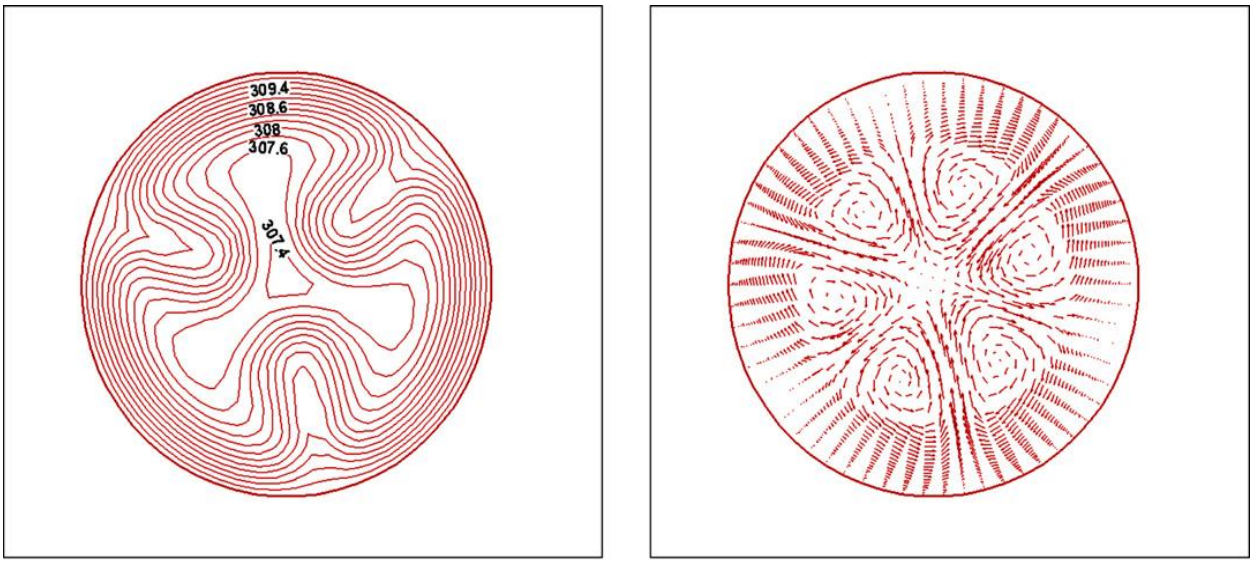

Figure 2.2: a and b, Temperature field and flow velocity vector with three multi- longitudinal vortex pairs. **Source; Liu et al (2012).**

The field synergy principle of boundary layer flow has been systematically expounded to show that convective heat transfer not only depends on thermal physics properties like temperature difference and fluid flow velocity but also depends on the angle between velocity vector and temperature gradient. Li *et al.* (2014) studied the flow and heat transfer characteristics of spiral corrugated tube by numerical simulation. Sivakumar *et al*. (2015) an experimental investigation was carried out to measure heat transfer, Reynolds number and friction factor fitted in concentric tube with twisted tape inserts. The different twist ratios are 2.52, 3.00 and 3.20 were studied for the laminar flow using computational fluid dynamics software. A copper twisted tape of different twist ratio was inserted and the plain tube data were compared with twisted tape inserts. The result shows that twisted tape access high heat transfer with increase in friction factor. The exit temperature of hot fluid decreases with increase of mass flow rate and high temperatures were

obtained in the twisted tape insert. The mean temperature of twisted tube increased from 2% to 4% compared to plain tube. It was observed that increase in heat transfer rate by 7% to 10% with twisted inserts fitted in the concentric circular tube. Aghayari *et al.* (2016) studied the performance of water - iron oxide nano fluid in a double pipe heat exchanger with perforated twisted tapes was investigated under turbulent flow regime. Iron oxide nano particles with diameter of 15 nm are used as nano fluid with concentration range from 0.12% to 0.2% by volume. The result shows that addition of nano particles increases the heat transfer and Nusselt number. Also reducing the twist ratio of perforated twisted tape and using the nano fluid with concentration of 0.2% v/v increase this value by 130%. Maximum increase in Nusselt number is achieved for the 0.2% v/v Iron oxide nanofluid and twist ratio of 2.5. This increase occurs in Reynolds number of 2500 which is 132.2% compared to the experiment performed with water and without the twisted tape inserts. Bhuiya *et al*. (2016) determined that inserting turbulators with different spacing ratio of 11, 6.4 and 4.2 gives enhancement efficiency with rate more than unity. This indicates that enhancing heat transfer is more than the effect of increasing friction loss with the maximum heat transfer enhancement achieved at 4.2 with a rate of 9.8 %.

CHAPTER THREE

EQUATIONS GOVERNING THE FLUID FLOW

3.1 Introduction

This chapter discusses how to generate multi- longitudinal vortices and state assumptions made in the flow problem to obtain governing equations of the fluid flow in cylindrical coordinates. Governing equations of the flow past a diverging conical ring insert are expressed using the renormalized group κ-ε turbulence model but flow in the inner core is best estimated by the Navier -Stokes equations for an incompressible flow in a cylindrical pipe. The governing equations are then non dimensionalised and physical interpretation of non dimensional numbers is described. Describing the relation between continuity equation and vorticity which is defined as an axial component for the curl of velocity vector.

3.2 Designing a diverging conical ring insert with slits

To obtain conical ring insert a circular is cut out of a circle designed as shown in Figure 3.1 below.

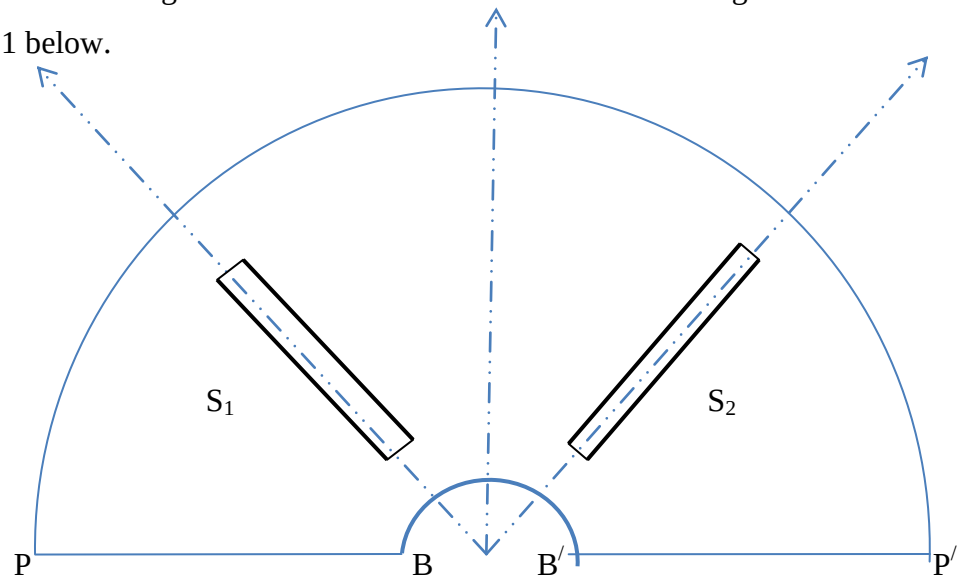

Figure 3.1: **Plate design for a diverging conical ring with two slits.**

By folding it such that points $PP^{/}$ coincide on the tube's inner circumference and $BB^{/}$ becomes the inlet circumference at the vertex. The slits S_1 and S_2 provide pathway for the injected fluid in axial direction that generate multi-longitudinal vortex flow. They are cut out on the slant surface of a conical insert, while the vertex is cut out to obtain the insert inlet circumference $BB^{/}$ to maintain a laminar flow along the centre line of the cylindrical tube with a steady stream of fluid. The conical insert is fixed at the end of an inlet piece of pipe with length of the exit piece set at a determined distance to ensure it provides properties of both displacement enhancement and a swirl flow device. The ratio of the inserts inlet to outlet diameter provides the pitch ratio given by d/D. Setting a conical insert with a divergence half angle of 7.5^0 then an inlet diameter of 0.036 m and outlet diameter of 0.05 m provides a pitch ratio of 0.72 with a horizontal distance of 0.07 m between the inlet and outlet.

The choice of these dimensions is in agreement with existing research on a divergent diffuser that provides a relationship of diffuser performance against the angle of divergence as shown in Figure 4.2 which establishes that maximum output is obtained at an angle of 7^0 on the vertex. For internal flows the fluid is completely encompassed in a duct or any other carrier with its cross sectional filled by the fluid. In a situation involving cylindrical pipes where the fluid flow fills the tube, forces are virtually identical in all radial directions therefore it is best analyzed using cylindrical coordinates. Since fluid motion is under pressure then the effects of gravity are negligible.

3.3 Conditions for the fluid flow

In this research hot water is used as the test fluid entering the diverging conical ring (DCR) insert placed in a cylindrical tube with the fluid in laminar flow. When using water to simulate a case of heat transfer in the fluid, note that if pressurized

water heats up to 374^0C at 22 MPa but at normal atmospheric pressure, it can only be in liquid state in the range between 0^0 C and 100^0 C. Water has good thermal conductivity, a large thermal capacity and low viscosity.

The cut out vertex provides an inlet diameter while the slant edges diverge at a half angle of α^0. The slits are placed in symmetrical positions to subdivide the pipe's cross section into equal parts so that fluid passing through the slits generates multi-longitudinal vortex pairs. The conical ring insert intersection of the walls at the vertex has a solid angle $2\alpha^0$ which is illustrated in Figure 3.2 used to determine the inserts divergence.

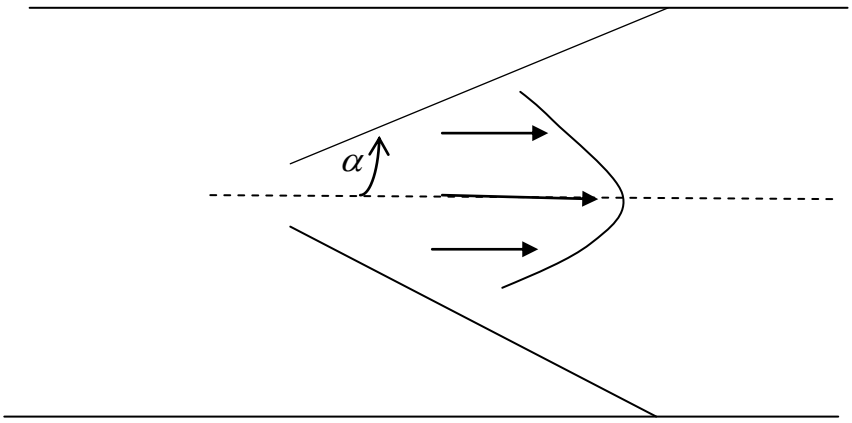

Figure 3.2: **Angle of inclination at the vertex of a diverging conical ring insert**

The conical ring insert is a divergent pipe and the Reynolds number (Re) is highest when an angle of divergence is zero. The Re is a decreasing function of the stream wise axial direction along the z coordinate and the flow non – parallelism is larger for a given divergence in which case two sets of approach are used. Mathematical investigations of incompressible viscous fluid flow through convergent or divergent channels were pioneered by Jeffery (1915) and Hamel (1916) as a special case of two dimensional flow through a channel with inclined plane walls tending to meet at a point and with a source or sink at the vertex. For the mean flow an axisymmetric Jeffery Hamel (JH) equation is derived, which is valid at small

divergence angles. At larger divergence angles greater than 2^0, the Navier -Stokes equation is solved directly in the axisymmetric geometry with a divergent portion of finite values. It is also known that at small divergence angles and high Re above 1000 a parallel flow stability analysis is conducted on the axisymmetric JH profile, while at lower Re the partial differential equations for non parallel stability are solved as an extended Eigen value problem.

3.4 Assumptions in the study

In this study the following assumptions are made:

i) The fluid flow is steady and in axial direction.

ii) The fluid is Newtonian, implying stress is proportional to the rate of shear force.

iii) The no-slip condition is satisfied, implying on the surface of a solid wall the velocity of the fluid layer adjacent to it moves at the speed of the wall.

iv) The fluid is considered incompressible.

v) The body forces are negligible.

3.5 Navier - Stokes equations governing an incompressible fluid flow in a cylindrical pipe

Using the gradient operator $\nabla = \hat{i}\frac{\partial}{\partial x} + \hat{j}\frac{\partial}{\partial y} + \hat{k}\frac{\partial}{\partial z}$ and the velocity vector in cylindrical coordinates $\vec{U} = u_r \vec{l}_r + u_\theta \vec{l}_\theta + u_z \vec{l}_z$ the continuity equation for an unsteady flow is $\frac{\partial \rho}{\partial t} + \nabla \cdot \left(\rho \vec{U} \right) = 0$ hence

$$\frac{\partial \rho}{\partial t} + \rho \left(\nabla \cdot \vec{U} \right) = 0 \qquad (3.1)$$

Where $\nabla \cdot \vec{U} = \frac{1}{r}\frac{\partial (ru_r)}{\partial r} + \frac{1}{r}\frac{\partial u_\theta}{\partial \theta} + \frac{\partial u_z}{\partial z}$ the cylindrical polar coordinates, of the velocity vector gives

$$\frac{\partial \rho}{\partial t} + \frac{1}{r}\frac{\partial (r\rho u_r)}{\partial r} + \frac{1}{r}\frac{\partial (\rho u_\theta)}{\partial \theta} + \frac{\partial (\rho u_z)}{\partial z} = 0 \tag{3.2}$$

The continuity equation in cylindrical polar coordinates best describes flows involving rotational or radial motion. A point in the flow with coordinates $P(r,\theta,z)$ has velocity components in the respective directions as u_r, u_θ and u_z, where transformation between Cartesian and polar systems is obtained by the relations,

$$r = \sqrt{x^2 + y^2 + z^2}, \quad \theta = \tan^{-1}\frac{y}{x} \quad and \; z = z. \tag{3.3}$$

The governing equations for a Newtonian incompressible three dimensional axisymmetric laminar flow in a pipe are:

a) The continuity equation

$$\frac{1}{r}\frac{\partial (ru_r)}{\partial r} + \frac{1}{r}\frac{\partial u_\theta}{\partial \theta} + \frac{\partial u_z}{\partial z} = 0 \tag{3.4}$$

b) The momentum equations:

i) In radial direction is

$$\rho\left(\frac{\partial u_r}{\partial t} + u_r\frac{\partial u_r}{\partial r} + \frac{u_\theta}{r}\frac{\partial u_r}{\partial \theta} - \frac{u_\theta^2}{r} + u_z\frac{\partial u_r}{\partial z}\right) =$$

$$-\frac{\partial p}{\partial r} + \rho g_r + \mu\left[\frac{1}{r}\frac{\partial}{\partial r}\left(r\frac{\partial u_r}{\partial r}\right) - \frac{u_r}{r^2} + \frac{1}{r^2}\frac{\partial^2 u_r}{\partial \theta^2} - \frac{2}{r^2}\frac{\partial u_\theta}{\partial \theta} + \frac{\partial^2 u_r}{\partial z^2}\right] \tag{3.5}$$

ii) In axial direction

$$\rho\left(\frac{\partial u_z}{\partial t}+u_r\frac{\partial u_z}{\partial r}+\frac{u_\theta}{r}\frac{\partial u_z}{\partial \theta}-\frac{u_\theta^2}{r}+u_z\frac{\partial u_z}{\partial z}\right)=$$

$$-\frac{\partial p}{\partial z}+\rho g_z+\mu\left[\frac{1}{r}\frac{\partial}{\partial r}\left(r\frac{\partial u_z}{\partial r}\right)+\frac{1}{r^2}\frac{\partial^2 u_z}{\partial \theta^2}+\frac{\partial^2 u_z}{\partial z^2}\right] \qquad (3.6)$$

iii) In tangential direction

$$\rho\left(\frac{\partial u_\theta}{\partial t}+u_r\frac{\partial u_\theta}{\partial r}+\frac{u_\theta}{r}\frac{\partial u_\theta}{\partial \theta}-\frac{u_r u_\theta}{r}+u_z\frac{\partial u_\theta}{\partial z}\right)=$$

$$-\frac{\partial p}{\partial z}+\rho g_\theta+\mu\left[\frac{1}{r}\frac{\partial}{\partial r}\left(r\frac{\partial u_\theta}{\partial r}\right)+-\frac{u_\theta}{r^2}+\frac{1}{r^2}\frac{\partial^2 u_\theta}{\partial \theta^2}+\frac{2}{r^2}\frac{\partial u_r}{\partial \theta}+\frac{\partial^2 u_\theta}{\partial z^2}\right] \qquad (3.7)$$

c) The energy equation is

$$\rho C_p\left(\frac{\partial T}{\partial t}+u_r\frac{\partial T}{\partial r}+\frac{u_\theta}{r}\frac{\partial T}{\partial \theta}+u_z\frac{\partial T}{\partial z}\right)=k\left[\frac{1}{r}\frac{\partial}{\partial r}\left(r\frac{\partial T}{\partial r}\right)+\frac{1}{r^2}\frac{\partial^2 T}{\partial \theta^2}+\frac{\partial^2 T}{\partial z^2}\right]+\phi \qquad (3.8)$$

where ϕ is the dissipation function.

The governing equations are used to describe the flow of a fluid past an axisymmetric diverging conical ring. The internal flow occurs when the fluid is completely encompassed by a pipe or a duct as the fluid carrier. In a situation involving a round pipe or a tube it is best analyzed using the cylindrical coordinates because the flow is virtually identical in all radial directions when the pipe is full, then the effects of gravity can be ignored.

3.6 Flow of a viscous fluid through a DCR insert with slits

When fluid flows through a circular diverging ring with slits, at the vertex of a DCR insert the flow is well defined by an axisymmetric divergent pipe flow problem of an incompressible viscous fluid. The cut out slits generate a swirl flow that decays downstream. The term swirling flow indicates a loosely defined class of flow, whose main characteristic is that the flow has both axial and radial velocity component. As shown in Figure 3.3 an insert provides an obstruction to the smooth fluid flow motion, causing a swirl flow with a pressure drop and a rise in friction factor to enhance heat transfer in the system.

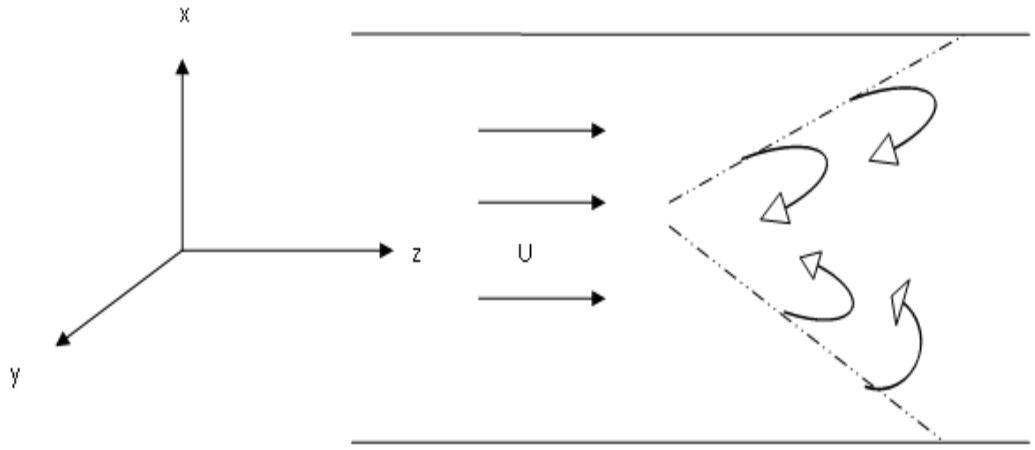

Figure 3.3: **Schematic view of fluid flow past a diverging conical ring insert**

Swirling fluid flow in a confined pipe and free flows unify a number of complexities which occur in other turbulent flows like, streamline curvature and rotation in three dimensional flow.

This research work is a case of swirl decay flow where rotation dies downstream due to friction. Whether a flow is turbulent or laminar depends on characteristics of both the fluid (viscosity) and flow velocity in a length scale.

The general properties of a turbulent flow are such that:

i) Turbulent flows are irregular or chaotic in space and time.

ii) Turbulent flows are diffusive; heat, momentum and mass are mixed then transported efficiently, which in many applications is a desirable feature of turbulence.

iii) Turbulence is essentially rotational and three dimensional; where rotating patches of a fluid i.e. eddies, have length scales ranging from size of flow domain and down to the smallest visible fluid motion.

Turbulence occurs in flows from a specific value of the Reynolds number, beyond 4000 in water at which point the non linear terms in the governing equations dominate over the linear viscous terms.

iv) Turbulent flows are dissipative and kinetic energy of velocity fluctuations produced at the largest scales is dissipated at the smallest scales into heat through viscous diffusion.

To analyze a swirl flow the two most common techniques are Renormalization Group (RNG) κ-ε model and Reynolds- stress model methods which are derived from an application of a statistical derivation to the instantaneous Navier- Stokes equations similar in form to the standard k-ε equations but includes; additional term in ε equation for interaction between turbulence dissipation and mean shear. Effects of swirl on turbulence and a differential formula for effective viscosity, which gives an improved prediction for high streamline curvature and strain rate. These features make RNG k-ε and Reynolds- stress models more accurate and reliable for a wide class of fully enclosed flows. The equations of motion and energy for a Newtonian incompressible flow are given in cylindrical coordinates (r,θ,z). The instantaneous velocity components are $u_z, u_r \text{ and } u_\theta$ respectively in axial, radial and azimuthal directions respectively. Temporal mean velocities are $\overline{u_z}, \overline{u_r} \text{ and } \overline{u_\theta}$ and their corresponding fluctuating components of velocities are $u_z^{/}, u_r^{/} \text{ and } u_\theta^{/}$. Using Reynolds decomposition in the governing equations the mean and fluctuation part are:

Axial component (z):

$$\bar{u}_z = u_z + u_z^{/}, \tag{3.9}$$

Radial component (r):

$$\bar{u}_r = u_r + u_r^{/}, \tag{3.10}$$

Tangential component (θ):

$$\bar{u}_\theta = u_\theta + u_\theta^{/}, \tag{3.11}$$

Temperature:

$$\bar{T} = T + T^{/}, \tag{3.12}$$

and Pressure:

$$\bar{p} = p_m + p^{/}. \tag{3.13}$$

Where $T^{/}$ and $p^{/}$ are fluctuating temperature and pressure p_m, is the local pressure minus hydrostatic pressure. If flow is assumed to be steady, the time variation terms are omitted and the following equations are obtained: Continuity equation

$$\frac{1}{r}\frac{\partial\left(r\overline{u_r}\right)}{\partial r} + \frac{1}{r}\frac{\partial\overline{u_\theta}}{\partial\theta} + \frac{\partial\overline{u_z}}{\partial z} = 0 \tag{3.14}$$

Momentum equation in axial direction obtained from equation (3.6) since $u_\theta = 0$ and the flow is steady obtaining

$$\bar{u}_r\frac{\partial\bar{u}_z}{\partial r} + \bar{u}_\theta\left(\frac{1}{r}\frac{\partial\bar{u}_z}{\partial\theta}\right) + \bar{u}_z\frac{\partial\bar{u}_z}{\partial z} = -\frac{1}{\rho}\frac{\partial\bar{p}}{\partial z} + \rho g +$$

$$\frac{1}{\rho}\left[\frac{\partial}{\partial z}\left(\mu\frac{\partial\bar{u}_z}{\partial z}\right) + \frac{1}{r}\frac{\partial}{\partial r}\left(r\mu\left(\frac{\partial\bar{u}_z}{\partial r} + \frac{\partial\bar{u}_r}{\partial z}\right)\right) + \frac{1}{r}\frac{\partial}{\partial\theta}\left(\mu\left(\frac{\partial\bar{u}_\theta}{\partial z} + \frac{1}{r}\frac{\partial\bar{u}_z}{\partial\theta}\right)\right)\right] \tag{3.15}$$

Also the momentum equation in radial and tangential direction exists. The assumption of constant viscosity is practical for swirling flow equations therefore

these terms change to $\mu\nabla^2\bar{U}$. In natural convection equations the viscosity term should be kept inside the divergence since μ varies with temperature. Substituting these terms into the momentum equations the RNG k-ε equations are obtained. The general two equations model for κ and ε together with the eddy – viscosity and stress – strain relationship constitute the κ-ε turbulence model where ε is the dissipation rate of k. The Reynolds stress model (RSM) also called second order closure model copes with more complex flows by taking into account anisotropic features of turbulence. The Reynolds stresses are expressed in terms of known mean flow quantities such as convective and diffusive nature of turbulence to solve the fluid governing equations in turbulence models. The equations are then combined with the Navier – Stokes equations in order to solve the flow problem in a closed set of seven partial differential equations. In turbulent flow there are both time averaged quantity and instantaneous fluctuation. The general turbulent flow equations are also valid for laminar flow when considering fluctuations to be negligible. The different models of solving turbulent flow can be selected upon use of computational fluid dynamics software to improve on accuracy of the solution.

In this research work simulation done of the flow past a DCR insert showed that the turbulence effects are not dominate and the swirl flow decay as the fluid exists the insert. Therefore the general Navier –stokes equations provide an acceptable prediction of the fluid flow being investigated.

3.7 Navier- Stokes equations for fluid flow in the DCR insert

An incompressible viscous fluid flows through a conical diffuser tube with slits generating longitudinal vortex pairs and experiences a flow condition that can be determined by the Navier – Stokes governing equations where a no slip condition at the interface between fluid and the walls is fundamental. The fluid element in motion has translation, linear deformation, rotation and angular deformation (also called rate of shearing strain). The rate of angular deformation is related to a

corresponding shearing stress. The differential form of momentum equation is derived by applying control volume with both body and surface forces. The body forces are due to external fields such as gravity, while surface forces are due to stresses that act on the sides of the control surfaces equal to normal pressure plus viscous stress. For Newtonian fluids the shear stress is proportional to the rate of strain. This stress tensor is included in the axial momentum governing equation. Considering a system of cylindrical polar coordinates (r,θ,z) the steady two dimensional flow of an incompressible viscous fluid from source at the inlet of a cylindrical pipe along the z axis is considered in Figure 3.3. Given that $u_\theta = 0$, meaning there is no change in angular velocity with respect to tangential direction (θ). The motion is therefore purely in axial and radial directions, depending on r and z. Considering a steady flow of viscous incompressible fluid in a tube with an axisymmetric diverging conical ring insert given velocity components (u,v).

The equation of continuity (3.4) becomes:

$$\frac{1}{r}\frac{\partial(ru_r)}{\partial r}+\frac{\partial(u_z)}{\partial z}=0 \text{ hence } \frac{u_r}{r}+\frac{\partial u_r}{\partial r}+\frac{\partial u_z}{\partial z}=0 \tag{3.16}$$

The equations for conservation of momentum (3.5) gives:

Radial momentum conservation equation which reduces since the flow is steady and gravity acts perpendicular to the axial flow which is negligible and the fluid injected from the slits on a slant edge parallel to the flow becomes

$$\rho\left(u_r\frac{\partial u_r}{\partial r}+u_z\frac{\partial u_r}{\partial z}\right)=-\frac{\partial p}{\partial r}+\mu\left[\frac{1}{r}\frac{\partial}{\partial r}\left(r\frac{\partial u_r}{\partial r}\right)-\frac{u_r}{r^2}+\frac{\partial^2 u_r}{\partial z^2}\right] \tag{3.17}$$

Similarly axial momentum conservation equation (3.6) reduces to:

$$\rho\left(u_r\frac{\partial u_z}{\partial r}+u_z\frac{\partial u_z}{\partial z}\right)=-\frac{\partial p}{\partial z}+\mu\left[\frac{1}{r}\frac{\partial}{\partial r}\left(r\frac{\partial u_z}{\partial r}\right)+\frac{\partial^2 u_z}{\partial z^2}\right]+\tau_{zz} \tag{3.18}$$

For a horizontal circular pipe with a Newtonian incompressible internal fluid flow, with only one non zero velocity in the direction of flow u_z. The additional term is obtained from a shear stress tensor component in cylindrical coordinates has

$$\tau_{zz} = \frac{-\mu}{r}\frac{\partial u_z}{\partial z}. \tag{3.19}$$

Then axial momentum equation becomes

$$\rho\left(u_r\frac{\partial u_z}{\partial r} + u_z\frac{\partial u_z}{\partial z}\right) = -\frac{\partial P}{\partial z} + \mu\left[\frac{1}{r}\frac{\partial}{\partial r}\left(r\frac{\partial u_z}{\partial r}\right) + \frac{\partial^2 u_z}{\partial z^2}\right] - \frac{\mu}{r}\frac{\partial u_z}{\partial z} \tag{3.20}$$

$$u_r\frac{\partial u_z}{\partial r} + u_z\frac{\partial u_z}{\partial z} = -\frac{1}{\rho}\frac{\partial P}{\partial z} + \frac{\mu}{\rho}\left[\frac{1}{r}\frac{\partial}{\partial r}\left(r\frac{\partial u_z}{\partial r}\right) + \frac{\partial^2 u_z}{\partial z^2} - \frac{\partial u_z}{r\,\partial z}\right] \tag{3.21}$$

Energy conservation equation (3.8) becomes:

$$\rho C_p\left(u_z\frac{\partial T}{\partial z} + u_r\frac{\partial T}{\partial r}\right) = k\left[\frac{1}{r}\frac{\partial}{\partial r}\left(r\frac{\partial T}{\partial r}\right) + \frac{\partial^2 T}{\partial z^2}\right] + \phi \tag{3.22}$$

The dissipation function for the energy equation is always positive in value and the term is rarely important for high speed flows in long or narrow capillaries where viscous heating is significant. The bulk viscosity does not appear in a momentum equation because divergence of the velocity vector is zero for incompressible flows. Body force per unit volume in the respective directions provides a means by which the presence of external entities is introduced into the momentum equations.

3.8 Stream function and vorticity formulation

A vortex line is an analogy to a streamline in the fluid such that at each point on the line a vorticity vector is a tangent to the line. The strength of a vorticity vector is not constant along a vortex line in the same way velocity is not necessarily constant along a streamline. While a vortex path in space whose surface elements are composed of vortex lines passing through the same closed curve. For irrotational and incompressible two dimensional fluid flows both the stream function and

velocity potential obey the same differential equation, where the azimuthal component of vorticity vector is

$$\omega = -\left(\frac{\partial u_r}{\partial z} - \frac{\partial u_z}{\partial r} \right) \tag{3.23}$$

In a potential vortex flow, fluid moves in concentric circles with an angular velocity u_θ that decreases inversely to radial distance from the centre of a vortex.

The Navier Stokes equations need to be expressed in terms of the stream function ψ and vorticity ω to be able to determine the fluid flow's vorticity and swirl velocity. On axisymmetric flow no velocity gradient exists in the θ direction and then the continuity equation for steady incompressible flow reduces to $\frac{1}{r}\frac{\partial (r u_r)}{\partial r} + \frac{\partial u_z}{\partial z} = 0$. This can be rearranged to give $\frac{1}{r}\frac{\partial (r u_r)}{\partial r} = -\frac{\partial u_z}{\partial z}$ hence the expression $r u_z dr - r u_r dz = d\psi$ where $\psi(r,z)$ is the Stokes stream function. The stream function ψ can be defined for any two dimensional flow, whether flow is irrotational or not. At least two of the velocity components are non zero, thus expressing the axial and radial velocities in cylindrical coordinates has:

$$u_z = \frac{1}{r}\frac{\partial \psi}{\partial r} \text{ and } u_r = \frac{-1}{r}\frac{\partial \psi}{\partial z} \tag{3.24}$$

This satisfies the continuity equation $\nabla \cdot \vec{U} = 0$ so that velocity field is determined through a Poisson equation for the stream function. The divergence will be equal to zero because of equivalence in the mixed second derivative of the stream function. The change in streamline function between a pair of streamlines is equal to volumetric flow rate between those two streamlines. Lines of constant streamlines are perpendicular to lines of constant velocity potential lines since the slopes are negative reciprocals of one another.

3.9 Field synergy and heat transfer performance

Each particle in a fluid has different physical quantities, such as temperature and pressure have definite physical meanings but no directions therefore no direct synergy relation among them. However the scalar gradient and velocity vector of a fluid particle in the flow field reflect not only intensity of heat transfer but also direction of transport process so that coupling of vectors represents a direct synergy relation therefore revealing the mechanism of physical quantity synergy to help explain heat transfer and flow process. Synergy correlation between velocity $\vec{U}$, velocity gradient $\nabla\vec{U}$, temperature gradient ∇T and pressure gradient ∇P is obtained where $\nabla\vec{U}$ serves as a reference vector, as shown in Figure 3.4 so that for a certain fluid particle P, there are five inter section angles to reflect the synergy relation among physical quantities.

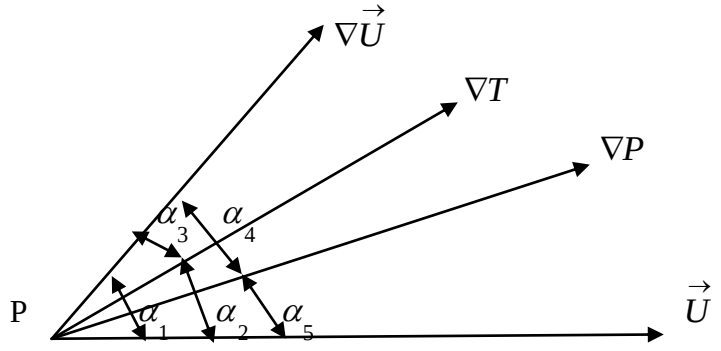

Figure 3.4: Intersection angles between physical quantities to determine synergy correlation. **Source: Liu et al. (2009)**

The angle between α_1 velocity and velocity gradient of a fluid particle P in laminar flow field given as

$$\alpha_1 = \cos^{-1} \frac{\vec{U} \cdot \nabla \vec{U}}{\left|\vec{U}\right\| \left|\nabla \vec{U}\right|}. \tag{3.25}$$

Velocity and temperature gradient is

$$\alpha_2 = \cos^{-1} \frac{\vec{U} \cdot \nabla T}{|\vec{U}|\left|\nabla T\right|}. \tag{3.26}$$

The vector relation of a fluid particle P as a synergy angle between temperature gradient ∇T and velocity gradient $\nabla \vec{U}$ is expressed has

$$\alpha_3 = \cos^{-1} \frac{\nabla T \cdot \nabla \vec{U}}{\left|\nabla T\right| |\nabla \vec{U}|}. \tag{3.27}$$

In two dimensional laminar flow field the vectors are coplanar hence all fluid particles on a stream line satisfy

$$\alpha_3 \equiv \left|\alpha_1 - \alpha_2\right|. \tag{3.28}$$

The pressure gradient ∇P not only drives flow of fluid but also affects heat transfer and flow process. For a fluid particle there exists synergy relation between pressure gradient and velocity gradient which is expressed has

$$\alpha_4 = \cos^{-1} \frac{\nabla P \cdot \nabla \vec{U}}{\left|\nabla P\right| |\nabla \vec{U}|}. \tag{3.29}$$

In a potential flow with no viscosity in a parallel fluid flow ∇P is orthogonal to $\nabla \vec{U}$ hence $\alpha_4 = 90^0$ so that flow resistance is zero. In viscous flow then $\alpha_4 < 90^0$ due to viscous dissipation. Similarly synergy angle between $\vec{U}$ and ∇P is expressed has

$$\alpha_5 = \cos^{-1} \frac{\vec{U} \cdot \nabla P}{|\nabla P| |\vec{U}|}. \tag{3.30}$$

Liu et al. (2009) showed that if the synergy relation of every fluid particle in the entire fluid field is improved then heat transfer and flow can be effectively organized to achieve better temperature uniformity in the flow field and flow resistance can also be reduced. There are three kinds of problems in terms of heat transfer enhancement. First if convective heat transfer is to be enhanced then the synergy between velocity and temperature gradient should be considered. The smaller the synergy angle α_2 is the larger the convective heat transfer coefficient *h* will be. Secondly if the flow resistance is to be reduced then the synergy between velocity and pressure gradients should be considered. The smaller a synergy angle α_5 is the smaller the pressure drop ΔP. Third if the purpose is to raise the overall performance of a heat transfer unit then the synergy between temperature gradient and velocity gradient should be considered.

According to the principle of physical quantity synergy it is possible to design excellent heat transfer surfaces and structures ensuring that the increased amplitude of convective heat transfer is close to or bigger than that of flow resistance by improving synergetic relation among physical quantities. The principle of field synergy in enhancement of convective heat transfer provides that better synergy of velocity and temperature gradients, gives higher convective heat transfer rate under the same conditions. Synergy of these two vector fields or the three scalar fields implies that the included angle between the velocity and temperature gradients should be as small as possible i.e. velocity and temperature gradient should be as parallel as possible. Local values of the three scalar fields should be simultaneously large i.e. larger values of the angle should correspond to larger values of velocity and temperature gradient. The velocity and temperature profiles at each cross section should be as uniform as possible. Better synergy

among the scalar fields will lead to a larger value of Nusselt number. By decreasing the included angle between velocity vector and temperature gradient, then synergy will make the integration value larger i.e. enhancing the heat transfer. Field synergy number $Fc = \frac{Nu}{\mathrm{Re}\ \mathrm{Pr}}$ represents the degree of synergy between velocity and temperature gradient fields for the entire domain. Fc stands for the dimensionless heat source strength i.e. the dimensionless convection term over the entire domain which physically is an indication of the degree of synergy between velocity and temperature gradient fields. Its value can be anywhere between zero and one depending on the type of heat transfer surface. Field synergy number and Stanton number have identical formulas relating to the Nusselt number. However this equation is always valid regardless of type of flow and heat transfer surface geometry. Stanton number is an alternate to Nusselt number for expressing dimensionless heat transfer coefficient for convective heat transfer over the heat transfer surface.

3.10 Non – dimensionalisation of the governing equations

It is necessary to determine non dimensional numbers that provide effects of varying flow parameters which gives a comparison between experimental and theoretical results. Dimensionless parameters allow application of results obtained in a model to be applied in any other geometrically similar case. We let L, U and P denote characteristic length, velocity and pressure respectively and express the non dimensional variables by indentifying them with an asterisk primed quantities.

$$r^* = \frac{r}{L,} \qquad u_z^* = \frac{u_z}{U,} \qquad u_r^* = \frac{u_r}{U,} \qquad p^* = \frac{p}{P,} \qquad z^* = \frac{z}{L} \text{ and } T^* = \frac{T}{\Delta T}. \qquad (3.31)$$

where ΔT is the characteristic driving temperature difference for heat transfer.

In the continuity equation (3.16) the parameters are replaced to obtain $\frac{u_r^* U}{r^* L} + \frac{\partial (u_r^* U)}{\partial (r^* L)} + \frac{\partial (u_z^* U)}{\partial (z^* L)} = 0$ factoring out the characteristic dimensions to get

$$\frac{U}{L}\left(\frac{u_r^*}{r^*} + \frac{\partial u_r^*}{\partial r^*} + \frac{\partial u_z^*}{\partial z^*} \right) = 0$$

which gives $\frac{u_r^*}{r^*} + \frac{\partial u_r^*}{\partial r^*} + \frac{\partial u_z^*}{\partial z^*} = 0.$ (3.32)

The radial momentum conservation equation (3.17) becomes

$$\rho\left(\frac{(u_r^* U)\partial (u_r^* U)}{\partial (r^* L)} + \frac{\left(u_z^* U\right)\partial\left(u_r^* U\right)}{\partial (z^* L)} \right) = \frac{-\partial\left(p^* P\right)}{\partial\left(r^* L\right)} + \mu\left[\frac{1}{\left(r^* L\right)} \frac{\partial}{\partial\left(r^* L\right)}\left(\frac{\left(r^* L\right)\partial\left(u_r^* U\right)}{\partial (r^* L)} \right) + \frac{\partial^2 (u_r^* U)}{\partial\left(z^* L\right)^2} \right]$$

$$\frac{U^2}{L}\left(\frac{u_r^* \partial u_r^*}{\partial r^*} + \frac{u_z^* \partial u_r^*}{\partial z^*} \right) = -\frac{P\partial p^*}{L\rho\partial r^*} + \frac{\mu}{\rho}\left[\frac{U}{L^2} \frac{\partial}{r^* \partial r^*}\left(\frac{r^* \partial u_r^*}{\partial r^*} \right) + \frac{U}{L^2} \frac{\partial^2 u_r^*}{\partial\left(z^*\right)^2} \right].$$

Factoring out the dimensional variables and multiplying by $\frac{L}{U^2}$

$$\frac{u_r^* \partial u_r^*}{\partial r^*} + \frac{u_z^* \partial u_r^*}{\partial z^*} = \frac{-P}{\rho U^2} \frac{\partial p^*}{\partial r^*} + \frac{\mu}{\rho L U}\left[\frac{\partial}{r^* \partial r^*}\left(\frac{r^* \partial u_r^*}{\partial r^*} \right) + \frac{\partial^2 u_r^*}{\partial (z^*)^2} \right]$$

This simplifies to:

$$\frac{u_r^* \partial u_r^*}{\partial r^*} + \frac{u_z^* \partial u_r^*}{\partial z^*} = -P_C \frac{\partial p^*}{\partial r^*} + \frac{1}{\mathrm{Re}}\left[\frac{\partial^2 u_r^*}{\partial (r^*)^2} + \frac{\partial u_r^*}{r^* \partial r^*} + \frac{\partial^2 u_r^*}{\partial\left(z^*\right)^2} \right] \quad (3.33)$$

The axial momentum conservation equation (3.21) becomes

$$\frac{(u_r^* U)\partial (u_z^* U)}{\partial\left(r^* L\right)} + \frac{(u_z^* U)\partial (u_z^* U)}{\partial (z^* L)} = \frac{-1}{\rho} \frac{\partial (p^* P)}{\partial (z^* L)} + \frac{\mu}{\rho}\left[\frac{1}{(r^* L)} \frac{\partial}{\partial (r^* L)}\left(\frac{(r^* L)\partial (u_z^* U)}{\partial (r^* L)} \right) + \frac{\partial^2 (u_z^* U)}{\partial (z^* L)^2} - \frac{\partial (u_z^* U)}{(r^* L)\partial (z^* L)} \right]$$

$$\frac{U^2}{L}\left(\frac{u_r^*\partial u_z^*}{\partial r^*}+\frac{u_z^*\partial u_z^*}{\partial z^*}\right)=\frac{-P}{\rho L}\frac{\partial p^*}{\partial z^*}+\frac{\mu}{\rho}\left[\frac{U}{L^2}\frac{\partial}{r^*\partial r^*}\left(\frac{r^*\partial u_z^*}{\partial r^*}\right)+\frac{U\partial^2 u_z^*}{L^2\partial(z^*)^2}-\frac{U\partial u_z^*}{L^2 r^*\partial z^*}\right]$$

Multiplying with $\frac{L}{U^2}$ it reduces this equation to:

$$\frac{u_r^*\partial u_z^*}{\partial r^*}+\frac{u_z^*\partial u_z^*}{\partial z^*}=\frac{-P}{\rho U^2}\frac{\partial p^*}{\partial z^*}+\frac{\mu}{\rho UL}\left[\frac{\partial}{r^*\partial r^*}\left(\frac{r^*\partial u_z^*}{\partial r^*}\right)+\frac{\partial^2 u_z^*}{\partial(z^*)^2}-\frac{\partial u_z^*}{r^*\partial z^*}\right]$$

$$\frac{u_r^*\partial u_z^*}{\partial r^*}+\frac{u_z^*\partial u_z^*}{\partial z^*}=-P_C\frac{\partial p^*}{\partial z^*}+\frac{1}{\mathrm{Re}}\left[\frac{\partial^2 u_z^*}{\partial(r^*)^2}+\frac{1}{r^*}\frac{\partial u_z^*}{\partial r^*}+\frac{\partial^2 u_z^*}{\partial(z^*)^2}\right]-\frac{1}{\mathrm{Re}}\frac{\partial u_z^*}{r^*\partial z^*} \qquad (3.34)$$

Energy conservation equation (3.22) becomes:

$$\rho C_p\left(u_z\frac{\partial T}{\partial z}+u_r\frac{\partial T}{\partial r}\right)=k\left[\frac{\partial^2 T}{\partial r^2}+\frac{1}{r}\frac{\partial T}{\partial r}+\frac{\partial^2 T}{\partial z^2}\right].$$

Which gives

$$\rho C_p\left(\frac{(u_z^*U)\partial(T^*\Delta T)}{\partial(z^*L)}+\frac{(u_r^*U)\partial(T^*\Delta T)}{\partial(r^*L)}\right)=k\left[\frac{\partial^2(T^*\Delta T)}{\partial(r^*L)^2}+\frac{1}{(r^*L)}\frac{\partial(T^*\Delta T)}{\partial(r^*L)}+\frac{\partial^2(T^*\Delta T)}{\partial(z^*L)^2}\right]$$

$$\frac{U\Delta T}{L}\left(\frac{u_z^*\partial T^*}{\partial z^*}+\frac{u_r^*\partial T^*}{\partial r^*}\right)=\frac{k}{\rho C_P}\frac{\Delta T}{L^2}\left[\frac{\partial^2 T^*}{\partial(r^*)^2}+\frac{\partial T^*}{r^*\partial r^*}+\frac{\partial^2 T^*}{\partial(z^*)^2}\right]$$

to become

$$\frac{u_z^*\partial T^*}{\partial z^*}+\frac{u_r^*\partial T^*}{\partial r^*}=\frac{k}{\mu C_P}\frac{\mu}{\rho UL}\left[\frac{\partial^2 T^*}{\partial(r^*)^2}+\frac{\partial T^*}{r^*\partial r^*}+\frac{\partial^2 T^*}{\partial(z^*)^2}\right].$$

$$\frac{u_z^*\partial T^*}{\partial z^*}+\frac{u_r^*\partial T^*}{\partial r^*}=\frac{1}{\mathrm{PrRe}}\left[\frac{\partial^2 T^*}{\partial(r^*)^2}+\frac{\partial T^*}{r^*\partial r^*}+\frac{\partial^2 T^*}{\partial(z^*)^2}\right] \qquad (3.35)$$

Where Pr and Re are non dimensional numbers.

3.11 Non -dimensional numbers

Dimensionless numbers are of key importance in parametric analysis of engineering problems since they help in understanding similarity between problems with similar type of fluid flow.

i) Reynolds number Re this is ratio of inertia force to viscous force,

$$\mathrm{Re} = \frac{\rho UL}{\mu} = \frac{UL}{\vartheta}. \tag{3.36}$$

ii) Pressure coefficient Pc this is a ratio of pressure force to inertia force,

$$Pc = \frac{P}{\rho U^2}. \tag{3.37}$$

iii) Prandtl number Pr is the ratio of momentum diffusivity (Kinematic viscosity) to thermal diffusivity,

$$\mathrm{Pr} = \frac{\mu C_P}{k} \tag{3.38}$$

which is a ratio of viscous to thermal force. In heat transfer involving convection mode, warm and cold particles mix because of their pressure difference which involves momentum transfer hence a measure of relative ability of fluid to allow momentum and thermal diffusion.

iv) Nusselt number,

$$\mathrm{Nu} = \frac{hD}{k} = \frac{QL}{k\Delta T} \tag{3.39}$$

Nu provides a dimensionless temperature gradient at a point. It is a ratio of actual to conductive heat flux.

v) Field synergy number

$$F_C = \frac{Nu}{\mathrm{Re}\,\mathrm{Pr}} \tag{3.40}$$

F_C represents the degree of synergy between velocity and temperature gradient fields in a domain.

The non dimensional numbers will be used to determine the behavior of fluid flow in geometrically similar cases when obtaining pressure and temperature profiles in the next chapter after discretization of the governing equations.

CHAPTER FOUR

SIMULATION OF THE FLUID FLOW

4.1 Introduction

In this chapter simulation is done using ‘solid works’ to obtain values of velocity components along the pipe to be used in solving other variables in the flow. The Governing equations of fluid flow in cylindrical coordinates are expressed in terms of central finite difference and discretization of equation done to determine flow parameters at different points of the pipe. The multi-longitudinal vortex pairs formed by an incompressible Newtonian fluid passing through a diverging conical ring insert with slits cut out on the slant edge are observed by obtaining cross sections of the flow simulations. Then comparison is done on flow pattern obtained when a diverging conical ring insert with slits is used and those of other solutions obtained by other researchers on heat transfer enhancement.

4.2 Pipe entrance effect

A fluid entering a circular pipe at uniform velocity experiences the no- slip condition when particles in the outer layer are in contact with the pipe inner surface and come to a complete rest. The no- slip condition causes the fluid particles in the adjacent layers to slow down as a result of fluid friction therefore a velocity gradient develops along the pipe. The region of flow in which effects of viscous shearing forces caused by fluid viscosity are felt is called the velocity boundary layer. Thickness of this boundary layer increases in direction of flow until the boundary layer reaches a centre line of the pipe; this part is called the hydrodynamic entrance region. The part beyond an entrance region has velocity profile fully developed and remains unchanged with the temperature remaining constant. The region starting from pipe entrance of fluid to the meeting point of boundary layer on opposite sides of a cylindrical pipe is called the hydrodynamic entrance region. Thereafter a hydro dynamically fully developed region is formed

and its within this section that a DCR insert is placed where there exist a fully developed velocity profile. Figure 4.1 shows variation of the boundary layer due to wall shear stress in the flow direction of a pipe from the entrance region into a fully developed region. In laminar flow the hydrodynamic entry length is given by $L_h \cong 0.05\mathrm{Re}D$.

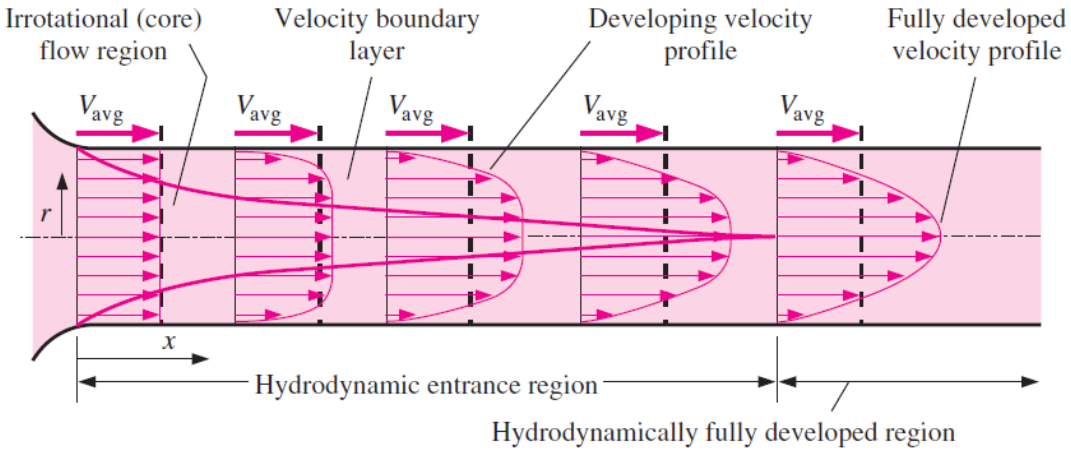

Figure: 4.1 Variation of boundary layer from the pipe entrance. Source: Fluid dynamics (2005)

The shear stress at the pipe wall is proportional to the slope of velocity profile which remains unchanged in the hydro dynamically fully developed region therefore wall shear stress is highest at the pipe inlet where thickness of boundary layer is small and decreases gradually to a fully developed value while pressure drop is higher at the entrance of a pipe. Placing the DCR at a fully developed region ensures that fluid flow at that section of the pipe is laminar during entry into the DCR insert, therefore providing a uniform velocity input in both the cone's inlet as well as at the slits. In this case swirl flow generated by the slits will have stronger vortices which ensure better heat transfer enhancement.

4.3 Simulation of fluid flow past a diverging conical ring insert

To determine the flow variables we simulate a physical situation by modeling a cylindrical tube with a diverging conical ring insert having two slits on opposite sides of the slant edge. A computer modeling software 'Solid works' is used to simulate the flow by construction of pipe geometry to demonstrate a case of hot water flowing in a horizontal pipe. The following physical properties of water at a temperature of 373 K are used in the simulation: density at 957.9 kg/m^3, specific heat (C_p) is 4217 kJ/Kg.K, thermal conductivity (k) is 0.679 W/m.k, dynamic viscosity is 2.82 X 10^{-4} Kg/m.s and a volume expansion coefficient is 7.5 X 10^{-4} k^{-1}. A cross section diagram at the DCR insert outlet displays the path lines indicating a multi-longitudinal vortex pair generated by one slit. As illustrated in Figure 4.2 with a key on the colour code provided on the left side showing values of pressure.

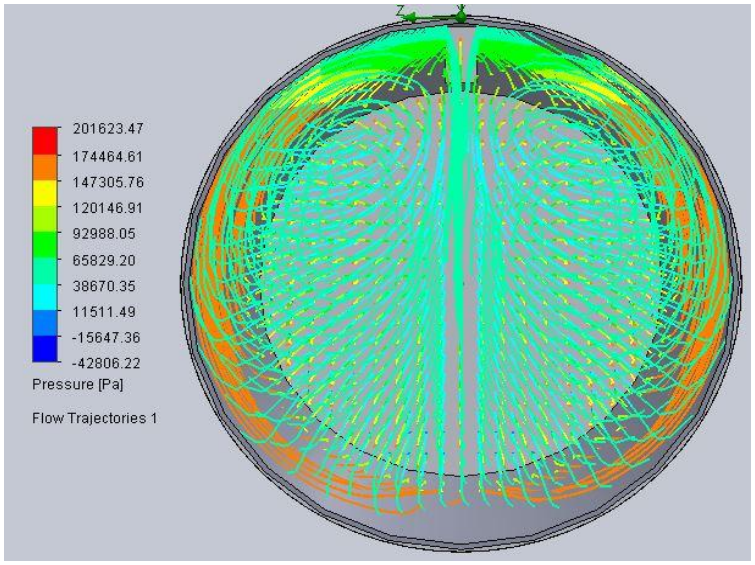

Figure 4.2: Pressure distribution of fluid flow generated by one slit

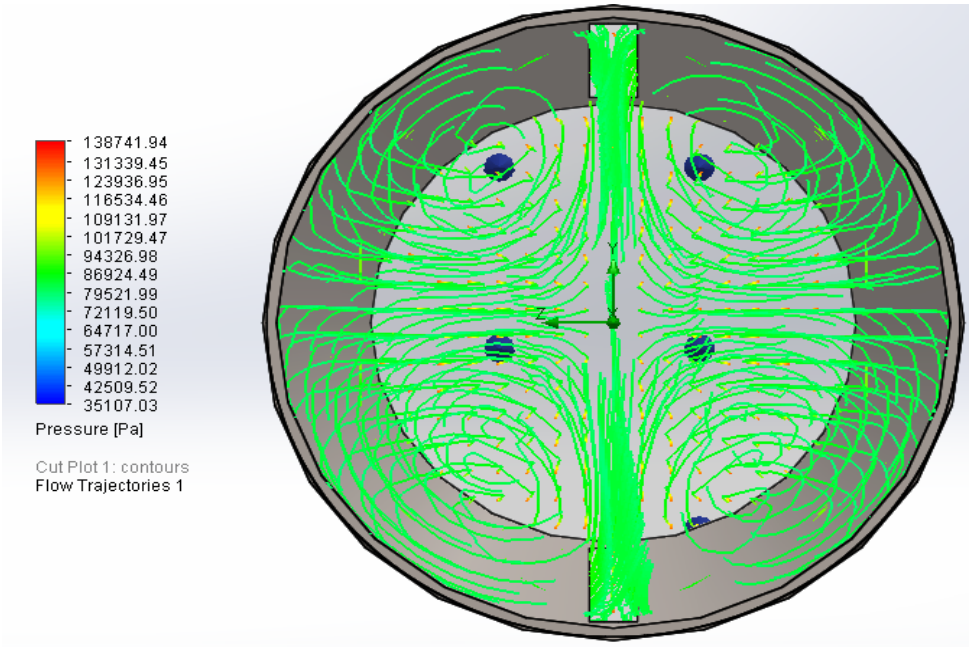

Figure 4.3: Pressure distribution for fluid flow generated by two slits

The uniform green colour implies that pressure is the same at the cross section but the fluid exhibits a pair of multi longitudinal vortices.

A cross section diagram at the DCR insert outlet displays the path lines indicating two multi-longitudinal vortex pairs generated by the two slits. As illustrated in Figure 4.3 with a key on the colour code provided on the left side showing values of pressure.

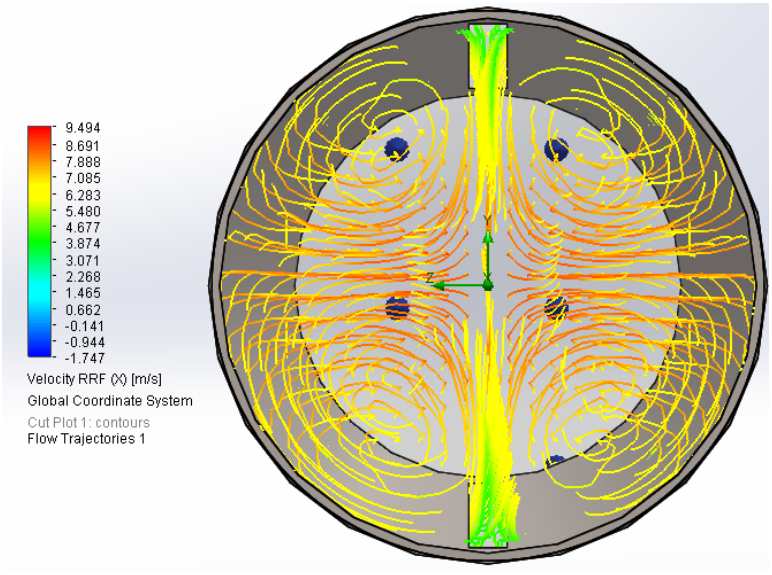

Figure 4.4: Fluid velocity vectors forming two pairs of multi– longitudinal vortices

The illustration on Figure 4.4 shows the velocity path lines of the fluid at different positions in a given cross section at the DCR insert outlet. The colour code is provided in a key on the left hand side.

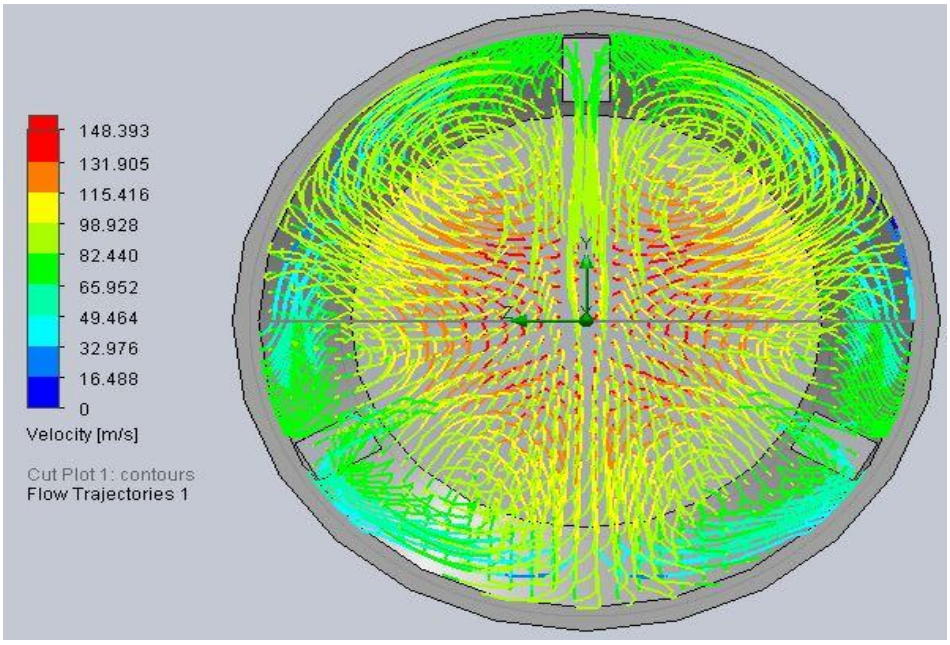

Figure 4.5: Fluid velocity vectors generated by three slits

The fluid velocity is highest at the regions with orange and lowest where it is green in colour. Figure 4.5 show a case of three slits indicating velocity variations.

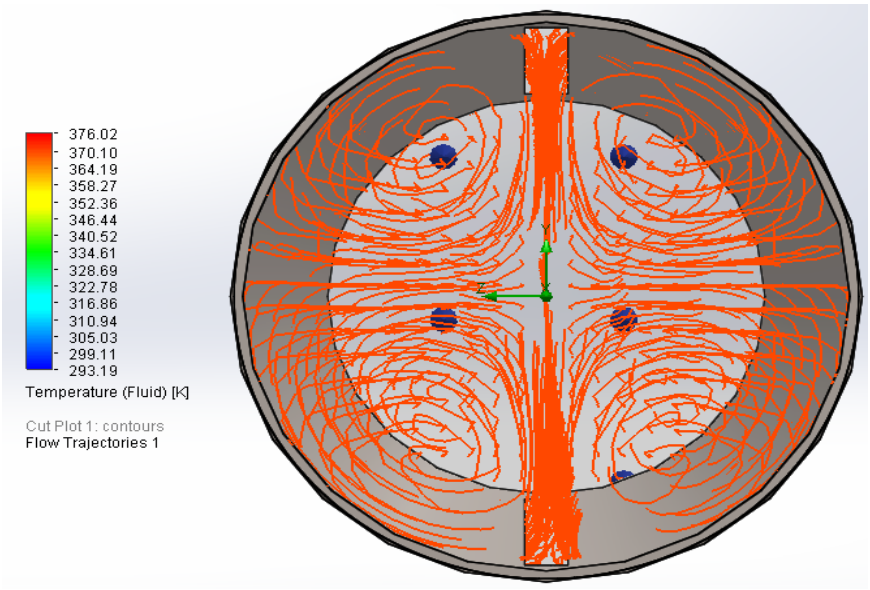

Figure 4.6: Temperature variation along path lines of multi longitudinal vortices

The diagram on Figure 4.6 shows the values of temperature obtained at the same cross section used to observe pressure and velocity of the fluid to establish fluid synergy that enables heat transfer enhancement.

The uniform red colour show uniform temperature along the cross section. The number of vortex pairs is equal to the number of slits on the cone and this causes a mixture of inner core and near wall fluid which enhances heat transfer. Different patterns of multi longitudinal vortex pairs are then compared with the level of heat transfer enhancement.

4.4 Synergy of physical quantities

The field synergy principle has two types of applications: first it facilitates in having a better understanding of known heat transfer phenomena or experimental

results and second it is to guide the development of novel enhancement of heat transfer structures. The velocity field in a duct flow can be varied by changing the duct configuration. For example vortices occurring when the flow goes through a specially designed alternatively twisted elliptic tube give comparative results for the Nusselt number and friction factor between the test results for water. Heat enhancement can be made with a reasonable increase in friction and for laminar flow cases the ratio of heat transfer enhancement is even much larger than that of the friction factor increase. Vortices significantly improve the synergy between the velocity and the temperature field. Inserts are used in a circular tube to increase the uniformity of temperature profile which improves the field synergy between the velocity and heat flow fields. The field synergy principle is used in enhancing our understanding of the heat transfer phenomena. It also provides a rule to improve any surface structure for a better heat transfer performance. There are several ways to improve the synergy between velocity and temperature gradient (heat flow fields) including varying the velocity and temperature boundary conditions.

4.5 Comparing vortices generated by insert with theoretical models

Numerical solutions of the field synergy equation for laminar convection heat transfer in a straight circular tube together with other governing equations indicate that multi- longitudinal vortex flow is the best way for heat transfer enhancement in laminar convection on cylindrical pipes. The swirl flow field with multi-longitudinal vortices has better heat transfer capability than a bare tube without additional volume force and its heat intensity grows much faster than the flow resistance increase.

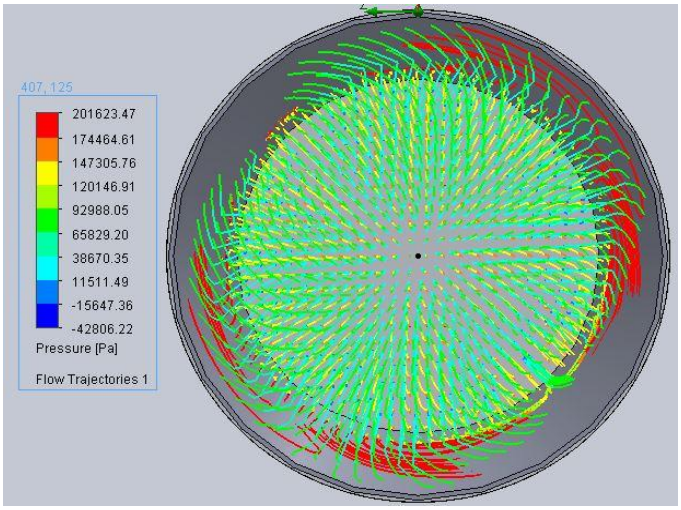

Figure 4.7: Flow velocity vector generated by a turbulator with no slits

This flow simulation in Figure 4,7 compares favorably with research work done using other methods has illustrated in Figure 4.8 below.

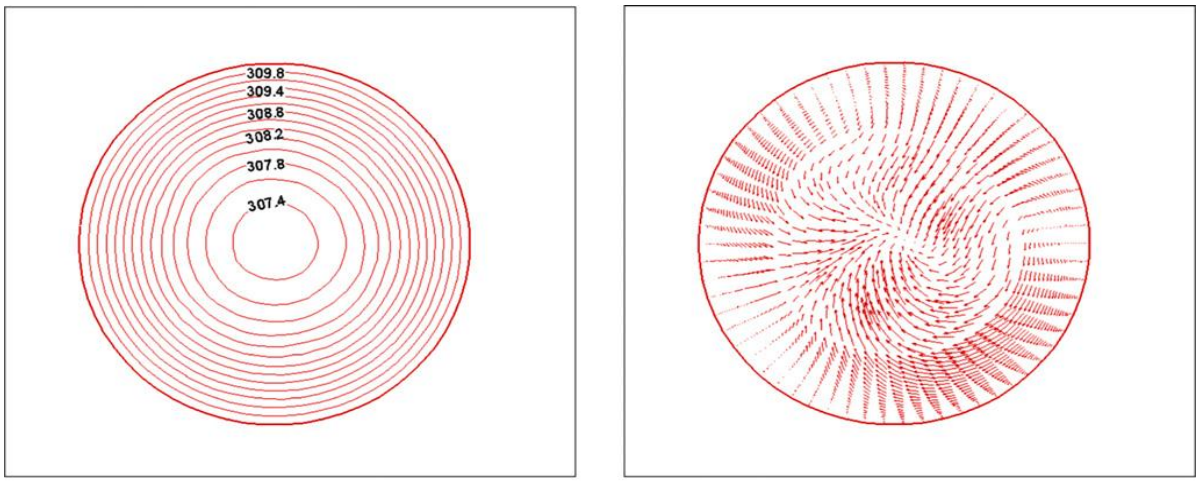

(a) Temperature field (b) Velocity vector

Figure 4.8 a and b: Temperature field and a flow velocity vector for a single vortex

Source: **Liu et al (2012).**

This kind of flow field is consistent with the principle of heat transfer enhancement in core flow of the tube proposed by Liu et al. (2012) who intended to design a flow field in which disturbance in the boundary flow is kept at relatively lower level while disturbance in the core is enhanced greatly.

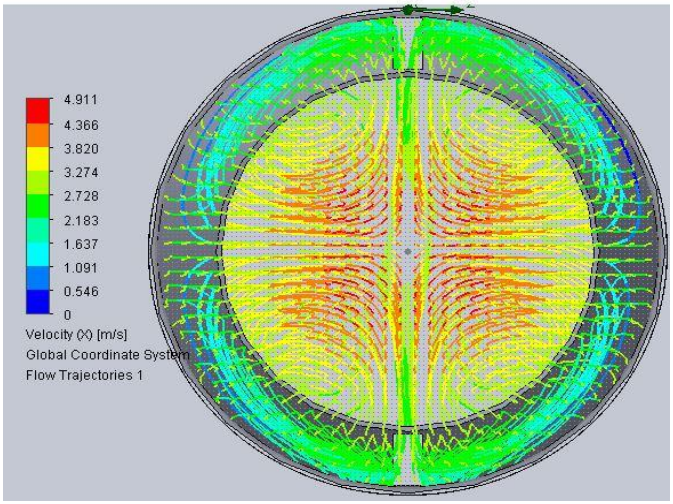

Figure 4.9: **Flow circulation by a turbulator with two slits**

The colours in Figure 4.9 illustrate variation of velocity along the path lines showing faster movements at the pipes centre line where the two pairs of multi-longitudinal vortices meet which agrees Figure 4.10 below.

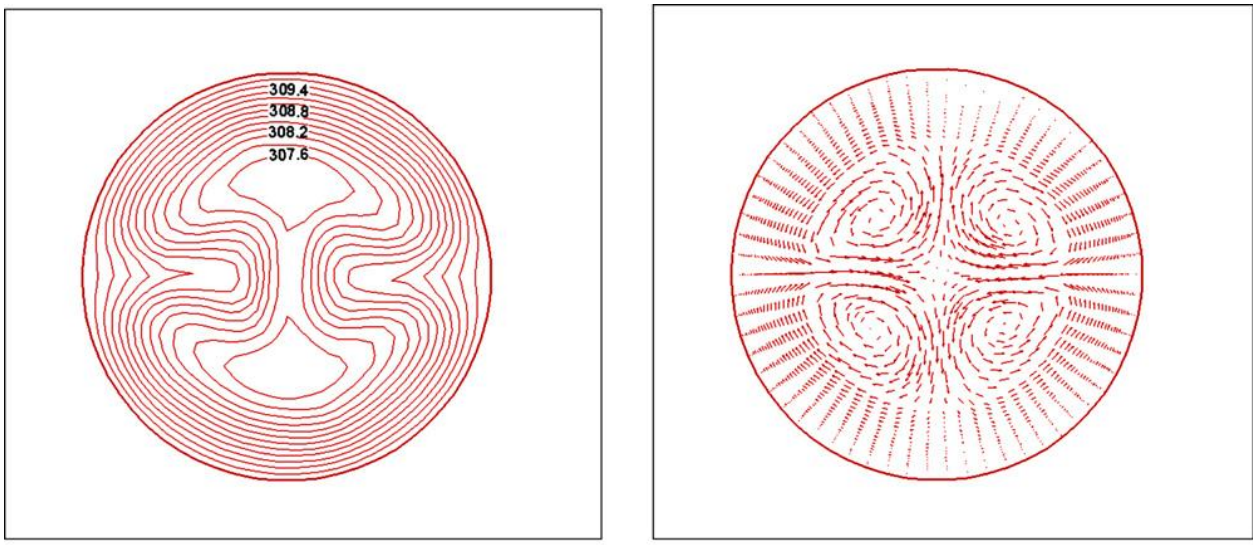

(a) Temperature field (b) Velocity vector

Figure 4.10 a and b: Temperature field and flow field structure with two multi-longitudinal vortex pairs. **Source: Liu et al (2012)**

The vortices are distributed symmetrically around a central part of the tube area such that velocity gradient near the tube wall is not increased to a large extent. This is indicated in the Figures 4.7 and 4.9 which are comparing simulation in this research work and those done by *Liu et al.* (2012). In practical applications when inserts are adopted to obtain longitudinal swirl flow with multiple- vortices in a tube, friction resistance will be much higher due to longitudinal vortices generated which decay gradually in stream wise direction due to viscous shear force.

4.6 Diverging cylindrical pipe internal surface friction

A diffuser is an expanding duct whose primary objective is to recover fluid static pressure from a fluid stream while reducing the flow velocity. A portion of the kinetic energy in the flow is converted into potential energy for fluid pressure. In a diffuser the pressure gradient opposes the flow and as a result fluid in the boundary layer decelerates and thickens rapidly. If it separates from the walls large unsteady eddies are formed that block the diffuser flow. Separation of fluid from diffuser walls is called a stall and it degrades diffuser pressure recovery which limits performance. It is largely governed by boundary layer growth and onset of separation influenced by flow profile whose cross section area at the entrance is A_1 and at the exit A_2. For a specific case of steady flow in a diffuser the loss coefficient is defined has

$$K = \frac{2g\Delta H}{u^2} \tag{4.1}$$

and the value of the diffuser efficiency is

$$\xi = 1 - \frac{K}{\left\{1 - \frac{A_2^2}{A_1^2}\right\}}. \tag{4.2}$$

This efficiency would be zero if there is no pressure recovery and unity in the case of full pressure recovery. Figure 4.11 shows the variation of diffuser performance

efficiency against the angle of divergence which establishes that maximum output is obtained when a cone has an angle of 7^0 at the vertex.

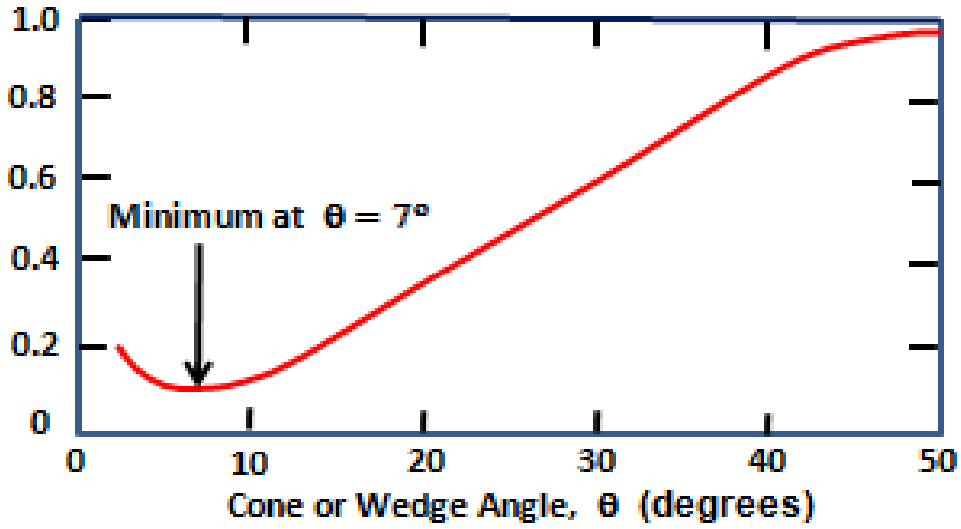

Figure 4.11: Diffuser performance efficiency against the cone angle of divergence.

Source: Idelchik (1994).

In practice the actual efficiency ξ depends on the diffuser geometry and sometimes other factors such as uniformity of the entering flow. Larger angles lead to flow separation within the diffuser which causes large viscous losses. Smaller angles imply diffusers become too long leading to larger viscous wall friction losses. The basic data set that is needed by a fluids engineer is knowledge of the loss coefficients for a straight cylindrical pipe. In this instance the loss coefficient will clearly be proportional to the length of the pipe and therefore we need to define a loss coefficient per unit length given by $\frac{K}{L}$ where L is the pipe length. But in order to keep the quantity dimensionless we need to multiply this by a length and the obvious choice is the pipe diameter, d. The resulting loss coefficient is called the friction factor f which is defined has

$$f = \frac{Kd}{L} = \frac{2gd\Delta H}{u^2 L} \quad . \tag{4.3}$$

Where u is the volume averaged fluid velocity equal to the volume flow rate divided by the internal cross sectional area of the pipe.

The friction factor is a function of Reynolds number for flow in the pipe is $\mathrm{Re} = \frac{ud}{\vartheta}$.

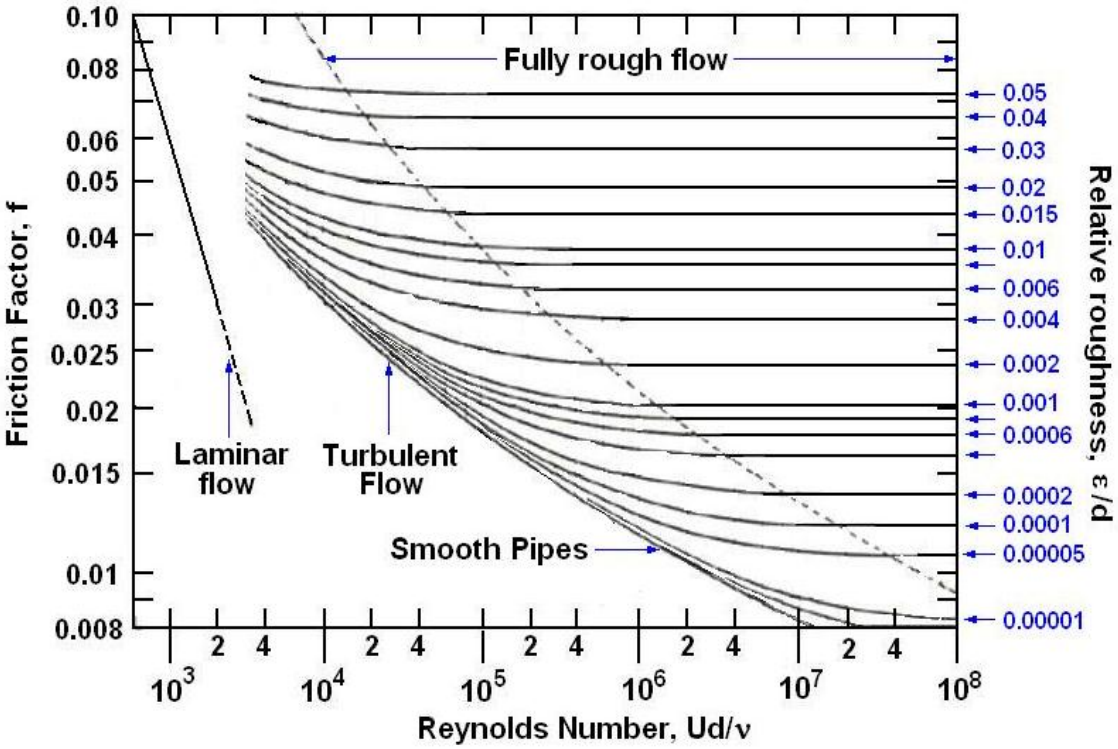

Figure 4.12: Moody diagram for pipe friction factor as a function of Reynolds number. **Source: Lewis F. Moody (1944).**

In addition f depends on nature of flow in the pipe, whether it is laminar or turbulent. The friction factor also depends on roughness of the interior surface of a pipe. This information is contained in a chart known as a Moody diagram whose content is in Figure 4.12 showing the friction factor plotted against the pipe Reynolds number. To help determine the best values of Re to perform the fluid flow past the DCR insert in a cylindrical tube. The diagram is semi empirical based on principles of research in measurement of surface roughness and understanding of velocity distribution within a boundary layer.

It is regarded as a temporary solution until sufficient further scientific advances are made but it continues to fulfill the function that Moody attributed to the graph. 'A simple means of estimating the friction factor'. It has relevance for a very broad range of situations from flow in micro tubes to flow in large pipe lines or tunnels. The Moody diagram helps in determining the range of Reynolds number at which the flow can remain laminar from the inlet to a DCR insert at a specific value of the friction factor.

4.7 Coefficient of skin friction

The resistance coefficient inside the tube is determined by skin friction

$$C_f = \frac{\tau}{\frac{1}{2}\rho u^2}. \tag{4.4}$$

Where $C_f = \frac{\mu \frac{\partial u_z}{\partial r}}{\frac{1}{2}\rho u^2} = \frac{2\mu\, a}{\rho u^2}$ given $a = \frac{F}{m} = \frac{F}{\rho \pi\, r^2 L} = \frac{F}{\rho A L}$

$$C_f = \frac{\mu}{\rho u L}\frac{2F}{\rho u A} = \frac{1}{\mathrm{Re}}\frac{F}{A}\frac{2}{\rho u} = \frac{2}{\rho \mathrm{Re}}\frac{P}{u_z}$$

In discrete form it becomes

$$C_{f\,i,k} = \frac{2}{\rho \mathrm{Re}}\left[\frac{P_{i,k}}{u_{z_{i,k}}}\right]. \tag{4.5}$$

From which a graph is be plotted to show variation of the coefficient of skin friction with pressure gradient at fixed Re Number. To determine the fluid friction characteristic in a cylindrical pipe, the skin friction is plotted against Re. Skin friction is defined as the ratio of wall shear stress to dynamic pressure.

4.8 Boundary conditions

Considering the theory of diffuser performance, when using hot water the flow parameters have been selected to ensure laminar flow during simulation as follows: at the pipe inlet axial velocity $u_z = 4\ m/s$ while some distance into the pipe where there is no entrance effect at the diverging conical ring insert inlet $u_z = 6\ m/s$, inlet pressure is P_0 =110,000 Pa and temperature is T_0=370 K. While Reynolds number (Re) satisfies the inequality 1000 < Re < 4000, pressure coefficient (P_C) = 6.5 and Prandtl number (Pr) = 1.75. Figure 4.13 shows the position of a conical ring insert in the cylindrical tube with the coordinate axis indicated. The DCR insert inlet radius is 18 mm and the outlet radius is 25mm, with the length along the z axis as 70 mm, to provide an angle that is less than 15^0 at the vertex and an half angle of 7^0 between the horizontal axis and the slant edge.

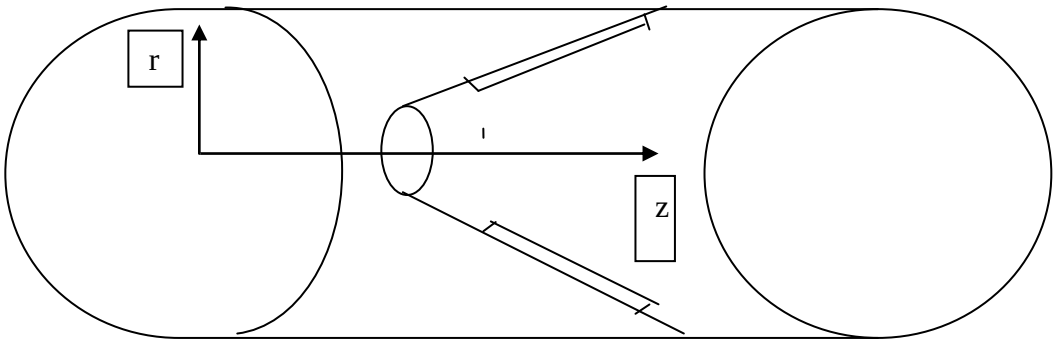

Figure 4.13: **Schematic diagram of a diverging conical ring insert with two slits**

Momentum flux on the fluid force through the ring at the DCR is obtained by

$$m = 2\pi\rho\int_0^\infty u^2 r dr \tag{4.6}$$

The flux is a constant and on the surface of a conical insert temperature

$$T_{\text{hot water}} = T_{\text{wall.}} \tag{4.7}$$

Simulating the fluid flow using solid works, a computational fluid dynamics software programme, reveals that the velocity profile before and after the DCR insert is as indicated in Figure 4.14 showing a rise of velocity within the insert and a flow separation thereafter in the region appearing blue past the insert.

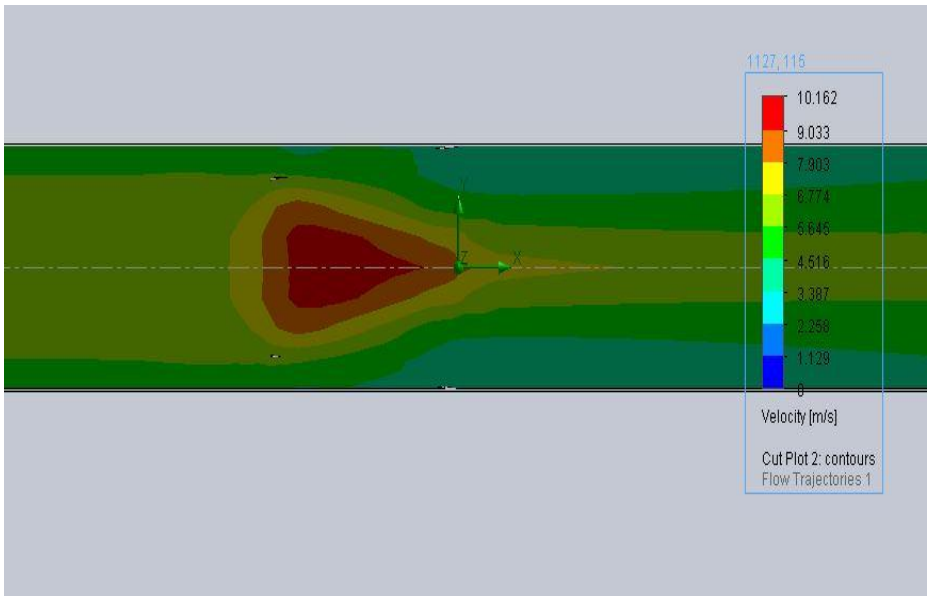

Figure 4.14: **Fluid velocity in the neighborhood of a DCR insert.**

Observation of the region along the centre line at a radial distance of 1.8 cm which is equivalent to the DCR insert inlet radius the fluid flow is laminar. The fluid separation occurring as the fluid exits the DCR insert does not affect the inner region of the fluid flow and agrees with the theory of a divergent diffuser.

4.9 Variation of pressure along the tube.

Results are obtained using a 4 m long tube of internal radius 0.05 m, to compare what happens when the diverging conical ring insert has different number of slits if it is placed in the tube a distance 3.5 m from the entrance.

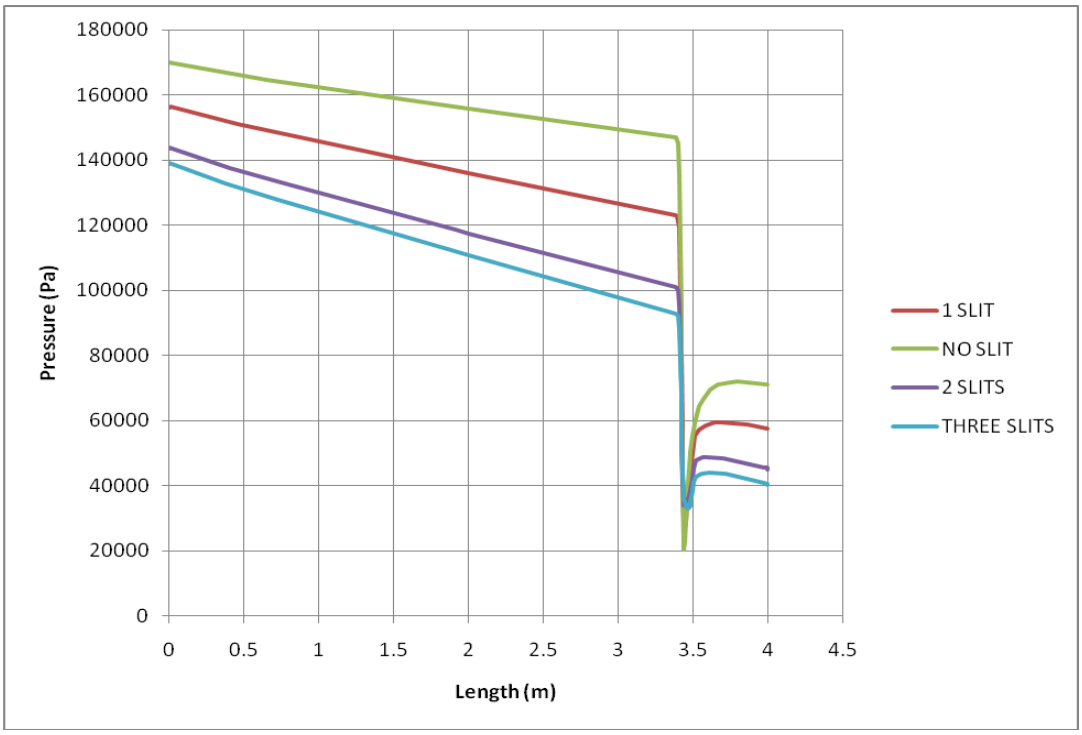

Figure 4.15: **Graph showing pressure variation due to number of slits on an insert.**

Figure 4.15 shows pressure change for four distinct cases of diverging conical insert. With no slit, one, two and three slits providing pressure variations with distance along the pipe axial plotted for values along a path at the pipe's centre line. A pressure drop is observed in the four different cases with an abrupt drop noted at the DCR insert, although a higher pressure drop is noted when the number of slits decreases.

The pressure drop is observed at the DCR insert inlet which is placed a distance of 3.5 m from the pipe inlet. To avoid the pipe entrance effect in a cylindrical pipe to ensure the flow is laminar while the fluid passes through the DCR insert. An increase in the number of slits allows more fluid flow in the pipe hence low pressure due to an increase in effective cross section area allowing the fluid to pass through.

4.10 Determining coefficient of skin friction

The simulation provides horizontal velocity components u_z and pressure P at specific radial distance $r_{i,k}$ along the pipe's centre line. The horizontal components of axial velocities are obtained along the lines marked in Figure 5.1 with plains chosen before fluid enters the DCR insert, when within the insert and after it passes through.

Table 4.1: **Variation of horizontal distance with pressure and horizontal velocity component**

Horizontal distance from pipe inlet (m)	Velocity $u_{z_{i,k}}$	Pressure $P_{i,k}$	$\frac{P_{i,k}}{u_{z_{i,k}}}$
6.50	6.394	107914.51	16877.4
6.55	6.394	107826.91	16863.76
6.60	6.394	107739.31	16850.06
6.65	6.394	107651.70	16836.36
6.70	6.394	107564.11	16822.66
6.75	6.394	107476.49	16808.95
6.80	6.395	107388.89	16792.63
6.85	6.395	107301.29	16778.93
6.90	6.373	107213.69	16759.99
6.95	8.501	93609.95	11011.64
7.00	8.338	83779.35	10047.89
7.05	6.738	86570.29	12848.07
7.10	6.418	86936.02	13545.65
7.15	6.233	87011.55	13959.82
7.20	6.104	86867.07	14231.17
7.25	6.059	86722.6	14313.02
7.30	6.046	86578.13	14319.9
7.35	6.033	86433.65	14326.81

7.40	6.030	86244.64	14302.59
7.45	6.035	86055.63	14259.42
7.50	6.040	85866.61	14216.32
7.55	6.045	85677.60	14173.3
7.60	6.051	85488.59	14128.01
7.65	6.064	85299.58	14066.55
7.70	6.078	85110.57	14003.05

Plotting the horizontal distance in the cylindrical pipe against a quotient of pressure divided by horizontal velocity a graph is obtained as shown below in Figure 4.16. The analysis is done from a distance of 6.5 m to avoid the hydrodynamic entrance region effect, where viscous shearing forces are felt. The part beyond an entrance region has velocity profile fully developed and remains unchanged with the temperature remaining constant.

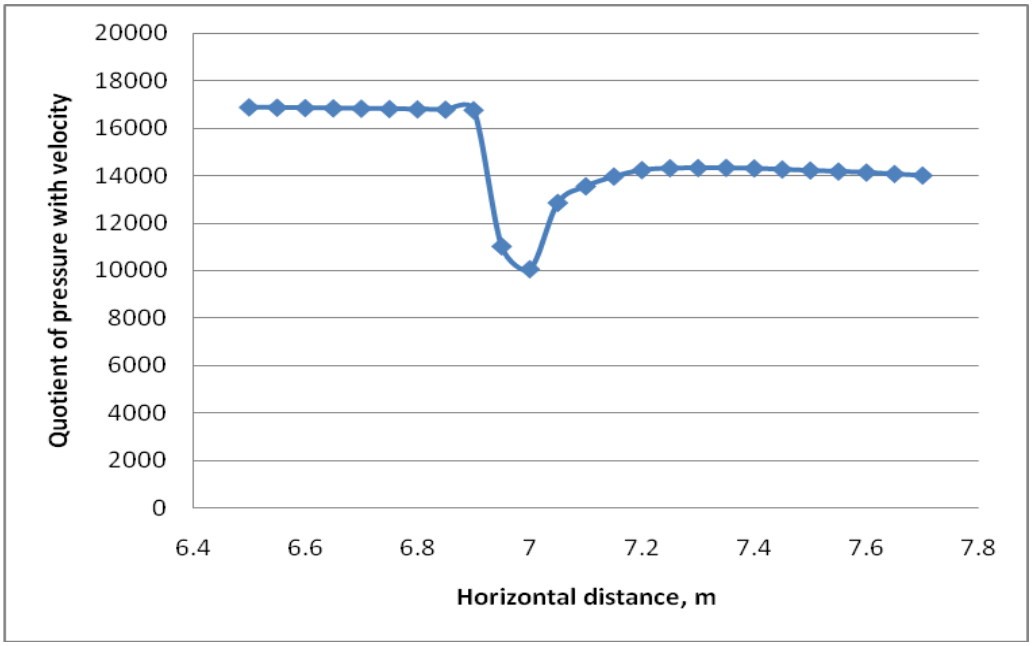

Figure 4.16: **Graph showing quotient of pressure with horizontal velocity component against horizontal distance**.

This observation describes the variation of coefficient of skin friction along the pipe in presence of a turbulator. An abrupt change of velocity and a drop in pressure are noted at the point where a DCR insert is placed on the pipe, which also generates the heat transfer enhancement.

Table 4.2: **Variation of Reynolds number with coefficient of skin friction**

Reynolds number (Re)	Re ρ	Coefficient of Skin friction (C_f)	
		After insert	Before insert
1000	957,900	0.02923	0.03445
1500	1,436,850	0.01948	0.02297
2000	1,915,800	0.01461	0.01723
2500	2,394,750	0.01169	0.01378
3000	2,873,700	0.00974	0.01148
3500	3,352,650	0.00835	0.00984

With the quotient considered to be 16500 before insert and have stabilized at 14,000 after fluid passes the insert then the coefficient of skin friction is determined on a range of Reynolds number as tabulated in Table 4.2 above. From equation 4.5 the coefficient of skin friction is determined which provide comparison of Reynolds number to skin friction has shown in Figure 4.17 below indicating that values of coefficient of skin friction after the fluid passes through the DCR insert are lower.

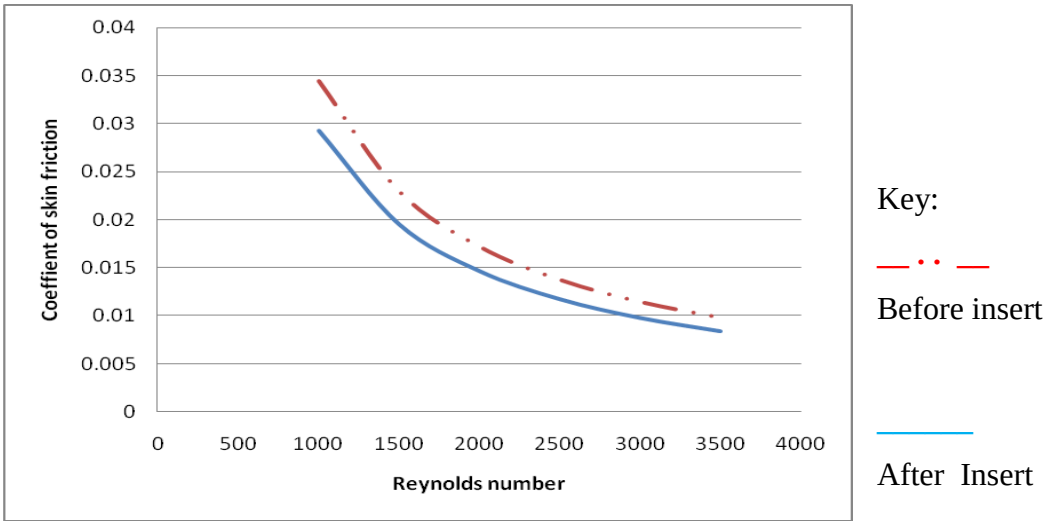

Figure 4.17: **A graph of coefficient of skin friction against Reynolds number**

The fluids coefficient of skin friction reduces with increase in Reynolds number or decreasing value of the quotient of fluid pressure to horizontal velocity component.

4.11 Grid points in the fluid flow domain

Given that $r_i = i\Delta r$ and $z_k = k\Delta z$ representing a plane along the cylindrical tube such that (i, k) = (0,0) is at the centre of the inlet on a DCR insert. Figure 4.6 below shows the position of each point in the neighbourhood of (i,k) which are required in the numerical determination of solutions to the discretized equation.

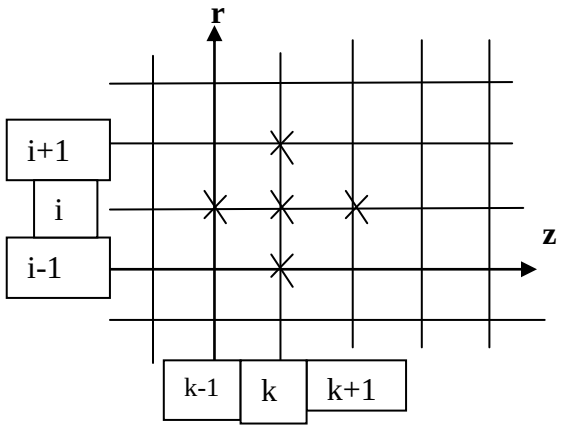

Figure 4.18: **Discrete grid points.**

Figure 4.18 illustrates a finite difference grid to determine the mesh points of flow parameters, each nodal point is identified by an ordered pair (i, k) that defines a specific location.

4.12 Discretization of governing equations

The finite central difference method is applied since it provides more accurate approximation of values at the middle of a given set of data on a grid. To enable us solve the nonlinear partial differential equations obtained after non dimensionalising the governing equations and writing variables in discrete form to obtain.

Continuity equation (3.32) in discrete form is

$$\frac{u_{r_{i,k}}}{r_{i,k}} + \left(\frac{u_{r_{i+1,k}} - u_{r_{i-1,k}}}{2\Delta r} \right) + \left(\frac{u_{z_{i,k+1}} - u_{z_{i,k-1}}}{2\Delta z} \right) = 0$$

$$\left(\frac{u_{z_{i,k+1}} - u_{z_{i,k-1}}}{2\Delta z} \right) = \left(\frac{u_{r_{i-1,k}} - u_{r_{i+1,k}}}{2\Delta r} \right) - \frac{u_{r_{i,k}}}{r_{i,k}} \tag{4.8}$$

The radial momentum equation (3.33) in discrete form is

$$u_{r_{i,k}} \left(\frac{u_{r_{i+1,k}} - u_{r_{i-1,k}}}{2\Delta r} \right) + u_{z_{i,k}} \left(\frac{u_{r_{i,k+1}} - u_{r_{i,k-1}}}{2\Delta z} \right) = -P_C \left(\frac{p_{i+1,k} - p_{i-1,k}}{2\Delta r} \right) + \frac{1}{\mathrm{Re}} \left(\frac{u_{r_{i-1,k}} - 2u_{r_{i,k}} + u_{r_{i+1,k}}}{(\Delta r)^2} + \frac{u_{r_{i+1,k}} - u_{r_{i-1,k}}}{2r_{i,k}\Delta r} + \frac{u_{r_{i,k-1}} - 2u_{r_{i,k}} + u_{r_{i,k+1}}}{(\Delta z)^2} \right)$$

$$u_{z_{i,k}} \left(\frac{u_{r_{i,k+1}} - u_{r_{i,k-1}}}{2\Delta z} \right) = -P_C \left(\frac{p_{i+1,k} - p_{i-1,k}}{2\Delta r} \right) + \frac{1}{\mathrm{Re}} \left(\frac{u_{r_{i-1,k}} - 2u_{r_{i,k}} + u_{r_{i+1,k}}}{(\Delta r)^2} + \frac{u_{r_{i+1,k}} - u_{r_{i-1,k}}}{2r_{i,k}\Delta r} + \frac{u_{r_{i,k-1}} - 2u_{r_{i,k}} + u_{r_{i,k+1}}}{(\Delta z)^2} \right) - u_{r_{i,k}} \left(\frac{u_{r_{i+1,k}} - u_{r_{i-1,k}}}{2\Delta r} \right)$$

$$u_{z_{i,k}} = \left(\frac{2\Delta z}{u_{r_{i,k+1}} - u_{r_{i,k-1}}} \right) \left\{ -P_C \left(\frac{p_{i+1,k} - p_{i-1,k}}{2\Delta r} \right) + \frac{1}{\mathrm{Re}} \left[\left(\frac{u_{r_{i-1,k}}}{(\Delta r)^2} + \frac{\mathrm{Re} u_{r_{i,k}} u_{r_{i-1,k}}}{2\Delta r} - \frac{u_{r_{i-1,k}}}{2r_{i,k}\Delta r} \right) - \left(\frac{2u_{r_{i,k}}}{(\Delta r)^2} + \frac{2u_{r_{i,k}}}{(\Delta z)^2} \right) + \left(\frac{u_{r_{i+1,k}}}{(\Delta r)^2} + \frac{u_{r_{i+1,k}}}{2r_{i,k}\Delta r} - \frac{\mathrm{Re} u_{r_{i,k}} u_{r_{i+1,k}}}{2\Delta r} \right) + \left(\frac{u_{r_{i,k-1}} + u_{r_{i,k+1}}}{(\Delta z)^2} \right) \right] \right\}$$

Therefore to obtain the horizontal velocity component requires the initial values of pressure and the radial velocity component to be known to solve the discrete equation.

$$u_{z_{i,k}} = \left(\frac{2\Delta z}{u_{r_{i,k+1}} - u_{r_{i,k-1}}} \right) \left\{ -P_C \left(\frac{p_{i+1,k} - p_{i-1,k}}{2\Delta r} \right) + \frac{1}{\mathrm{Re}} \left[\left(\frac{1}{(\Delta r)^2} + \frac{\mathrm{Re} u_{r_{i,k}}}{2\Delta r} - \frac{1}{2r_{i,k}\Delta r} \right) u_{r_{i-1,k}} - \frac{2u_{r_{i,k}}}{(\Delta r)^2} + \left(\frac{1}{(\Delta r)^2} + \frac{1}{2r_{i,k}\Delta r} - \frac{\mathrm{Re} u_{r_{i,k}}}{2\Delta r} \right) u_{r_{i+1,k}} + \left(\frac{u_{r_{i,k-1}} - 2u_{r_{i,k}} + u_{r_{i,k+1}}}{(\Delta z)^2} \right) \right] \right\} \tag{4.9}$$

The axial momentum conservation equation (3.34) in discrete form is

$$u_{r_{i,k}} \left(\frac{u_{z_{i+1,k}} - u_{z_{i-1,k}}}{2\Delta r} \right) + u_{z_{i,k}} \left(\frac{u_{z_{i,k+1}} - u_{z_{i,k-1}}}{2\Delta z} \right) = -P_C \left(\frac{p_{i,k+1} - p_{i,k-1}}{2\Delta z} \right) + \frac{1}{\mathrm{Re}} \left(\frac{u_{z_{i-1,k}} - 2u_{z_{i,k}} + u_{z_{i+1,k}}}{(\Delta r)^2} + \frac{u_{z_{i+1,k}} - u_{z_{i-1,k}}}{2r_{i,k}\Delta r} + \frac{u_{z_{i,k-1}} - 2u_{z_{i,k}} + u_{z_{i,k+1}}}{(\Delta z)^2} \right) - \frac{1}{\mathrm{Re}} \left(\frac{u_{z_{i,k+1}} - u_{z_{i,k-1}}}{2r_{i,k}\Delta z} \right)$$

$$P_C\left(\frac{p_{i,k+1}-p_{i,k-1}}{2\Delta z}\right)=-u_{z_{i,k}}\left(\frac{u_{z_{i,k+1}}-u_{z_{i,k-1}}}{2\Delta z}\right)-u_{r_{i,k}}\left(\frac{u_{z_{i+1,k}}-u_{z_{i-1,k}}}{2\Delta r}\right)+$$

$$+\frac{1}{\mathrm{Re}}\left(\frac{u_{z_{i-1,k}}-2u_{z_{i,k}}+u_{z_{i+1,k}}}{(\Delta r)^2}+\frac{u_{z_{i+1,k}}-u_{z_{i-1,k}}}{2r_{i,k}\Delta r}+\frac{u_{z_{i,k-1}}-2u_{z_{i,k}}+u_{z_{i,k+1}}}{(\Delta z)^2}\right)-\frac{1}{\mathrm{Re}}\left(\frac{u_{z_{i,k+1}}-u_{z_{i,k-1}}}{2r_{i,k}\Delta z}\right)$$

$$P_C\left(\frac{p_{i,k+1}-p_{i,k-1}}{2\Delta z}\right)=\left(\frac{u_{r_{i,k}}}{2\Delta r}+\frac{1}{\mathrm{Re}(\Delta r)^2}-\frac{1}{2r_{i,k}\,\mathrm{Re}\,\Delta r}\right)u_{z_{i-1,k}}-\frac{2}{\mathrm{Re}}\left(\frac{1}{(\Delta r)^2}+\frac{1}{(\Delta z)^2}\right)u_{z_{i,k}}$$

$$+\left(\frac{1}{\mathrm{Re}(\Delta r)^2}+\frac{1}{2\,\mathrm{Re}\,r_{i,k}\Delta r}-\frac{u_{r_{i,k}}}{2(\Delta r)}\right)u_{z_{i+1,k}}-\left(\frac{u_{z_{i,k}}}{2\Delta z}-\frac{1}{\mathrm{Re}(\Delta z)^2}+\frac{1}{2r_{i,k}\,\mathrm{Re}\,\Delta z}\right)u_{z_{i,k+1}}+\left(\frac{u_{z_{i,k}}}{2\Delta z}+\frac{1}{2r_{i,k}\,\mathrm{Re}\,\Delta z}+\frac{1}{\mathrm{Re}(\Delta z)^2}\right)u_{z_{i,k-1}}$$

$$p_{i,k+1}=p_{i,k-1}+\frac{2\Delta z}{P_C}\left\{\left(\frac{u_{r_{i,k}}}{2\Delta r}+\frac{1}{\mathrm{Re}(\Delta r)^2}-\frac{1}{2r_{i,k}\,\mathrm{Re}\,\Delta r}\right)u_{z_{i-1,k}}-\frac{2}{\mathrm{Re}}\left(\frac{1}{(\Delta r)^2}+\frac{1}{(\Delta z)^2}\right)u_{z_{i,k}}+\left(\frac{1}{\mathrm{Re}(\Delta r)^2}+\frac{1}{2r_{i,k}\,\mathrm{Re}\,\Delta r}-\frac{u_{r_{i,k}}}{2\Delta r}\right)u_{z_{i+1,k}}\right.$$

$$\left.-\left[\frac{u_{z_{i,k}}}{2\Delta z}-\frac{1}{\mathrm{Re}(\Delta z)^2}+\frac{1}{2r_{i,k}\,\mathrm{Re}\,\Delta z}\right]u_{z_{i,k+1}}+\left[\frac{u_{z_{i,k}}}{2\Delta z}+\frac{1}{2r_{i,k}\,\mathrm{Re}\,\Delta z}+\frac{1}{\mathrm{Re}(\Delta z)^2}\right]u_{z_{i,k-1}}\right\}$$

(4.10)

The energy conservation equation (3.35) in discrete form

$$u_{z_{i,k}}\left(\frac{T_{i+1,k}-T_{i-1,k}}{2\Delta z}\right)+u_{r_{i,k}}\left(\frac{T_{i,k+1}-T_{i,k-1}}{2\Delta r}\right)=\frac{1}{\mathrm{Re}\,\mathrm{Pr}}\left[\frac{T_{i-1,k}-2T_{i,k}+T_{i+1,k}}{(\Delta r)^2}+\frac{1}{r_{i,k}}\left(\frac{T_{i+1,k}-T_{i-1,k}}{2\Delta r}\right)+\frac{T_{i,k-1}-2T_{i,k}+T_{i,k+1}}{(\Delta z)^2}\right]$$

$$\frac{u_{z_{i,k}}}{2\Delta z}\left(T_{i+1,k}-T_{i-1,k}\right)+\frac{u_{r_{i,k}}}{2\Delta r}\left(T_{i,k+1}-T_{i,k-1}\right)=\frac{1}{\mathrm{Re}\,\mathrm{Pr}}\left[\left(\frac{1}{(\Delta r)^2}-\frac{1}{2r_{i,k}\Delta r}\right)T_{i-1,k}-\left(\frac{2}{(\Delta r)^2}+\frac{2}{(\Delta z)^2}\right)T_{i,k}+\left(\frac{1}{(\Delta r)^2}+\frac{1}{2r_{i,k}\Delta r}\right)T_{i+1,k}+\frac{T_{i,k-1}+T_{i,k+1}}{(\Delta z)^2}\right]$$

$$\left(\frac{u_{r_{i,k}}}{2\Delta r}-\frac{1}{\mathrm{RePr}(\Delta z)^2}\right)T_{i,k+1}=\frac{1}{\mathrm{RePr}}\left[\left(\frac{1}{(\Delta r)^2}-\frac{1}{2r_{i,k}\Delta r}+\frac{u_{z_{i,k}}\mathrm{RePr}}{2\Delta z}\right)T_{i-1,k}-\left(\frac{2}{(\Delta r)^2}+\frac{2}{(\Delta z)^2}\right)T_{i,k}+\left(\frac{1}{(\Delta r)^2}+\frac{1}{2r_{i,k}\Delta r}-\frac{u_{z_{i,k}}\mathrm{RePr}}{2\Delta z}\right)T_{i+1,k}+\frac{T_{i,k-1}}{(\Delta z)^2}+\frac{u_{r_{i,k}}\mathrm{RePr}}{2\Delta r}T_{i,k-1}\right]$$

$$\left(\frac{\mathrm{RePr}(\Delta z)^2u_{r_{i,k}}-2\Delta r}{2(\Delta r)\mathrm{RePr}(\Delta z)^2}\right)T_{i,k+1}=\frac{1}{\mathrm{RePr}}\left[\begin{array}{l}\left(\frac{1}{(\Delta r)^2}-\frac{1}{2r_{i,k}\Delta r}+\frac{u_{z_{i,k}}\mathrm{RePr}}{2\Delta z}\right)T_{i-1,k}-\left(\frac{2}{(\Delta r)^2}+\frac{2}{(\Delta z)^2}\right)T_{i,k}+\\ \left(\frac{1}{(\Delta r)^2}+\frac{1}{2r_{i,k}\Delta r}-\frac{u_{z_{i,k}}\mathrm{RePr}}{2\Delta z}\right)T_{i+1,k}+\left(\frac{1}{(\Delta z)^2}+\frac{u_{r_{i,k}}\mathrm{RePr}}{2\Delta r}\right)T_{i,k-1}\end{array}\right]$$

$$T_{i,k+1}=\left(\frac{2(\Delta r)(\Delta z)^2}{u_{r_{i,k}}\mathrm{RePr}(\Delta z)^2-2\Delta r}\right)\left[\begin{array}{l}\left(\frac{1}{(\Delta r)^2}-\frac{1}{2r_{i,k}\Delta r}+\frac{u_{z_{i,k}}\mathrm{RePr}}{2\Delta z}\right)T_{r-1,k}-\left(\frac{2}{(\Delta r)^2}+\frac{2}{(\Delta z)^2}\right)T_{i,k}+\left(\frac{1}{(\Delta r)^2}+\frac{1}{2r_{i,k}\Delta r}-\frac{u_{z_{i,k}}\mathrm{RePr}}{2\Delta z}\right)T_{i+1,k}\\ +\left(\frac{1}{(\Delta z)^2}+\frac{u_{r_{i,k}}\mathrm{RePr}}{2\Delta r}\right)T_{i,k-1}\end{array}\right] \qquad (4.11)$$

Therefore determination of the flow variables can be predicted using the Navier-Stokes governing equations for fluid flow in a cylindrical pipe given in equations 3.32, 3.34 and 3.35 which are in non dimensional form after being discretized using central finite difference to obtain equations 4.8, 4.10 and 4.11 that are then coded using Matlab to generate graphs of pressure and temperature, in which the Reynolds number can be varied to determine the possible variations within the range of a laminar fluid flow. In the next chapter different maximum values of temperature obtained from the different number of slits are used to achieve the thermal performance factor to determine the most efficient number of symmetrically positioned slits on a conical ring insert.

CHAPTER FIVE

ANALYSIS AND DISCUSSIONS OF RESULTS

5.1 Introduction

Since the flow within the insert is not a perfect laminar flow, horizontal velocity components are determined using the CFD simulation software which is then used to solve the mathematical model provided. Where the discretized continuity equation is solved using a tri diagonal matrix whose right hand side is determined by obtaining differences in the horizontal velocities to compute using row reduction the radial velocity components to be used the pressure and temperature profiles

A theoretical determination of the heat transfer enhancement factor is obtained, then analysis is done for different set ups. The results obtained in simulation of this flow are presented graphically and discussed to ensure they are correctly interpreted. Other sets of results are also generated for different number of slits in the DCR insert to determine its effect on the rate of heat transfer enhancement.

5.2 Determination of pressure and temperature profiles

To determine the pressure and temperature profiles inside the conical ring insert values of horizontal velocity u_z are obtained along several plains perpendicular to the fluid flow direction which is the axial length along this tube as indicated in Figure 5.1. The horizontal axial velocity components are approximated using a computer simulation software ‘solid works’.

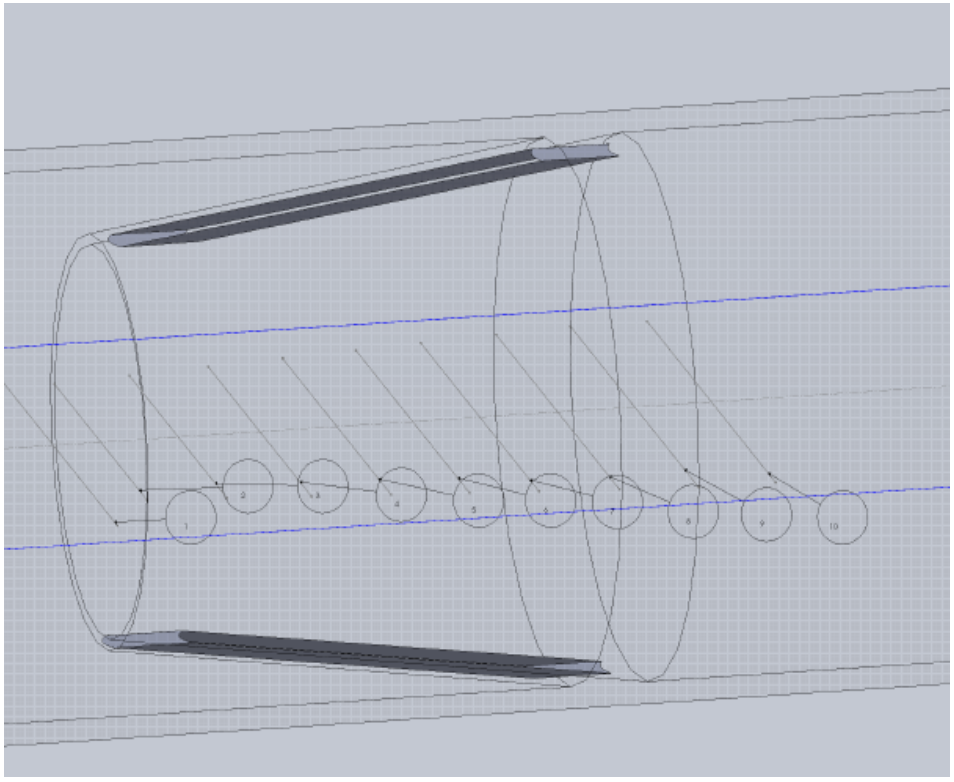

Figure 5.1: **Shows numbered lines along which velocities values Uz are obtained**

A second case of simulation done where a conical insert as a half angle of $\alpha = 5^0$ in a pipe of radius R= 2.5 cm and a vertex inlet of radius r = 1.8 cm, where the initial fluid velocity at the tube's inlet is u_z= 4 m/s is used and a pressure difference of 10 k Pa between pipe inlet and outlet of length 8 m. The simulation provides horizontal velocity components u_z at specific radial distance $r_{i,k}$ along the pipe with special preference given to the region inside the diverging conical ring insert. Three regions are selected at different radial distances within the conical insert as shown in Table 4.3 representing the tube's inner core (i = 0,1,2), the middle region (*i* = 8,9,10) and the inner path next to DCR insert inlet
(*i* = 16,17,18). The step size along the horizontal direction is Δz =0.01 and in the radial direction is

Δr =0.001. Fluid velocity values provided in a tabulated form is provided in Table 5.1. which is the axial velocity u_z along the axial planes.

Table 5.1: Axial velocity values of points across a DCR insert

Step size Δz=0.0	Radial distance Δi = 0.001m									
	≈0.00	0.00	0.00	…	0.00	0.00	0.01	…	0.01	0.01	0.01
	i=0	*i=1*	*i=2*		*i=8*	*i=9*	*i=10*		*i=16*	*i=17*	*i=18*
k=1	6.438	6.41	6.39		6.23	6.20	6.19		5.92	5.87	5.77
k=2	6.452	6.42	6.40		6.23	6.20	6.19		5.94	5.90	5.80
k=3	6.453	6.42	6.40		6.21	6.18	6.16		5.85	5.81	5.71
k=4	6.453	6.45	6.42		6.24	6.21	6.18		5.84	5.77	3.39
k=5	6.453	6.42	6.40		6.24	6.21	6.19		5.85	5.78	5.70
k=6	6.440	6.41	6.39		6.25	6.23	6.20		5.90	5.82	5.75
k=7	6.454	6.42	6.40		6.24	6.21	6.19		5.85	5.78	5.70
k=8	6.454	6.42	6.40		6.25	6.22	6.20		5.88	5.81	5.74
k=9	7.152	7.15	7.15		7.02	6.93	6.84		6.12	5.97	5.82
k=10	8.332	8.32	8.31		8.29	8.30	8.31		8.07	7.95	7.83
k=11	9.158	9.15	9.16		9.18	9.19	9.20		8.69	8.53	8.38
k=12	9.495	9.54	9.59		9.70	9.67	9.65		8.54	8.27	8.01
k=13	9.204	9.34	9.48		9.50	9.43	9.35		7.55	7.20	6.87
k=14	8.913	9.10	9.29		9.05	8.94	8.82		6.54	6.26	5.98
k=15	8.621	9.15	9.34		8.32	8.05	7.68		5.60	5.39	5.17
k=16	8.330	8.72	9.11		7.45	7.10	6.75		4.99	4.81	4.63
k=17	8.039	7.82	7.61		6.30	6.03	5.77		4.42	4.24	4.05
k=18	7.354	7.25	7.05		5.86	5.66	5.46		4.27	4.08	3.88
k=19	6.184	6.09	6.02		5.65	5.59	5.53		5.06	4.96	4.87
k=20	6.076	6.04	6.00		5.80	5.76	5.73		5.42	5.36	5.29
k=21	6.097	6.06	6.05		5.87	5.84	5.82		5.61	5.57	5.49

The horizontal components of axial velocities are obtained along the lines marked in Table 5.1 with some plains chosen before the fluid enters the DCR insert, when within the insert and after it leaves. Along each plain three sets of values are provided at equally spaced intervals from the centre line to the edge of the inlet of the DCR insert. This gives the values of axial velocity at the centre, middle and outer region of the fluid flow within the insert.

5.3 Solving the discretized equations

Using boundary conditions and non dimension numbers in the discretized governing equations for the flow of hot water in a cylindrical tube in the region just before and after the conical ring insert. If $\Delta z = 0.01$, $\Delta r = 0.001$, axial velocity at the tube inlet is $u_z = 4$ m/s and at the DCR insert inlet is $u_z = 6$ m/s rising due to the constriction which reduces the mass flow rate causing rise in velocity. In which the horizontal component starts reducing as radial velocity increases from zero and $r_{i,k}$ is the radial distance from the centre of the tube with a singularity existing at $r_{0,k}$. Parameters are predetermined at the centre line with boundary conditions $P_o=1.1x10^5$ Pa, T_o =370 K, 1000<Re<3000, Pr =1.75 and P_C = 6.5 then the governing equations are solved to obtain the various flow profiles.

Equation (4.9) is expressed has

$$u_{r_{i-1,k}} - \frac{2\Delta r u_{r_{i,k}}}{r_{i,k}} - u_{r_{i+1,k}} = \frac{\Delta r}{\Delta z}\left(u_{z_{i,k+1}} - u_{z_{i,k-1}}\right)$$

$$u_{r_{i-1,k}} - \frac{0.002 u_{r_{i,k}}}{r_{i,k}} - u_{r_{i+1,k}} = \frac{\Delta r}{\Delta z}(u_{z_{i,k+1}} - u_{z_{i,k-1}}) \qquad (5.1)$$

At the DCR insert inlet boundary values are estimated from a flow simulation using solid works. The equation is expressed as a tri diagonal matrix shown in Figure 5.2 which uses the coefficients occurring in the three middle terms of the matrix to obtain the radial velocities the matrix is solved using Matlab algorithm given in Appendix 1, to determine radial velocities which vary with radial distance. Values of u_z's provide for differences on the column in the right hand side of Equation (5.1) to be able to solve the tri-diagonal matrix to determine the value of u_r's. At the DCR insert inlet k = 0 for i=1 to i=18; then at

k =1 the rows are tabulated starting from i=1 to i=18 on the diverging conical ring insert where i= 0 is at the centre line of the pipe up to i =18 the inlets inner radius for each of values of k given upto k =21.

$$
\begin{bmatrix}
-2 & -1 & 0 & 0 & 0 & 0 & 0 & 0 & 0 & 0 & 0 & 0 & 0 & 0 & 0 & 0 & 0 & 0 \\
1 & -1 & -1 & 0 & 0 & 0 & 0 & 0 & 0 & 0 & 0 & 0 & 0 & 0 & 0 & 0 & 0 & 0 \\
0 & 1 & \frac{-2}{3} & -1 & 0 & 0 & 0 & 0 & 0 & 0 & 0 & 0 & 0 & 0 & 0 & 0 & 0 & 0 \\
0 & 0 & 1 & \frac{-1}{2} & -1 & 0 & 0 & 0 & 0 & 0 & 0 & 0 & 0 & 0 & 0 & 0 & 0 & 0 \\
0 & 0 & 0 & 1 & \frac{-2}{5} & -1 & 0 & 0 & 0 & 0 & 0 & 0 & 0 & 0 & 0 & 0 & 0 & 0 \\
0 & 0 & 0 & 0 & 1 & \frac{-1}{3} & -1 & 0 & 0 & 0 & 0 & 0 & 0 & 0 & 0 & 0 & 0 & 0 \\
0 & 0 & 0 & 0 & 0 & 1 & \frac{-2}{7} & -1 & 0 & 0 & 0 & 0 & 0 & 0 & 0 & 0 & 0 & 0 \\
0 & 0 & 0 & 0 & 0 & 0 & 1 & \frac{-1}{4} & -1 & 0 & 0 & 0 & 0 & 0 & 0 & 0 & 0 & 0 \\
0 & 0 & 0 & 0 & 0 & 0 & 0 & 1 & \frac{-2}{9} & -1 & 0 & 0 & 0 & 0 & 0 & 0 & 0 & 0 \\
0 & 0 & 0 & 0 & 0 & 0 & 0 & 0 & 1 & \frac{-1}{5} & -1 & 0 & 0 & 0 & 0 & 0 & 0 & 0 \\
0 & 0 & 0 & 0 & 0 & 0 & 0 & 0 & 0 & 1 & \frac{-2}{11} & -1 & 0 & 0 & 0 & 0 & 0 & 0 \\
0 & 0 & 0 & 0 & 0 & 0 & 0 & 0 & 0 & 0 & 1 & \frac{-1}{6} & -1 & 0 & 0 & 0 & 0 & 0 \\
0 & 0 & 0 & 0 & 0 & 0 & 0 & 0 & 0 & 0 & 0 & 1 & \frac{-2}{13} & -1 & 0 & 0 & 0 & 0 \\
0 & 0 & 0 & 0 & 0 & 0 & 0 & 0 & 0 & 0 & 0 & 0 & 1 & \frac{-1}{7} & -1 & 0 & 0 & 0 \\
0 & 0 & 0 & 0 & 0 & 0 & 0 & 0 & 0 & 0 & 0 & 0 & 0 & 1 & \frac{-2}{15} & -1 & 0 & 0 \\
0 & 0 & 0 & 0 & 0 & 0 & 0 & 0 & 0 & 0 & 0 & 0 & 0 & 0 & 1 & \frac{-1}{8} & -1 & 0 \\
0 & 0 & 0 & 0 & 0 & 0 & 0 & 0 & 0 & 0 & 0 & 0 & 0 & 0 & 0 & 1 & \frac{-2}{17} & -1 \\
0 & 0 & 0 & 0 & 0 & 0 & 0 & 0 & 0 & 0 & 0 & 0 & 0 & 0 & 0 & 0 & 1 & \frac{-1}{9}
\end{bmatrix}
\begin{pmatrix}
u_{r_{1,1}} \\ u_{r_{2,1}} \\ u_{r_{3,1}} \\ u_{r_{4,1}} \\ u_{r_{5,1}} \\ u_{r_{6,1}} \\ u_{r_{7,1}} \\ u_{r_{8,1}} \\ u_{r_{9,1}} \\ u_{r_{10,1}} \\ u_{r_{11,1}} \\ u_{r_{12,1}} \\ u_{r_{13,1}} \\ u_{r_{14,1}} \\ u_{r_{15,1}} \\ u_{r_{16,1}} \\ u_{r_{17,1}} \\ u_{r_{18,1}}
\end{pmatrix}
= \frac{1}{10}
\begin{pmatrix}
u_{z_{1,2}} - u_{z_{1,0}} \\ u_{z_{2,2}} - u_{z_{2,0}} \\ u_{z_{3,2}} - u_{z_{3,0}} \\ u_{z_{4,2}} - u_{z_{4,0}} \\ u_{z_{5,2}} - u_{z_{5,0}} \\ u_{z_{6,2}} - u_{z_{6,0}} \\ u_{z_{7,2}} - u_{z_{7,0}} \\ u_{z_{8,2}} - u_{z_{8,0}} \\ u_{z_{9,2}} - u_{z_{9,0}} \\ u_{z_{10,2}} - u_{z_{10,0}} \\ u_{z_{11,2}} - u_{z_{11,0}} \\ u_{z_{12,2}} - u_{z_{12,0}} \\ u_{z_{13,2}} - u_{z_{13,0}} \\ u_{z_{14,2}} - u_{z_{14,0}} \\ u_{z_{15,2}} - u_{z_{15,0}} \\ u_{z_{16,2}} - u_{z_{16,0}} \\ u_{z_{17,2}} - u_{z_{17,0}} \\ u_{z_{18,2}} - u_{z_{18,0}}
\end{pmatrix}
$$

Figure 5.2: **Tri diagonal matrix to determine radial velocities.**

Solution of the tri- diagonal matrix equation is used to solve Equation (5.2) to obtain the pressure profile in Figure 5.3, the algorithm used to obtain the pressure is given in Appendix 2. Given velocities in axial and radial directions obtained, which

are used with a step size in axial direction and radial distance from the pipes centre line.

$$p_{i,k+1} = p_{i,k-1} + \frac{2\times 0.01}{P_C}\left\{\left(\frac{u_{r_{i,k}}}{2(0.001)} + \frac{1}{\mathrm{Re}(0.001)^2} - \frac{1}{2r_{i,k}\,\mathrm{Re}(0.001)}\right)u_{z_{i-1,k}} - \frac{1}{\mathrm{Re}}\left[\frac{2}{(0.001)^2} + \frac{2}{(0.01)^2}\right]u_{z_{i,k}} + \right.$$

$$\left.\left(\frac{1}{\mathrm{Re}(0.001)^2} + \frac{1}{2r_{i,k}\,\mathrm{Re}(0.001)} - \frac{u_{r_{i,k}}}{2(0.001)}\right)u_{z_{i+1,k}} - \left(\frac{u_{z_{i,k}}}{2(0.01)} - \frac{1}{\mathrm{Re}(0.01)^2} + \frac{1}{2\mathrm{Re}(0.01)}\right)u_{z_{i,k+1}} + \left(\frac{u_{z_{i,k}}}{0.02} + \frac{1}{0.02\mathrm{Re}} + \frac{1}{\mathrm{Re}(0.01)^2}\right)u_{z_{i,k-1}}\right\}$$

$$p_{i,k+1} = p_{i,k-1} + \frac{0.02}{P_C}\left\{\left(\frac{500u_{r_{i,k}}}{1} + \frac{1x10^6}{\mathrm{Re}} - \frac{500}{r_{i,k}\,\mathrm{Re}}\right)u_{z_{i-1,k}} - \frac{1}{\mathrm{Re}}\left[2\times 10^6 + 2x10^4\right]u_{z_{i,k}} + \right.$$

$$\left.+\left(\frac{10^6}{\mathrm{Re}} + \frac{500}{r_{i,k}\,\mathrm{Re}} - \frac{u_{r_{i,k}}}{0.002}\right)u_{z_{i+1,k}} - \left(\frac{u_{z_{i,k}}}{0.02} - \frac{10^4}{\mathrm{Re}} + \frac{50}{\mathrm{Re}}\right)u_{z_{i,k+1}} + \left(50u_{z_{i,k}} + \frac{50}{\mathrm{Re}} + \frac{10^4}{\mathrm{Re}}\right)u_{z_{i,k-1}}\right\}$$

$$p_{i,k+1} = p_{i,k-1} + \frac{1}{50P_C}\left\{\left(500u_{r_{i,k}} + \frac{1{,}000{,}000}{\mathrm{Re}} - \frac{500}{r_{i,k}\,\mathrm{Re}}\right)u_{z_{i-1,k}} - \frac{2{,}020{,}000\,u_{z_{i,k}}}{\mathrm{Re}} + \left(\frac{1{,}000{,}000}{\mathrm{Re}} + \frac{500}{r_{i,k}\,\mathrm{Re}} - 500u_{r_{i,k}}\right)u_{z_{i+1,k}}\right.$$

$$\left.-\left(50u_{z_{i,k}} - \frac{9{,}950}{\mathrm{Re}}\right)u_{z_{i,k+1}} + \left(50u_{z_{i,k}} + \frac{10{,}050}{\mathrm{Re}}\right)u_{z_{i,k-1}}\right\}$$

(5.2)

The pressure profiles are obtained for various axial velocities at specific radial distance using Equation (5.2) with a fixed step size in the axial direction. The investigation as established that internal flow of the fluid within the conical insert is different from the region immediately after the insert. Within the diverging conical insert the higher the Reynolds number the higher the pressure. While immediately after it pass the insert the lower the Reynolds number the higher the fluid pressure as indicated in Figure 5.3 below.

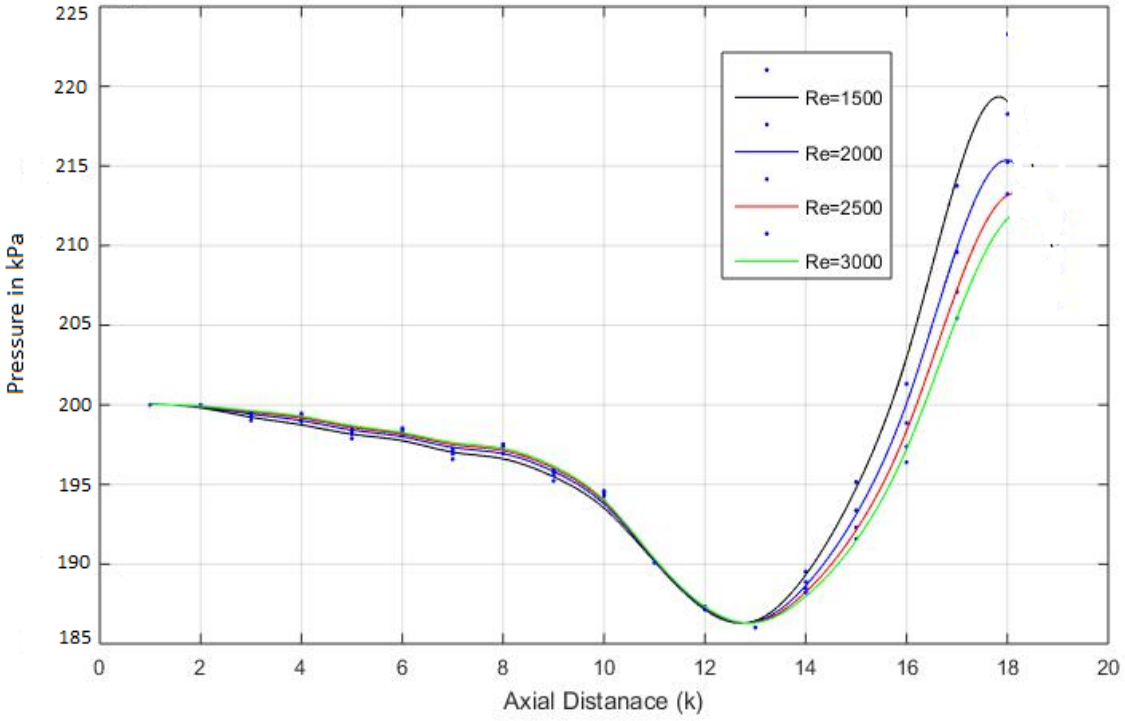

Figure 5.3: **Pressure variation along axial distance for 1500 ≤ Re ≤ 3000.**

The energy equation which is expressed in Equation (5.3) when substituted with the constants, non dimensional numbers and boundary conditions together axial velocity estimated by simulating in the flow determine temperature variations along the tube.

$$T_{i,k+1} = \left(\frac{2(\Delta r)(\Delta z)^2}{u_{r_{i,k}} \mathrm{RePr}(\Delta z)^2 - 2\Delta r} \right) \left[\left(\frac{1}{(\Delta r)^2} - \frac{1}{2r_{i,k}\Delta r} + \frac{u_{z_{i,k}} \mathrm{RePr}}{2\Delta z} \right) T_{i-1,k} - \left(\frac{2}{(\Delta r)^2} + \frac{2}{(\Delta z)^2} \right) T_{i,k} + \left(\frac{1}{(\Delta r)^2} + \frac{1}{2r_{i,k}\Delta r} - \frac{u_{z_{i,k}} \mathrm{RePr}}{2\Delta z} \right) T_{i+1,k} + \left(\frac{1}{(\Delta z)^2} + \frac{u_{r_{i,k}} \mathrm{RePr}}{2\Delta r} \right) T_{i,k-1} \right]$$

$$T_{i,k+1} = \left(\frac{2x10^{-7}}{(0.01)^2 u_{r_{i,k}} \mathrm{RePr} - 2(0.001)} \right) \left[\left(\frac{1}{(0.001)^2} - \frac{1}{0.002\, r_{i,k}} + \frac{u_{z_{i,k}} \mathrm{RePr}}{2(0.01)} \right) T_{i-1,k} - \left(2.02 \times 10^6 \right) T_{i,k} + \left(\frac{1}{(0.001)^2} + \frac{1}{0.002 r_{i,k}} - \frac{u_{z_{i,k}} \mathrm{RePr}}{0.02} \right) T_{i+1,k} + \left(10^4 + \frac{u_{r_{i,k}} \mathrm{RePr}}{0.002} \right) T_{i,k-1} \right]$$

$$T_{i,k+1} = \left(\frac{2 \times 10^{-7}}{0.0001\, u_{r_{i,k}} \mathrm{RePr} - 0.002} \right) \left[\left(1{,}000{,}000 - \frac{500}{r_{i,k}} + 50\, u_{z_{i,k}} \mathrm{RePr} \right) T_{i-1,k} - 2{,}020{,}000\, T_{i,k} + \left(1{,}000{,}000 + \frac{500}{r_{i,k}} - 50\, u_{z_{i,k}} \mathrm{RePr} \right) T_{i+1,k} + \left(10{,}000 + 500\, u_{r_{i,k}} \mathrm{RePr} \right) T_{i,k-1} \right]$$

(5.3)

This equation provides a temperature profile along the DCR insert for varying axial velocity.

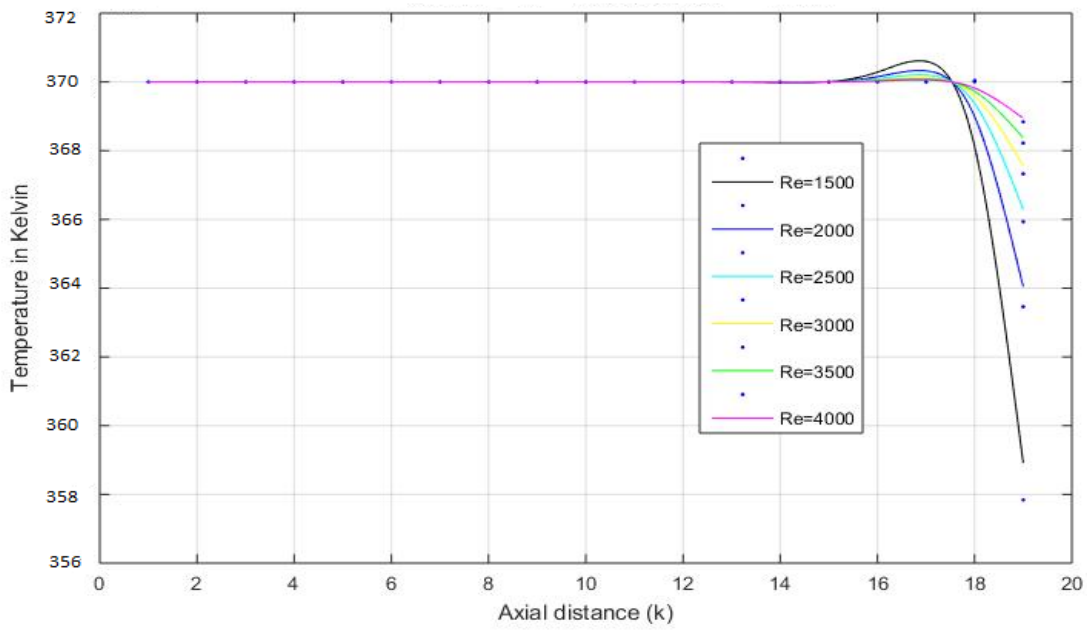

Figure 5.4: **Temperature profile along the pipe with variation of Reynolds number.**

5.4 Accuracy, stability and convergence of the numerical method

Accuracy is the extent of approximation for a numerical solution when compared with an exact solution. The truncation error associated with the diffusion term using a finite difference method is of order $(\Delta z)^2$. When the mesh is refined, it is true that the truncation error decreases. The order of a discretization method is *n* if its truncation error is of order $(\Delta z)^n$. A consistent numerical method is one in which truncation error tends to vanish as the mesh becomes finer. Stability is a property of the path to a solution. In a steady state problem we obtain a discretized set of algebraic equations to be solved. An iterative solution method is unstable or divergent if it fails to yield a solution to the discrete set. The term convergence has two common uses. First an iterative method is said to converge to a solution meaning it has successfully obtained a solution to a discrete algebraic set. Secondly there is convergence to mesh independence implying that the process of mesh refinement and its use in obtaining solutions remain essentially invariant with further refinement.

5.5. Variation of temperature along the tube

Temperature of the fluid along a tube is determined for the different set ups to compare the variations due to number of slits on the conical insert and rate of heat transfer.

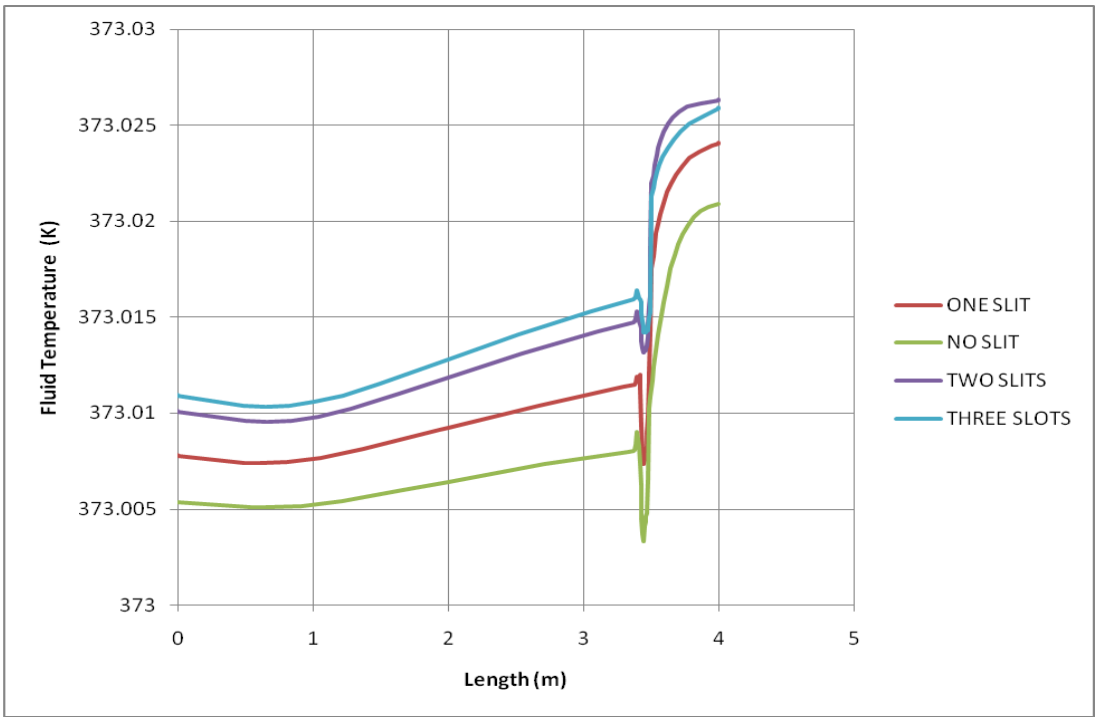

Figure 5.5: **Variation of temperature in different cases of DCR insert with slits.**

It is observed that the pressure drops abruptly in the insert while temperature increases. A case where the DCR insert has two slits attains the highest temperature past the insert outlet as well as the greatest temperature change between outlet and inlet values.

Fluid temperature is nearly constant immediately it enters the pipe but starts to rise as it approaches the DCR insert which is followed by an abrupt drop then a rise in temperature due to heat transfer enhancement. This is as a result of movement in fluid particles caused by the turbulator which releases the dissipation energy. As the fluid moves past a DCR insert it is noted that the case with two slits on opposite sides of the conical ring gains the highest temperature towards the pipes exit, since it generates multi longitudinal vortices that provide the best synergy. Obtaining the temperature difference between the inlet and outlet we realize that heat gain in a case with two slits on the DCR insert as the greatest enhancement among the different set ups.

5.6 Determination of thermal performance factor

The heat enhancement factor of a plain tube fitted with a DCR insert is obtained analytically by determining the non dimensional numbers and other physical values required to run the simulation software solid works. With hot water used as the test fluid, values of the physical properties used during flow simulation are: Inlet temperature T_0=373 K, tube inlet pressure P_0 = 110,000 Pa with tube outlet pressure P_1 =101,330 Pa (1 atmosphere). Maximum velocity v = 4 m/s at the pipe inlet, density of water at a temperature of 373 K is ρ = 957.9 kg/m^3 while specific heat at constant pressure C_p= 4217 J/Kg.K. Thermal conductivity k = 0.679 W/m.k and coefficient of dynamic viscosity μ =2.82X10^{-4} Kg/m.s. Taking the tube's inner diameter = 0.05 m which is equal to the inserts outlet and the DCR insert inlet diameter =0.036 m, at which point the fluid flow velocity = 6 m/s.

Mass flow rate ($\dot{m}$) is the product of fluid density (Kg/m^3), tube's cross sectional area (m^2) and flow velocity of fluid (m/s) then

$$\dot{m} = \rho A v = 957.9 \times \pi \left(\frac{0.05}{2} \right)^2 \times 4 = 7.52333 \text{ Kg/s.}$$

At the pipe's entrance and then

$$\dot{m} = 957.9 \times \pi \left(\frac{0.036}{2} \right)^2 \times 6 = 5.85014 \text{ Kg/s .}$$

At the DCR insert inlet the difference causing a rise of internal energy. When the fluid encounters the DCR insert which has a smaller radius than the inlet pipe therefore a pressure drop is experienced and a rise in fluid velocity within the conical tube.

Heat transfer rate in a tube where the DCR has no slits is

$$Q = \dot{m} C_p (T_{\text{out let}} - T_{\text{in let}}) = 5.85014 \text{X } 4217(373.0207\text{-}373.0054) = 377.45162 \text{ J/s.} \quad (5.4)$$

Heat transfer coefficient in a pipe in presence of a DCR insert with no slits is

$$h_{0slit} = \frac{Q}{\pi DL\Delta T} = \frac{377.45162}{\pi \times 0.036 \times 4(0.0153)} = 54{,}532.762 \quad (5.5)$$

A tube in presence of a DCR with one slits there is an approximate increase in inlet area.

For a slit with a length of 5 cm along the slant edge on a DCR insert of divergence angle 15^0 at the vertex, has a projected radial length of

$0.05 \text{x} \sin 7.5^0 = 6.5263 \text{x} 10^{-3}$ m.

Since the slit has a width of 0.005 m, the slits projected cross sectional area is $0.006526 \text{x} 0.005 = 3.26315 \text{x} 10^{-5}$ m^2.

Hence a DCR insert with one slit has an equivalent inlet area of

$\pi \text{ x} 3.24 \text{x} 10^{-4} + 3.26315 \text{x} 10^{-5} = 1.050506 \text{x} 10^{-3}$ m^2 .

Therefore mass flow rate $\dot{m} = 957.9 \times 0.0010505 \times 6 = 6.03767 kg/s$

Heat transfer rate has

$Q = \dot{m} C_p (T_{out\ let} - T_{in\ let}) = 6.03767 \text{x } 4217 \text{ x } (373.0262 - 373.0101) = 409.89485$ J/s. (5.6)

The inlet cross sectional area of a DCR insert with one slit as an equivalent diameter of $A = \pi r^2$ therefore $r = \sqrt{\frac{A}{\pi}} = \sqrt{\frac{1.050506}{\pi}} = 0.018286\ m$.

Hence equivalent diameter is 0.0365725 m.

Then heat transfer coefficient $h = \frac{Q}{\pi DL\Delta T}$.

For the DCR with 1 slits

$$h_{1slit} = \frac{Q}{\pi DL\Delta T} = \frac{409.89485}{\pi \times 0.0365725 \times 4(0.0161)} = 55{,}396.46877 \quad (5.7)$$

Thermal performance factor $\eta = \frac{h_{1slit}}{h_{0slit}} = \frac{55{,}396.468}{54{,}532.762} = 1.015838$ (5.8)

Similarly analysis is done on the other cases where the DCR insert as two and three slits with the results provided in table 5.2 to compare their rate of heat transfer and the thermal performance factor.

Table 5.2: **Coefficient of heat transfer by different number of slits on a DCR insert**

Number of slits	0	1	2	3
$\Delta T = T_{outlet} - T_{inlet}$	0.015356	0.016099	0.016128	0.014882
Estimated area of slits (m^2)	0	3.263×10^{-5}	6.526×10^{-5}	9.789×10^{-5}
Equivalent Radius (m)	0.0180	0.018286	0.018568	0.018845
Equivalent Diameter (m)	0.0360	0.036572	0.037136	0.037691
Q [rate of heat transfer] (J/s)	377.45162	409.89486	423.38799	402.44769
h [coefficient of heat transfer]	54,532.762	55,396.468	56,253.766	57,094.814
η [thermal performance factor]		1.01584	1.03156	1.04698

From this analytical results the rate of heat transfer is represented graphically as illustrated in Figure 5.6 which indicates the optimal number of slits for heat transfer enhancement in a cylindrical pipe is two slits in symmetrical positions directly opposite each other on the cones slant surface.

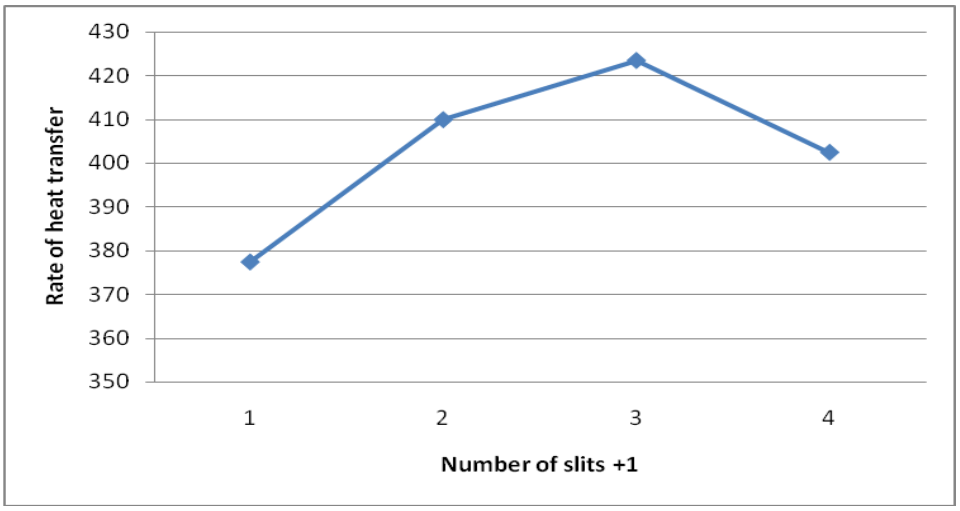

Figure 5.6: **Varation on rate of heat transfer with number of slits on the DCR insert.**

It is noted that two slits on opposite sides of the conical insert are observed to offer the highest heat transfer enhacentment potent when it generates two longitudinal vortex pairs.

5.7 Discussion of results

When the number of slits increases the amount of fluid passing through a conical insert increases thus decreasing the pressure as shown in Figure 4.15. The insert with no slit has its graph line showing the highest pressure drop while the case of three slits has the lowest change in pressure, the four graph lines plotted together show simillar behaviour of a sudden drop of pressure at the insert inlet.

An increase in velocity at the insert increases kinetic energy in the fluid, raising the collisions of fluid particles leading to a rise in temperature due to dissipation of heat in the boundary layer region.

As flow blockage increases the pressure drops, leading to increased viscous effects because of reduced free flow area causing a secondary flow. This creates a swirl flow that results in mixing of fluid particles and raising the temperature gradient which ultimately leads to a higher heat transfer enhancement.

The coefficient of heat transfer increases with increase in number of slits on the DCR insert which increases amount of fluid flowing past the turbulator.

The thermal performance fact also increases with rise in number of slits symmetricaly positioned on the conical inserts curved surface.

CHAPTER SIX

CONCLUSIONS AND RECOMMENDATIONS

6.1 Introduction

This chapter presents the main findings of the research study and recommendations for further research.

6.2 Conclusion

There is need to analyze the flow pattern when using a diverging conical ring insert with slits and its effect in determining the change in temperature and pressure for the different set ups. Comparing zero, one, two and three slits which attains the second specific objective.

There is a difference in values computed for rate of heat transfer with change in number of slits which shows that two multi-longitudinal vortex pairs in the diverging conical ring insert is a flow pattern that enhances heat transfer than the other cases. This is generated by two symmetrical slits on opposite sides of the conical insert, in relation to the first specific objective.

The rate of heat transfer was highest when a conical insert has two slits which is 423.3879 J/s in the analysis done in Table 5.2, while the thermal performance factor increases with the number of slits. This is a result of rise in the mass flow rate past the insert; this provides a result in relation to the third specific objective.

It is found that as Reynolds number increases then coefficient of skin friction reduces on the fluid flow past the diverging conical ring insert, as shown in Section 4.10 to achieve the fourth specific objective.

An increase in velocity at the insert increases kinetic energy in the fluid, raising the collisions of fluid particles leading to a rise in temperature due to dissipation of heat in the boundary layer region hence a temperature rise. Temperature rise provides heat transfer enhancement on the fluid.

There is variation in every set up for values are obtained to determine the variation of temperature along the pipe showing change of temperature due to the diverging conical insert in the cylindrical pipe. It is observed that heat transfer enhancement occurs has the fluid passes through the diverging conical ring insert.

6.3 Recommendation

Future researchers to investigate the effect of a diverging conical ring insert on compressible fluid flow, for example hot air passing through a turbulator fixed in a pipe on a combustion exhauster.

i) To determine effect of swirl flow generated by a divergent conical ring insert with slits using the stream function equation and vorticity equation to determine amount of heat enhancement due to fluid circulation.
ii) To investigate synergy between pressure, temperature and velocity vectors of the flow with multi-longitudinal vortices along the flow tube.
iii) To study effect of multiple diverging conical ring inserts with slits placed at fixed distances from each other along a tube to maintain swirl flow.

REFFERENCES

Abdullah, M.N., (2012) Heat transfer and pressure drop in turbulent flow through an eccentric converging diverging tube with twisted tape inserts. Journal of Engineering and Development, *16* (2) 178 -192.

AI-Fahed, S. and Chakroun, W., (1996) Effect of tube tape clearance on heat transfer for fully developed turbulent flow in a horizontal isothermal tube, *International Journal Heat and Fluid Flow*, 17, 173–178.

Aghayari R., Maddah H., Baghbani A. J., Mohammadiun H., and Nikpanje E. (2016), An experimental investigation of heat transfer of Fe_2O_3 Water nano fluid in a double pipe heat exchanger, *International Journal of Nano Dimensions*, *6* (5) 517-524.

Al-Fahed, S., Chamra, L.M. and Chakroun, W., (1999) Pressure drop and heat transfer comparison for both micro fin tube and twisted-tape inserts in laminar flow, *Experimental Thermal and Fluid Science*, 18, 323-333.

Anvari A., Lotfi R., Rashidi A. and Sattari S, (2011) Experimental research on heat transfer of water in tubes with conical ring inserts in transient regime, *International Communications in Heat and Mass Transfer*, 38, 668 -671.

Avinash S., (2015). Analysis of Heat Transfer in Pipe with Twisted Tape Inserts, International Conference on Fluid Flow. *Journal of Heat and Mass Transfer* Ottawa, 30, 120 -125.

Ayhan, T., Azak,Y., Demirtas, C. and Ayhan, B., (1999) Numerical and experimental investigation of enhancement of turbulent flow heat transfer in tubes by means of truncated hollow cone inserts, *Heat Transfer Enhancement of Heat Exchangers*, Kluwer Academic Publishers, 347–356.

Bankar, D. and Pathare, N.R., (2010) Analysis of heat transfer and friction factor characteristic in circular tube fitted with v-nozzle turbulators, *Emerging Trends in Engineering and Technology (ICETET), 3rd International Conference*, 675-679.

Bergles, A.E. and Rosennow, W.M., (1985) *Techniques to Augment Heat Transfer Reading: Handbook of Heat Transfer Application.* New York : McGraw-Hill.

Bhuiya, M. M. K., Azad, A. K., Chowdhury, M.S.U. and Saha. M., (2016). Heat transfer augmentation in a circular tube with perforated double counter twisted tape inserts. *International Communications in Heat and Mass Transfer,* 74, 18-26.

Bilen, K., Cetin, M., Gul, H. and Balta, T., (2009) The investigation of groove geometry effect on heat transfer for internally grooved tubes, *Applied Thermal Engineering,* 29, 753-761.

Chang, S.W., Yang T.L and Liou, J.S., (2007) Heat transfer and pressure drop in a tube with broken twisted tape insert, *Experimental Thermal and Fluid Science journal,* 32, 489-501.

Changzhong M., (2016). Experimental study on effect of heat transfer enhancement for single phase forced convective flow with twisted tape inserts. *International Journal of Heat and Mass Transfer*, 20, 160 - 168.

Chen, Q., Liang, X.G. and Guo, Z.Y., (2013) Entransy theory for the optimization of heat transfer. *International Journal of Heat Mass Transfer*, 63, 65-81.

Chokphoemphun, S., Monsak P., Chinaruk T. and Promvonge P. (2015). Heat transfer augmentation in a circular tube with winglet vortex generators. *Chinese Journal of Chemical Engineering, 23*(4) 605-614.

Chou, X.T., Wai, L.M., Yew, M.H., and Boon T.T., (2012) On the role of inserts in forced convection heat transfer augmentation. *International Communications in Heat and Mass Transfer,* 39, 1138 – 1145.

Curnia , J.C., Sasmito, A. and Mujumdar, A.S. (2012) Laminar convective heat transfer for in- plane spiral coils of non- circular cross-section ducts. *A Computational Fluid Dynamics Journal of Thermal Science,* 16, 109 -118

Dewan, A., Mahanda, P., Sumithra Raju, K. and Suresh Kumar, P., (2004) Review of passive heat transfer augmentation techniques, *Journal of Power and Energy,* 218-509.

Dewan, A., Mahanta, P., Sumithra Raju, K. and Suresh Kumar, P., (2015) Review of passive heat transfer augmentation techniques, *International Journal of Science, Engineering and Technology Research, 4* (4) 660.

Durmus, A. (2004) Heat transfer and energy loss in cut out conical turbulators. *Energy Conversion Management,* 45, 785-796.

Eiamsa-ard, S., Pethkool, S., Pong, C.T. and Promvonge, P., (2008) Turbulent flow heat transfer and pressure loss in a double pipe heat exchanger with louvered strip inserts. *International Communications in Heat and Mass Transfer,* 35, 120-129.

Eiamsa-ard, S. and Promvonge, P., (2006) Heat transfer characteristics in a tube fitted with helical screw -tape with / without core-rod inserts, *International Communications in Heat and Mass Transfer*, 34, 176-185.

Fan, A., Deng, J., Guo, J. and Liu, W., (2011) A numerical study on thermo- hydraulic characteristics of turbulent flow in a circular tube fitted with conical strip inserts. *Applications in Thermal Engineering*, 31, 2819- 2828.

Gambill, W.R. and Bundy,R.D., (1963) High flux heat transfer characteristics in turbulent swirl flow subjected to large transverse temperature gradients, *AICHE Journal*, 91, 55–59.

Guo, J., Yan, Y., Liu, W., Jiang, F. and Fan, A. (2015) Enhancement of laminar convective heat transfer relying on excitation of transverse secondary swirl flow. *International Journal of Thermal Sciences*, 87, 199-206.

Gupta, A. K., Lilley, D. G., and Syred, N., (1984) *Swirl Flows*, Ohu: Abacus Press.

Hasim, F., Yoshida, M. and Miiyashita, H., (2003) Compound heat transfer enhancement by a combination of a helically ribbed tube with twisted tape inserts. *Journal of Chemical Engineering of Japan* 36, 1116-1122.

Holit B. and Ozceyhan V., (2012) Heat transfer enhancement in a tube with twisted tape insert placed separately from the tube wall. *Journal of Experimental Thermal and Fluid Science*, 41, 51 -58.

Hong Y., Deng X. and Zhang L., (2012) 3D Numerical study on compound heat transfer enhancement of converging – diverging tubes equipped with twin twisted tapes. *Chinese journal of chemical engineering, 20* (3) 589 – 601.

Hossain, S., Dev, U.K. and Rahman K.A., (2015) The enhancement of heat transfer in a circular tube with insert and without insert by using finite element method. *Journal of Procedia Engineering*, 105, 81 – 88.

Idelchik, I. E., (1994) Handbook of hydraulic resistance, Londan: *CRC Press.*

Jia, H., Liu, Z.C. and Nakayam A., (2014) Convective heat transfer, *International Journal of Heat and Mass Transfer*, 73, 124-129.

Karakaya, H. and Durmus, A., (2013) Heat transfer and energy loss in conical spring turbulators, *International Journal of Heat and Mass Transfer*, 60, 756-762.

Kongkaitpaiboon, V., Nanan, K. and Eiamsa –ard, S., (2010) Experimental investigation of heat transfer and turbulent flow friction in a tube fitted with perforated conical rings. *Int. Communications in Heat and Mass Transfer*, 37, 560- 567.

Kreith, F. and Margolis, D., (1959) Heat transfer and friction in turbulent vortex flow, *Applied Science Resource*, 8, 457–473.

Li, L., Xiaoze, D. , Yuwen, Z., Lijun, Y., and Yongping. Y., (2014) "Numerical simulation on flow and heat transfer of fin-and-tube heat exchanger with longitudinal vortex generators", *International Journal of Thermal Sciences*, 92, 85-96.

Liu, W., Liu, Z. C. and Guo, Z. Y., (2009) Physical quantity synergy in laminar flow field of convective heat transfer and analysis of heat transfer enhancement. *China Science Bulletin, 54* (19) 3579- 3586.

Liu, W., Liu, Z.C. and Ma, L., (2012) Application of a multi- field synergy principle in the performance evaluation of convective heat transfer enhancement in a tube. *China Science Bulletin*, 57, 1600- 1607.

Manglik, R.M. and Bergles, A.E., (1994) Fully developed laminar heat transfer in circular-segment ducts with uniform wall temperature, *Numerical Heat Transfer Journal of Applications*, 26, 499–519.

Meng, J.A., Liang, X.G., (2005) Field synergy optimization and enhanced heat transfer by multi-longitudinal vortices flow in tube, *International Journal of Heat and Mass Transfer*, 48, 3331- 3337.

Mirzaei, M. and Sohankar, A., (2013) Heat transfer augmentation in plate finned tube heat exchangers with vortex generators: a comparison of round and flat tubes. *International Journal of Science and Technology Transactions of Mechanical Engineering, 37*(1) 39 -51.

Mohammed A.A., Bashar A.M. and Raheem J.M., (2014) Heat transfer enhancement in a tube fitted with nozzle turbulators, *Engineering and Technology Journal*, 32, 10.

Moody L. F., (1944) Friction factors for pipe flow. *Transactions of the A.S.M.E*, 671-684.

Muhammad K. R., Suhaimi H. and Aklilu T. (2015), Experimental Investigation on Heat TransferEnhancement By Using Porous Twisted Plate As An Insert in A Fitted Tube, *Journal of Engineering and Applied Sciences, 10* (21) 1819-6608.

Nagarajan G. and Ranganatan S., (2015) Heat transfer enhancement in double pipe heat Exchanger with twisted type insert in ANSYS fluent, *International Electronic Research journal, 3* (2) 981-993.

Nakate, D.S., Channapattana, S.V., and Ravi. H.C., (2015) .Enhancement in the Performance of Heat Exchanger by Inserting Twisted Tape Turbulators, *International Electronic Research journal,* 2, 1563-1570.

Naphon, P., (2006) Heat transfer and pressure drop in horizontal double pipes with and without twisted tape insert, *International Communications in Heat and Mass Transfer*, 33, 166-175.

Nuntadusit, C., Wae-hayee, M., Bunyajitradulya, A. and Eiamsa-ard, S. (2012) Heat transfer enhancement by multiple swirling impinging jets with twisted tape swirl generators, *International Communications in Heat and Mass Transfer*, 39, 102 – 107.

Parra, T., Szasz, R.Z., Duwig, C., Perez, R., Mendoza, V. and Castro, F., (2013) Acoustic instabilities on swirling flames, *International Journal of Mechanical Engineering*. *7*(9) 742 -745.

Pradip R. B. and Dinesh K. K. (2013) A study on the heat transfer enhancement for air flow through a duct with various rib inserts. *International Journal of Latest Trends in Engineering and Technology, 2* (4) 201 -202.

Promvonge, P. and Eiamsa-ard, S., (2007) Heat transfer behaviors in a tube with combined conical–ring and twisted tape insert, *International Communication in Heat and Mass Transfer*, 34, 849-859.

Putkaradze, V. and Vorobieff, P., (2006) Instability, bifurcations and solutions in expanding channel flows, *Journal of Fluid Mechanics*, 97, 144 -152.

Sadri Reza M., (1997) Channel Entrance Flow, *PhD. Thesis Department of Mechanical Engineering the University of Western Ontario.*

Saha, S.K. and Dutta, A., (2001) Thermo-hydraulic study of laminar swirl flow through a circular tube fitted with twisted-tapes, *Transaction ASME Journal Heat Transfer*, 2, 417–421.

Sahu, K. C. and Govindarajan R., (2005) Stability of flow through a slowly diverging pipe, *Journal of Fluid Mechanics*, 531, 325 – 334.

Saqr, K.M. and Wahid, M.A., (2014) Effects of swirl intensity on heat transfer and entropy generation in turbulent decaying swirl flow, *Applied Thermal Engineering,* 70, 486-493.

Shivalingaswamy, B.P. and Narahari, G.A., (2014) Numerical investigation of convective heat transfer and pressure loss in round tube fitted with conical ring turbulator, *International Journal of Scientific and Research Publications, 4* (4) 2250.

Sivakumar K. and Rajan K., (2015). Experimental Analysis of Heat Transfer Enhancement In a Circular Tube With Different Twist Ratio of Twisted Tape Inserts, *International Journal of Heat and Technology,* 33, 236 -241.

Sivashanmugam, P. and Suresh, S., (2006) Experimental studies on heat transfer and friction factor characteristics of laminar flow through a circular tube fitted with helical screw-tape inserts, *Journal Applied Thermal Engineering,* 26, 990-997

Suresh, K. P., Mahanta,P. and Dewan, A., (2004) Study of heat transfer and pressure drop in a large hydraulic diameter annulus, *The 17th National Heat and Mass Transfer*

Conference and 6th ISHMT/ASME, Heat and Mass Transfer Conference, Indira Gandhi Centre for Atomic Research, Kalpakkam, India: 62–66.

Swaminathan, G., Sahu, K. C., Sameen, A. and Govindarajan R., (2011) Global instabilities in diverging channel flows, *Journal of Theoretical and Computational Fluid Dynamics*, 25, 53 – 64.

Van Rooyen, R.S. and Kroeger, D.G., (1978) Laminar flow heat transfer in internally finned tubes with twisted-tape inserts, *Journal Illumination of Engineering Science,National Research Council of Canada*, 2,7–11.

Vijay D., Shejwalkar M. and Nadar D., (2014). Experimental study on effect of area and turbulence on heat transfer through circular pipe by using internal threading in drying system. *Journal of Basic and Applied Engineering Research*, 1 (1) 24 -29.

Wang, L. and Sunden, B., (2002) Performance comparison of some tube inserts, *International Communications in Heat and Mass Transfer*, 29, 45-56.

Webb, R.L. and Hyun Kim, N., (2005) *Principles of Enhanced Heat Transfer,* 2nd edition, London: Taylor Francis Group press.

Wisam A. K., (2012) An experimental study on the effect of shape and location of vortex generators ahead of a heat exchanger; *Al – Khwarizmi Engineering Journal*, *8* (2) 12-29.

Yakut, K. and Sahin, B., (2006) Flow-induced vibration analysis of conical-rings used of heat transfer enhancement in heat exchanger, *Journal of Applied Energy* 78, 273–288.

Yakut, K. Sahin, B. and Canbazoglu, S., (2004) Performance and flow-induced vibration characteristics for conical-ring turbulators, *Journal of Applied Energy* 79, 65–76.

Yilmaz, M., Yapici, S., Jomakli, O. and Sara, O. N., (2002) Energy correlation of heat transfer and enhancement efficiency in decaying swirl flow, *International Communications in Heat and Mass Transfer*, 38, 351–358

Yongsiri K., Eiamsa-ard S., Chinaruk T. and Promvonge P., (2006) Effect of turbulent decaying swirl flow on heat transfer enhancement in a tube, *International Conference on Sustainable Energy and Environment*, 2006, 21 -23.

Zohir, A.E. and Gomaa, A.G. (2013) Heat transfer enhancement through sudden expansion pipe airflow using swirl generator with different angles, *Experimental Thermal and Fluid Science*, 45, 146 -154.

Zozulya, N.V. and Shkuratov, I.Y., (1974) Effect of length of twisted-tape turbulence promoter and its initial twisting pitch on augmentation of heat transfer inside a tube, *Journal of Heat Transfer*. Soviet Research 6, 98–100.

APPENDICIES

Appendix 1: Algorithm for solving tri diagonal matrix to obtain radial velocity

```
%numerical techniques of solving finite differences
%developed  to solve tri diagnol matrix
% a3=size(a1);
% constants
dz=0.001;
dr=0.01;
dz0=0;
dr0=0;
po=1e05; %pressure
To=370; % temperature
re=2000; % reynolds number
pr=4;    %
pc=160;  %
 row=18;
col=18;
mt=[2;1;2/3;1/2;2/5;1/3;2/7;1/4;2/9;1/5;2/11;1/6;2/13;1/7;2/15;1/8;2/17;1/9];
for i=1:row
   for j=1:col
      for i=j
      a3(i,j)=mt(i);
   end
  end
end
% disp(a3)
a3(1,2)==0;
find(a3==18)
```

```
a3(1,2:end)=0;  %take away the abnormality in matrix formation
% disp(a3)
% break
a4=a3-1*diag(ones(17,1),1);
% disp(a4)
% break
a5=a4+1*diag(ones(17,1),-1);
% disp(a5)
% break
% to display and plot the sparse matrix use spy(a5)
%  uz=[0 0 0.1 0 -0.2 -0.3 0.9 0.8 0.8 0.8 0.8 0.7 0.7 0.7 0 0.4 0.4 0];% values of uz
for k=0;
 file1='data_uz.txt';
 file2='data_all_uz.txt';
 data=load(file1);
 data1=load(file2);
 uz=data(:,1);
 ur=a5\uz;      %Mat divid for a case of Ax=b i.e x=A\b
ur2=pinv(a5)*uz; % least squares approach
% disp(ur2);
 k=[ur ur2]; %compare if the two techniques give the same value
   disp(k);  %try to check if the two technique are the same
   Ur=zeros(18,30);
    Ur=pinv(a5)*data1(:,1:end); % compute all the ur from all the uz values in data1
%   disp(Ur)
%% computation of the array of radial length variations r(i,k)
file3='radial.txt';
r=load(file3);
y2=r;
```

```
for i=1:18
   for j=1:30
      y2(i,j)=r(i,j);
   end
end
r2=y2;
a1=re.*r2;
%%  %% computation of pressure profile
 A=zeros(18,30);
 for i=1:18
    for k=1:30
       A=Ur/(0.002)+1000/(re)-500./(a1);
    end
 end
  for i=2:18
   for j=1:30
   uk(i,j)=data1(i-1,j);
    end
 end
A2=A.*uk;
w=2e06/re;
 B=w+2e06;
%  disp(B)
  %% C values to be redone
 C=zeros(18,30)
  data1(:,end)=[]
 uz=(data1(:,end)==0)
uz1=[data1 uz];
% disp(uz1)
```

```
uz2=[uz data1];
% disp(uz2)
C=uz1-uz2/(0.002);
b2=B-C;
%%
y=load(file2);
B2=b2.*y;
disp(B2);
% break
%% D values
  w2=1e06/re; w3=500./(re*r2); w4=Ur/0.002;
  w5=w2+w3; w6=w5-w4;
  for i=1:17
   for j=1:30
   uz(i,j)=y(i+1,j);
    end
end
D2=w6.*uz;
%% E value
  E2=C/re;
  fa=0.002/pc;
  bra=A2-B2+D2-E2;
  fas=fa+bra;
  pre=1e05+fas;
  %%  save the generated pressure data
 save_file='variables.txt';
 results_path=['F:\New folder'];
 if ~exist(results_path,'dir')
    mkdir(results_path);
```

```
end
  save(save_file,'pre');
  save Pressure_Profile.txt pre –ascii
```

Appendix 2: Matlab algorithm to obtain pressure profile

```
%for Ur values from simulation
 %Computing Pressure profile
   %defining parameters
   %let x be the size of vector Re
   z=1:4;
   %vector for Reynolds number
   Re(z)=[1500 2000 2500 3000];
   Pc=6.5;
   i=1:1:3;
   p(1,1:3,1:6)=2.0*10^5;
   p(2,1:3,1:6)=2.0*10^5;
   %defining r(i,k)
   r(1,1:18)=repelem(0.0001,18);
   r(2,1:18)=repelem(0.001,18);
   r(3,1:18)=repelem(0.002,18);
   %k ranges from 1 to 18
   k=1:18;
   r(i,k);
   %importing Ur
   Ur=xlsread('Ur from simulation.xlsx');
   %importing uz
   uz=xlsread('Erick.xlsx',2);
   Ur(k,i);
```

```
   %generate pressure profile
   for z=1:4
   for k=2:18
```

```
    %pressure equation
    for i=1:3
    %repeat for values of i

    p(k+1,i,z)=p(k-1,i)+(1/(50*Pc))*((500*Ur(k,i)+(1000000/Re(z))-
(500/(r(i,k)*Re(z))))*uz(k,1)...
     -((2020000*uz(k,2))/Re(z))+((1000000/Re(z))+(500/(r(i,k)*Re(z)))-
(500*Ur(k,i)))*uz(k,3)...
 -((50*uz(k,2))-(9950/Re(z)))*uz(k+1,i)+((50*uz(k,2))+(10050/Re(z)))*uz(k-1,i));
    end
    end
    end
```

```
    %partitioning the matrix p

    %Re=1500;
    p1=p(:,1,1);%P at the center
    p2=p(:,2,1);%P at the middle
    p3=p(:,3,1);%P at the outer
    %Re=2000
    p4=p(:,1,2);
    p5=p(:,2,2);
    p6=p(:,3,2);
    %Re=2500
    p7=p(:,1,3);
    p8=p(:,2,3);
    p9=p(:,3,3);
    %Re=3000
    p10=p(:,1,4);
```

```
p11=p(:,2,4);
p12=p(:,3,4);
```

```
%plotting curves

k=1:19;
k=transpose(k);

a=fit(k,p1,'smoothingspline');
hL1=plot(a,k,p1);
legend('Re=1500');
hold on;
b=fit(k,p4,'smoothingspline');
hL2=plot(b,k,p4);
legend('Re=2000');
hold on;
c=fit(k,p7,'smoothingspline');
hL3=plot(c,k,p7);
legend('Re=2500');
hold on;
d=fit(k,p10,'smoothingspline');
hL4=plot(d,k,p10);
legend('Re=3000');
hold off;
%Legend
legend(' ','Re=1500', ' ','Re=2000',' ','Re=2500', ' ', 'Re=3000');
grid on;
xlabel('Axial Distanace (k)');
set(hL1(2),'color','k');
```

```
set(hL2(2),'color','b');
set(hL3(2),'color','r');
set(hL4(2),'color','g');
hold off;
grid on;
xlabel('Axial Distance (K)');
```

Appendix 3: Matlab algorithm to obtain temperature profile

```
  %COMPUTING TEMPERATURE PROFILE
%============================
%importing Ur
Ur=xlsread('Ur from simulation.xlsx');
%importing uz
uz=xlsread('Erick.xlsx',2);
%parameter definition-Temperature boundary conditions
%defining r(i,k)
r(1,1:18)=repelem(0.0001,18);
r(2,1:18)=repelem(0.001,18);
r(3,1:18)=repelem(0.002,18);
i=1:3;
k=1:18;
%defining boundary values
%T(k,i-1)=370=370; T(k,i)=370 T(k,i+1)=370
z=1:6;
T(k,1:3,z)=370;
%T(i,k-1)=370;
T(1,2,:)=370;
Pr=1.75;
%defining Re vector
Re=[1500 2000 2500 3000 3500 4000];
for z=1:6;
for k=2:18
   for i=1:3
    T(k+1,i,z)=((2*10^-7)/(0.0001*Ur(k,i)*Re(z)*Pr-0.002))*((1000000-
(500/r(i,k))+(50*uz(k,2)*Re(z)*Pr))*T(k,1)...
```

```
    -2020000*T(k,2)+(1000000+(500/r(i,k))-(50*uz(k,2)*Re(z)*Pr))*T(k,3)...
    +(10000+(500*Ur(k,i)*Re(z)*Pr))*T(k-1,2));
   end
end
end
```

```
%partitioning matrix T
%for i=1 and Re=1:6;
T1=T(:,1,1);
T2=T(:,1,2);
T3=T(:,1,3);
T4=T(:,1,4);
T5=T(:,1,5);
T6=T(:,1,6);
%for i=2 and Re=1:6
T7=T(:,2,1);
T8=T(:,2,2);
T9=T(:,2,3);
T10=T(:,2,4);
T11=T(:,2,5);
T12=T(:,2,6);
%for i=3 and Re=1:6
T13=T(:,3,1);
T14=T(:,3,2);
T15=T(:,3,3);
T16=T(:,3,4);
T17=T(:,3,5);
T18=T(:,3,6);
```

```
    %Plotting Temperature profile
    k=1:19;
    k=transpose(k);
    figure(1);%i=1
    a=fit(k,T1,'smoothingspline');
    hL1=plot(a,k,T1);
    hold on;
    b=fit(k,T2,'smoothingspline');
    hL2=plot(b,k,T2);
    hold on;
    c=fit(k,T3,'smoothingspline');
    hL3=plot(c,k,T3);
    hold on;
    d=fit(k,T4,'smoothingspline');
    hL4=plot(d,k,T4);
    hold on;
    e=fit(k,T5,'smoothingspline');
    hL5=plot(e,k,T5);
    hold on;
    f=fit(k,T6,'smoothingspline');
    hL6=plot(f,k,T6);
    hold off;
    %legend
    legend(' ','Re=1500', ' ','Re=2000',' ','Re=2500', ' ', 'Re=3000',' ','Re=3500', '
','Re=4000');
    grid on;
    title('Temperature against Axial distance (k)-centre');
    xlabel('Axial distance (k)');
```

```
ylabel('Temperature in Kelvin');
set(hL1(2),'color','k');
set(hL2(2),'color','b');
set(hL3(2),'color','c');
set(hL4(2),'color','y');
set(hL5(2),'color','g');
set(hL6(2),'color','m');
```

Appendix 4: Publication 1

www.ijraset.com *Volume 5 Issue V, May 2017*
IC Value: 45.98 *ISSN: 2321-9653*
International Journal for Research in Applied Science & Engineering Technology (IJRASET)

Effect of Slits in A Diverging Conical Ring Insert on Heat Transfer Enhancement in A Cylindrical Tube

Kinyua Eric Mugambi[1], Mathew Kinyanjui[2], Murray Humphrey[3]
[1]*Dep. of Mathematics & Physics, Tech. U. of Mombasa*
[2]*Dep. of pure & applied Mathematics, J.K.U.A.T*
[3]*Department of statistics & actuarial science, Jomo Kenyatta University of Agriculture and Technology; Kenya.*

Abstract: *Diverging conical ring insert in a cylindrical tube is a passive augmentation technique aiming to improve the heat transfer enhancement. An insert disrupts the flow creating a mixture between core and near wall fluid leading to enhancement of heat. In this research work hot water is used as the test fluid in a simulation to establish the pressure and temperature variation along a tube 4m long with an insert placed at 3.5m from the entrance. At this position uniform velocity is attained to avoid the boundary layer and pipe entry effect. Analysis of the results shows a positive heat transfer enhancement rate compared with a plain tube, the highest rate achieved when two slits are placed on opposite sides of the conical ring.*
Key words: *heat transfer enhancement, multi longitudinal vortex, Slit, Diverging ring insert and Thermal performance factor.*

I. INTRODUCTION

Heat transfer is a study on exchange of thermal energy through a body or between bodies which occurs when there is a temperature difference. Thermal energy transfers occur from a body with a higher temperature to another with lower temperature. Heat transfer enhancement is an improvement in the performance of a thermal system by change of surface geometry to obtain higher energy efficiency also referred to as heat transfer augmentation. The heat transfer rate can be improved by introducing a disturbance in the fluid flow using different enhancement technologies breaking the viscous and thermal boundary layer. Augmentation techniques are broadly classified into three different categories: Passive, Active and Compound. Passive techniques are those that do not require any direct input of external power, rather they use it from the system itself which ultimately leads to an increase in fluid pressure drop. They are divided into displacement enhancement devices like conical rings and swirl flow devices that produce superimposed swirl flow or secondary recirculation on the axial flow in a tube e.g. helical strip or coiled screw type tube inserts and twisted tapes. Active techniques are those that have external power used to facilitate the desired flow modification and improvement in the rate of heat transfer like in the case of rotating tubes and surface vibration. Compound techniques occur when any two or more of these techniques are employed simultaneously to obtain enhancement in heat transfer that is greater than that produced by either of them when used individually.

II. LITERATURE REVIEW

Ayhan et al. [1] provided the effect of truncated hollow cone inserts on heat transfer and friction in a tube. Durmus [3] investigated the effect of cutting out conical turbulators on heat transfer with different types of turbulators and different conical-angles of 5^0, 10^0, 15^0 and 20^0 establishing that heat transfer rate as well as friction coefficients increased with the angles. Promvonge [11] conducted experiments by inserting several conical rings as turbulators over a test tube with conical rings of three different diameter ratios of the ring to the diameter (d/D = 0.5, 0.6, 0.7) were introduced in the tests and for each ratio the rings were placed with three different arrangements; Converging conical ring-CCR, Diverging conical ring-DCR, Converging diverging conical ring-CDCR in which cold air at ambient air temperature was passed through the tube with the DCR being the most efficient. Fan et al. [4] numerically investigated turbulent flow and heat transfer in a circular tube fitted with conical strip inserts using k-ε turbulence. Kongkaitpaiboon et al. [7] studied the perforated conical–ring with different pitch ratios and different numbers of perforated holes. They found that it leads to a heat transfer rate up to 137% over that in the plain tube. The perforated conical-rings enhanced heat transfer more than typical conical-rings on the basis of thermal performance factor of around 0.92 at the same pumping power which was found at the smallest pitch ratio and maximum number of holes. Karakaya and Durmus [6] devised the conical spring turbulators for three

different cone angles 30°, 45° and 60° in Reynolds number ranging from 10000 to 34000. They found that the best results in terms of direction of flow are diverging, converging –diverging and converging respectively, while the turbulator best results for the cone angle are 30°, 45° and 60° respectively. Guo et al. [5] carried out a theoretical study about the effect of a secondary flow on the laminar convection heat transfer, while Saqr and Wahid [12] proposed an empirical correlation for predicting the entropy augmentation as a function of the swirl number. Numtadusit et al. [10] studied the effect on Nusselt number of different set ups of multiple swirling jets. As for the design of swirl generators Zohir et al. [13] evaluated the increase of heat transfer rate when modifying the location and pitch angle of the swirl generator upwind the test chamber. Liu et al [8] explained the physical quantity synergy principle from field synergy by reflecting the physical mechanism of convective heat transfer in the laminar and turbulence flows and explained physical essentials on reducing flow resistance by revealing how heat transfer performance is influenced by physical quantity synergy relation on temperature, velocity and pressure. Chen et al. [2] proposed the entransy dissipation based thermal resistance method for heat exchanger performance design and optimization. By setting entransy dissipation as optimization objective and viscous dissipation as a constraint condition, the optimization flow field equation for convective heat transfer is expressed by Meng et al [9]. Therefore the optimum velocity field indicates the basic characteristics of the flow pattern that benefits the heat transfer most for the laminar flow heat transfer in a tube as between 2 to 4 multi-longitudinal vortex pairs.

III. ASSUMPTIONS IN THE STUDY.

In this research using a viscous Newtonian fluid, the following assumptions are made:

A. The fluid flow is steady and in the axial direction.
B. The fluid is Newtonian i.e. stress is proportional to the rate of shear force.
C. The no-slip condition is satisfied i.e. on the surface of the solid wall the velocity of the fluid layer adjacent to it is stationary.
D. The fluid is incompressible i.e. density of the fluid is assumed to be a constant.

IV. BOUNDARY CONDITIONS

Using hot water the flow parameters at the inlet of the tube are $u_z = 3m/s$ while pressure P_0 =110,000 Pa and temperature T_0=370K. The Reynolds number (Re) satisfies the inequality 1000<Re<5000, pressure coefficient: P_C =6.5 and Prandtl number: Pr = 1.75, Figure 1 shows the position of a conical ring insert in the cylindrical tube, with the axis indicated. The DCR insert inlet radius is 18mm and the outlet radius is 25mm, with the length along the z axis as 70mm.

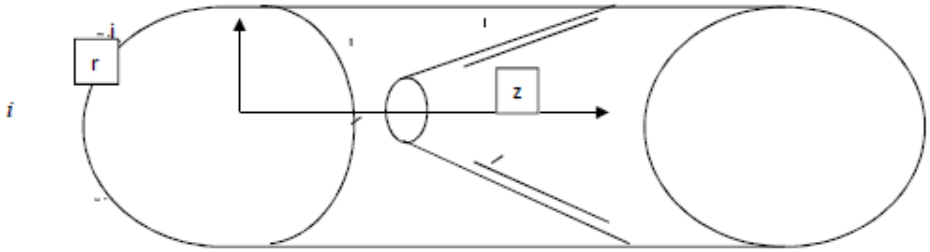

Fig 1: Schematic diagram of a diverging conical ring insert with two slits in a pipe.

Momentum flux on the fluid force through the ring at the DCR is $\dot{m} = 2\pi\rho\int_0^{\infty} u^2 r dr$ a constant and on the wall surfaces temperature $T_{\text{hot water}} = T_{\text{wall}}$.

The conical insert has a half angle of $\alpha = 7.5^0$ in a pipe of radius R= 2.5cm, and a pressure difference of 10k Pa.

V. PHYSICAL SIMULATION OF THE FLOW PROBLEM.

To determine the flow parameters we simulate a physical situation by modeling the cylindrical tube with a diverging conical ring insert having slits on the slant edge. A software 'Solid works' is used to simulate the flow after construction of the pipe geometry to

Volume 5 Issue V, May 2017
ISSN: 2321-9653
International Journal for Research in Applied Science & Engineering Technology (IJRASET)

demonstrate a case of hot water flowing in a horizontal pipe. Fluid velocity along the tube is illustrated by a colour code as shown in figure 2. The slits generate fluid circulation in the tube with axial velocity u_z along the axial planes. A cross section diagram at the DCR insert outlet displays the streamlines indicating two multi-longitudinal vortex pairs generated by two slits.

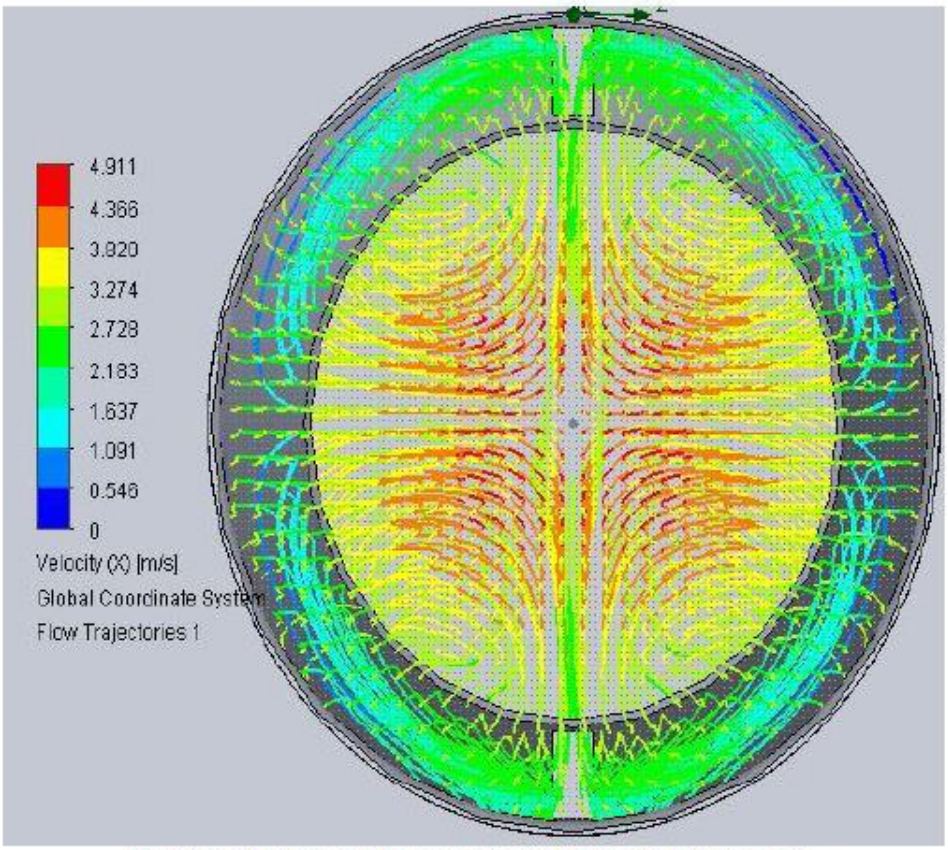

Fig. 2 Streamlines generated by 2 slits form two multi-longitudinal vortex pairs.

The number of vortex pairs is equal to the number of slits on the cone, these causes a mixture of inner core and near wall fluid which enhances heat transfer.

VI. GRAPHICAL REPRESENTATION OF THE RESULTS

A. Variation of Pressure

Results are obtained using a 4m long tube of internal radius 0.05m, to compare what happens when there is no conical ring insert and if one is placed in the tube a distance 3.5m from the entrance. Thereafter different DCR inserts are used by having four different cases i.e. with no slit, one, two and three slits. Pressure variation is observed at $i = 0$ which is the centre line of our pipe.

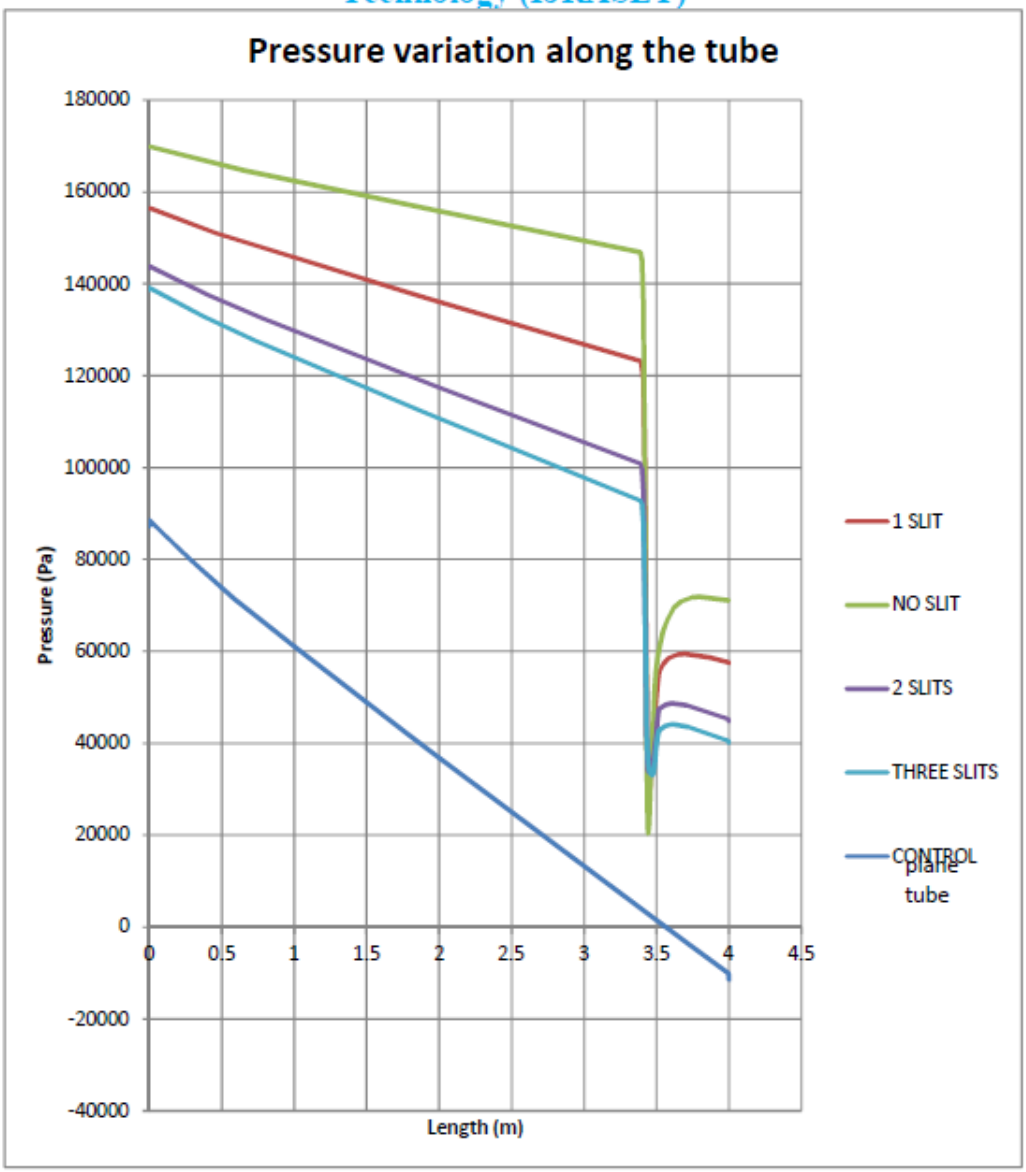

Figure 3: Pressure drop due to an insert placed in a plane tube.

A consistent pressure drop is observed in the four different cases with a DCR insert although a higher-pressure gradient is noted as the number of slits increases.

B. Variation of Temperature along the Tube.

Temperature of the fluid along a tube is determined for the different set ups to compare the effect due to number of slits on heat enhancement.

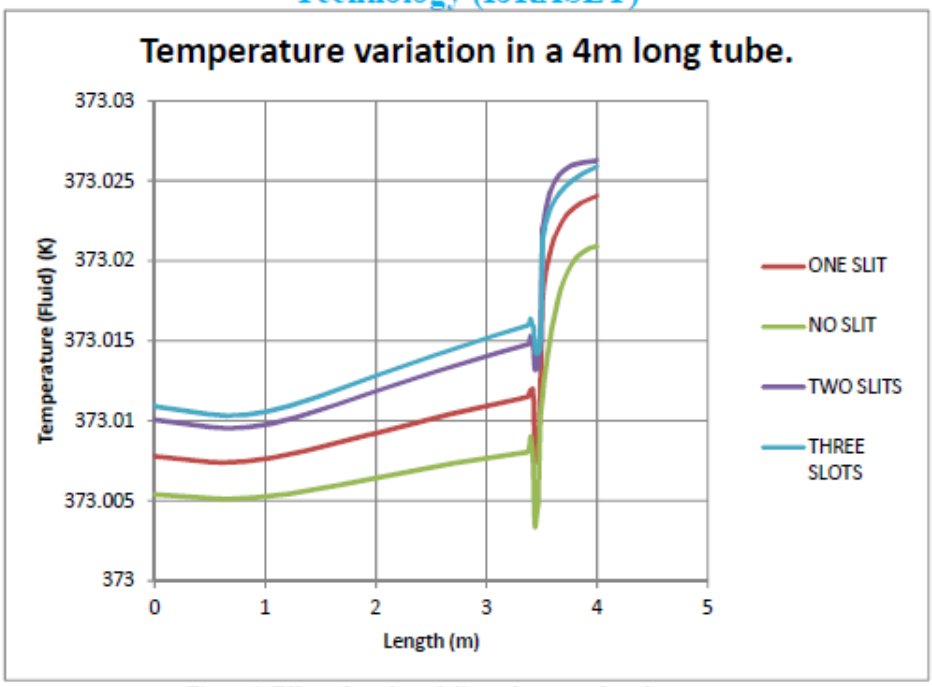

Figure 4: Effect of number of slits on heat transfer enhancement.

It is observed that after the pressure drop temperature in the case where DCR insert has two slits attains the highest temperature at the tube's outlet.

Number of slits on a DCR	0	1	2	3
$\Delta T = T_{outlet} - T_{inlet}$	0.015356	0.016099	0.016128	0.014882

Obtaining the temperature difference between the inlet and outlet we realize that heat gain for the 2 slit on a DCR is greatest among the different set ups.

VII. DETERMINATION OF THERMAL PERFORMANCE FACTOR

The overall heat enhancement factor for a plane tube fitted with a DCR insert is obtained analytically by obtaining several non dimensional factors. If hot water is used as the test fluid then the physical properties can be taken as follows: Inlet temperature T_0=370K, Tube inlet pressure P_0 = 110 000 Pa, while the tube outlet pressure is $P_{out\,let}$ =101 330Pa =1 atm, maximum velocity v= 4 m/s at the insert inlet, Density of water at 100^{0}c ρ = 957.9kg/m^3. Specific heat at constant pressure C_p= 4217kJ/Kg.K, Thermal conductivity k=0.679W/m.k , coefficient of Dynamic viscosity μ =2.82X10^{-4}Kg/m.s.

Using the tube's inner diameter =0.05m and fluid flow velocity = 3.5m/s. Mass flow rate (Kg/s) is the product of density (Kg/m^3), tube's cross sectional area (m^2) and fluid flow velocity then $\dot{m} = \rho A v = 957.9 \times \pi\left(\frac{0.05}{2}\right)^2 \times 3.5 = 6.5829$ Kg/s at the tubes inlet. When the fluid encounters the DCR with a smaller radius, a higher pressure drop is experienced and a rise in fluid velocity.

Heat transfer rate in a tube bearing a DCR with no slits is

$Q = \dot{m}\, C_p(T_{out\,let} - T_{in\,let}) = 6.5829 \times 4217(373.0207 - 373.0054) = 424.7294$ J/s.

Heat transfer coefficient in a tube bearing DCR insert with no slits is

$$h_{DCR0s} = \frac{Q}{\pi DL\Delta T} = \frac{424.7294}{\pi \times 0.0360 \times 4(0.0153)} = 61{,}363.2748$$

In a tube bearing a DCR with two slits an approximate increase in inlet area at $2.5\text{x}10^{-5}$ m^2 per slit, i.e length x width at 0.005m x 0.005m. Then a DCR with two slits as an equivalent inlet diameter of 0.0364m therefore heat transfer rate is

$Q=\dot{m}\, C_p(T_{out\ let}-T_{in\ let})$=6.5829X 4217X(373.0262-373.0101)=444.1614 J/s.

Heat transfer coefficient $h = \frac{Q}{\pi DL\Delta T}$.

For the DCR with 2 slits $h_{DCR2s} = \frac{Q}{\pi DL\Delta T} = \frac{444.1614}{\pi \times 0.0364 \times 4(0.0161)} = 60{,}311.9943$

Thermal performance factor $\eta = \frac{h_{DCR2s}}{h_{DCR0s}} = \frac{60{,}311.9943}{61{,}363.2748} = 0.9828$

In this analysis the wall is non conducting hence flow is adiabatic.

VIII. CONCLUSION

The investigation has been performed to determine heat transfer enhancement rate for varying number of slits on a common DCR insert with a constant pitch ratio.

The simulation of convection heat transfer in a straight circular tube shows that the two multi-longitudinal vortex pair in the tube is a flow pattern that enhances the heat transfer enormously.

IX. ACKNOWLEDGEMENTS

Authors wish to thank the Technical University of Mombasa for the financial support that has made this research work possible and also grateful to Charles Gathua who provided the expertise in the operations of Solid works which greatly assisted in this work.

A. Nomenclature

1) Roman Symbol — Quantity

C_P	Specific heat capacity at constant pressure
D	inner diameter of tube, m
d	inlet diameter of the diverging conical insert, m
h	heat transfer coefficient W/m^2k
k	thermal conductivity W/mk
L	Axial pitch tube length , m
$\dot{m}$	mass flow rate , Kg/s
Nu	Nusselt number
P	pressure, Pa (Nm^{-2})
P_o	pressure at the inlet, Pa (Nm^{-2})
Pr	Prandtl number
Q	convential heat transfer
r	tube radius
T	temperature, K

U	mean velocity of flow
u_z	axial velocity, m/s

2) Greek Symbols

	Quantity
Δ	Small change
α	Half angle at the vertex, rad
μ	Coefficient of dynamic viscosity kg/ms
ρ	Fluid density, kg/m^3
η	Thermal performance factor

3) List of Abbreviations

DCR	Diverging conical ring

REFERENCES

[1] Ayhan, T., Azak,Y., Demirtas, C. and Ayhan, B., (1999) Numerical and experimental investigation of enhancement of turbulent flow heat transfer in tubes by means of truncated hollow cone inserts, Heat Transfer Enhancement of Heat Exchangers, Kluwer Academic Publishers, 347–356
[2] Chen, Q., Liang, X.G. and Guo, Z.Y., (2013) Entransy theory for the optimization of heat transfer. Int Journal of Heat MassTransfer, 63 pp. 65-81.
[3] Durmus, A. (2004) Heat transfer and energy loss in cut out conical turbulators. Energy Conversion Management 45, 785-796
[4] Fan, A., Deng, J., Guo, J. and Liu, W., (2011) A numerical study on thermo- hydraulic characteristics of turbulent flow in a circular tube fitted with conical strip inserts. Applications in Thermal Engineering 31, 2819- 2828
[5] Guo, J., Yan, Y., Liu, W., Jiang, F. and Fan, A. (2015) Enhancement of laminar convective heat transfer relying on excitation of transverse secondary swirl flow. Int Journal of Thermal Sciences, vol. 87, pp. 199-206
[6] Karakaya, H. and Durmus, A., (2013) Heat transfer and energy loss in conical spring turbulators, International Journal of Heat and Mass Transfer, Volume 60, pp.756-762
[7] Kongkaitpaiboon, V., Nanan, K. and Eiamsa –ard, S., (2010) Experimental investigation of heat transfer and turbulent flow friction in a tube fitted with perforated conical rings. Int. Communications in Heat and Mass Transfer 37, 560- 567
[8] Liu, W., Liu, Z.C. and Ma, L., (2012) Application of a multi- field synergy principle in the performance evaluation of convective heat transfer enhancement in a tube. China Science Bulletin, 57. pp. 1600- 160
[9] Meng, J.A., Liang, X.G., (2005) Field synergy optimization and enhanced heat transfer by multi-longitudinal vortices flow in tube, Int. Journal of Heat and Mass transfer. 48: 3331- 3337
[10] Nuntadusit, C., Wae-hayee, M., Bunyajitradulya, A. and Eiamsa-ard, S. (2012) Heat transfer enhacement by multiple swirling impinging jets with twisted tape swirl generators, Int. Communications in Heat and Mass Transfer. Vol 39, pp 102 – 10
[11] Promvonge, P. and Eiamsa-ard, S., (2007) Heat transfer behaviors in a tube with combined conical–ring and twisted tape insert, Int. Communication in Heat and Mass Transfer 34: 849-859
[12] Saqr, K.M. and Wahid, M.A., (2014) Effects of swirl intensity on heat transfer and entropy generation in turbulent decaying swirl flow. Applied Thermal Engineering. Vol 70, pp.486- 493.
[13] Zohir, A.E. and Gomaa, A.G. (2013) Heat transfer enhancement through sudden expansion pipe airflow using swirl generator with different angles, Experimental Thermal and Fluid Science. Vol 45, pp. 146 -154.

Appendix 5: Publication 2

ISSN: 2319-5967
ISO 9001:2008 Certified
International Journal of Engineering Science and Innovative Technology (IJESIT)
Volume 7, Issue 3, May 2018

Determining coefficient of skin friction on a cylindrical pipe in the presence of a conical turbulator enhancing heat transfer

Kinyua Eric Mugambi[1], Mathew Kinyanjui[2], Surindar Mohan Uppal

Abstract— **In this study analysis is done on the effect of a fluids skin friction on heat transfer enhancement. The variation in fluid internal friction during flow is due to a diverging conical ring insert placed in a cylindrical pipe to generate multi longitudinal vortex. Using computational fluid dynamics software 'solid works' the values of pressure and horizontal velocity along the pipes centre line are determined. It is noted that the fluids skin friction increases with reduction of Reynolds number, which is affected by the ratio of fluid pressure to the velocity during flow.**

Index Terms— **Skin friction, Heat transfer enhancement.**

I. INTRODUCTION

Heat transfer enhancement is an active and essential field of research since it increases the effectiveness of heat exchangers. Suitable heat transfer techniques achieve considerable technical advantage in fluid transmission. Heat transfer enhancement methods are categorized into active, passive and compound techniques. A diverging conical ring insert with slits placed in a cylindrical pipe is a passive technique. Passive enhancement of convective heat transfer can be achieved in three ways:

i) Decreasing thermal boundary layer thickness – the enhancing surfaces such as offset fin in compact heat exchanger are adopted.

ii) Increasing interruption in the fluid – inserted devices belong to this type of enhancement where plates are obliquely positioned to an oncoming flow.

iii) Increasing velocity gradient near a heat transfer wall - by inserting a co-axial tube in a pipe it appreciably enhances heat transfer in the fluid flow.

In fixed flow rate the insertion makes velocity gradient near heat transfer wall larger than that without an insert, leading to enhancement of heat transfer. Many researchers focus on whether heat transfer is enhanced and to which degree it is enhanced, while ignoring the increase in flow resistance which sometimes may exceed the degree of heat transfer enhancement. With growing concern about energy saving in heat exchangers which are widely used in the industry, researchers are now devoted to develop heat transfer enhancement units which can work efficiently with low power consumption. Since the overall performance of convective heat transfer is heavily dependent on heat transfer process, great emphasis should be on the process of optimization. The power needed in transmission of an incompressible fluid flow is partly obtained from fluid viscosity reflecting frictional resistance and profile resistance as well as from momentum change.

II. LITERATURE REVIEW

Promvonge and Eiamsa-ard [8] performed an experimental investigation of heat transfer and friction factor characteristics for flow of air through horizontal pipe with and without conical turbulators, using conical rings with three different ratios of the ring to tube diameter (d/D = 0.5, 0.6, 0.7) and for each ratio the rings are placed with three different arrangements such as converging conical ring, diverging conical ring and converging–diverging conical ring. The boundary layer disruption causes a better chaotic mixing between the core and wall region fluid, thus enhancing the convective process. However diverging conical ring provides higher heat transfer and yields higher pressure loss at small Reynolds number than other arrangements. Kongkaitpaiboon [6] investigated experimentally the influences of perforated conical rings on the turbulent convective heat transfer, friction factor and thermal performance factor characteristics. The perforated conical-rings used were of three different pitch ratios (d/D= 4, 6 and 12) and three different numbers of perforated holes (N=4, 6 and 8 holes) and found that the thermal performance factor of all perforated conical-rings arrangements is higher than those of the conical ring over the range studied. The heat transfer rate and friction factor of perforated conical-rings increase with

ISSN: 2319-5967
ISO 9001:2008 Certified
International Journal of Engineering Science and Innovative Technology (IJESIT)
Volume 7, Issue 3, May 2018

decreasing pitch ratio and decreasing number of perforated holes. Shivalingaswamy and Narahari [9] analysed heat transfer enhancement in a tube fitted with circular-ring turbulator (CRT) as reported in a thesis simulated using ANSYS Fluent computational fluid dynamics (CFD) software. Insertion of turbulators in the flow passage is one of the favorable passive heat transfer augmentation techniques due to their advantages of easy fabrication and operation as well as low maintenance. Influence of the diameter ratio and pitch ratio on the heat transfer rate, friction factor and thermal performance factor behaviors was investigated under uniform wall heat flux condition. The CRTs with different diameter ratios (d/D=0.5, 0.6 and 0.7) and pitch ratios (4 and 8) were employed for the Reynolds number ranging between 4000 and 20,000. Over the entire range investigated CRTs propose heat transfer enhancement around 57% to 195% compared to that in the plain tube. Jia et al. [4] proposed the way to enhance convective heat transfer based on minimum power consumption principle and found that it could provide strong theoretical guidance for designing high-efficiency and low resistance heat transfer enhancement units. Karakaya and Durmus [5] devised the conical spring turbulators for three different conical arrangements (converging, diverging and converging diverging) and three different cone angles 30°, 45° and 60° in Reynolds number range of 10000 to 34000. It was found that the best results in terms of heat transfer are respectively diverging, converging diverging and converging arrangements, while the turbulator best results were obtained, for cone angles 30°, 45° and 60°; respectively. Mugambi et al. [7] investigated heat transfer enhancement in a cylindrical pipe with a diverging conical ring insert (DCR), using CFD flow simulation where the DCR insert had slits symmetrical positioned on the slant edges generates multi longitudinal vortices, to obtain the heat transfer enhancement, two slits have the highest rate of heat transfer when compared with a case of zero, one or three slits. Bhuiya et al [3] determined that inserting turbulators with different spacing ratio of 11, 6.4 and 4.2 gives enhancement efficiency with rate more than unity. This indicates that enhancing heat transfer is more than the effect of increasing friction loss with the maximum heat transfer enhancement achieved at 4.2 with rate a 9.8 %. Avinash et. al [1] gives an analysis of heat transfer in pipe with twisted tape inserts to understand the effect of change in pitch of twisted tape on the flow pattern, results at Re 800 and twist ratio 2, 3, 4 and 5 considered and conclude that variation of twist ratio and Re on heat transfer and flow characteristics using twisted tape inserts and also the heat transfer increases with decrease in twist ratio and increase in Re. Hossain, et. al. [3] analyzed heat transfer enhancement in circular tube with and without inserts for laminar flow in the range of Re= 1600~2400 by using COMSOL Multi physics to perform CFD simulation. Here a non-isothermal flow model was considered in which water was taken in the model and copper was considered as material of circular pipe under constant heat flux of 32.087 KW/h. Using governing equation of non-isothermal flow together with continuity equation, the dynamic behavior of the flow was described which transport heat. In the simulation four, six, eight inserts were used for experimental length 800mm and they got highest output temperature 319.28 K for four insert while the output temperature was 307.85 when there was no insert in the tube, also noting that not just increasing the number of inserts will increase the heat transfer but determining specific distance between the inserts also need to be considered.

III. CONICAL RING INSERT WITH SLITS

A conical ring insert with slits to generate multi-longitudinal vortex flow is placed in a cylindrical pipe at a point of detachment. The ratio of an inserts inlet to outlet diameter provides the pitch ratio i.e. d/D. If an angle at the vertex of a conical insert has a divergence half angle of 7.5^0 then an inlet diameter of 0.036 m and outlet diameter of 0.05 m provides a pitch ratio of 0.72 with a horizontal distance of 0.07 m between the inlet and outlet. Figure 1 below show the position of a conical ring insert in the cylindrical tube with two slits on opposite sides.

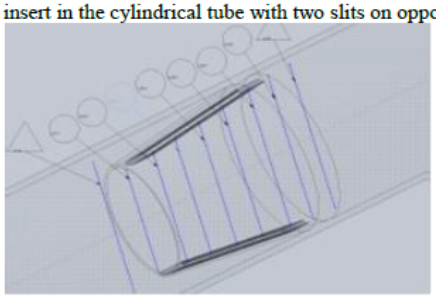

Fig 1. Schematic diagram of a diverging conical ring (DCR) insert with two slits.

ISSN: 2319-5967
ISO 9001:2008 Certified
International Journal of Engineering Science and Innovative Technology (IJESIT)
Volume 7, Issue 3, May 2018

The lines perpendicular to the pipe indicate points along which velocity and pressure of the fluid flow in the pipe are determined. 'Solid works' was used in simulation, which is a design analysis application fully integrated to provide a one screen solution. It is a three dimensional solid modeling package which allows users to develop full models of simulated environment.

IV. COEFFICIENT OF SKIN FRICTION

The fluid friction is a dimensionless quantity that depends on flow velocity, density, viscosity and diameter of the pipe. which similarly determined coefficient of skin friction $C_f = \frac{\tau}{\frac{1}{2}\rho u^2}$. (1)

Where $C_f = \frac{\mu \frac{\partial u_z}{\partial r}}{\frac{1}{2}\rho u^2} = \frac{2\mu\ a}{\rho u^2}$ given that an incompressible fluid of density ρ moving at a horizontal velocity component u_z in a pipe of radius r. The fluid accelerates when passing through the diverging conical ring insert at $a = \frac{F}{m} = \frac{F}{\rho \pi r^2 L} = \frac{F}{\rho A L}$

(2)

Substituting and grouping the terms $C_f = \frac{2\mu}{\rho u^2}\frac{F}{\rho A L} = \frac{\mu}{\rho u L}\frac{2F}{\rho u A} = \frac{1}{\mathrm{Re}}\frac{F}{A}\frac{2}{\rho u} = \frac{2}{\mathrm{Re}\,\rho}\frac{P}{u_z}$

In discrete form the coefficient of skin friction is proportional to the ratio in blankets, that is $C_{f_{i,k}} = \frac{2}{\mathrm{Re}\,\rho}\left[\frac{P_{i,k}}{u_{z_{i,k}}}\right]$ (3)

Which compares with fluid flow in a cylindrical pipe whose friction factor is $f = \frac{\Delta P}{\left(\frac{L}{D}\right)\left(\rho\frac{u^2}{2}\right)}$.

(4)

V. SIMULATION OF FLOW

When using hot water the flow parameters are set up as follows, at the pipe inlet axial velocity $u_z = 4m/s$ while at the diverging conical ring insert inlet $u_z = 6m/s$, inlet pressure is P_0 =110,000 Pa and temperature is T_0=370 K. While Reynolds number (Re) satisfies the inequality 1000 < Re < 3000, pressure coefficient (P_C) = 6.5 and Prandtl number (Pr) = 1.75. The thermo physical properties of water at the above temperature and pressure as used in the simulation are; density is 957.9kg/m^3, specific heat (C_p) is 4217kJ/Kg.K, thermal conductivity (k) is 0.679W/m.k, dynamic viscosity is 2.82X10^{-4}Kg/m.s and a volume expansion coefficient is 7.5X10^{-4}k^{-1}. Simulating the fluid flow using a soft ware solid works which reveals that velocity profile before and after a DCR insert is as indicated in figure 2 below showing a rise of velocity within the insert and a flow separation thereafter. Fluid velocity in the DCR insert is illustrated by a colour code with values along the pipe centre line provided in a tabulated form which is given in table 1.

ISSN: 2319-5967
ISO 9001:2008 Certified
International Journal of Engineering Science and Innovative Technology (IJESIT)
Volume 7, Issue 3, May 2018

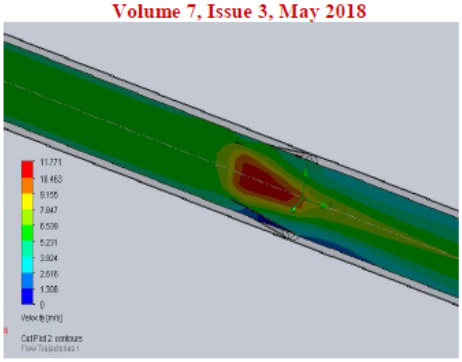

Fig 2: Fluid velocity contours in a pipe with diverging conical ring insert.

In the next part figure 3 presents contour of fluid pressure distribution through the smooth cylindrical pipe with a conical insert. The fluid pressure at the pipe centre line is provided in table 1. The figure below represents fluid pressure distribution through the smooth cylindrical pipe with a DCR insert, with variations shown by colour coding and a key provided indicating the values.

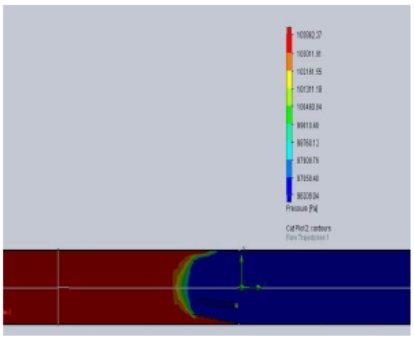

Fig 3: Fluid flow pressure distribution in a pipe with diverging conical ring insert.

The simulation provides horizontal velocity components u_z and pressure P at specific radial distance $r_{i,k}$ along the pipe's centre line. The horizontal components of axial velocities are obtained along the lines marked in figure 1 with plains chosen before fluid enters the DCR insert, when within the insert and after it passes through.

TABLE 1: VARIATION OF HORIZONTAL DISTANCE WITH PRESSURE, HORIZONTAL VELOCITY COMPONENT AND TEMPERATURE ALONG THE PIPE.

Horizontal distance from pipe inlet	Velocity $u_{z_{i,k}}$	Pressure P_{ik}	$\frac{P_{i,k}}{u_{z_{i,k}}}$	Temperature T_{ik}
6.50	6.394	107914.51	16877.4	370.00630
6.55	6.394	107826.91	16863.76	370.00633
6.60	6.394	107739.31	16850.06	370.00637
6.65	6.394	107651.70	16836.36	370.00641
6.70	6.394	107564.11	16822.66	370.00645

ISSN: 2319-5967
ISO 9001:2008 Certified
International Journal of Engineering Science and Innovative Technology (IJESIT)
Volume 7, Issue 3, May 2018

6.75	6.394	107476.49	16808.95	370.00648
6.80	6.395	107388.89	16792.63	370.00652
6.85	6.395	107301.29	16778.93	370.00656
6.90	6.373	107213.69	16759.99	370.00664
6.95	8.501	93609.95	11011.64	370.00643
7.00	8.338	83779.35	10047.89	370.00534
7.05	6.738	86570.29	12848.07	370.00972
7.10	6.418	86936.02	13545.65	370.01005
7.15	6.233	87011.55	13959.82	370.01030
7.20	6.104	86867.07	14231.17	370.01060
7.25	6.059	86722.6	14313.02	370.01065
7.30	6.046	86578.13	14319.9	370.01070
7.35	6.033	86433.65	14326.81	370.01075
7.40	6.030	86244.64	14302.59	370.01080
7.45	6.035	86055.63	14259.42	370.01085
7.50	6.040	85866.61	14216.32	370.01090
7.55	6.045	85677.60	14173.3	370.01095
7.60	6.051	85488.59	14128.01	370.01100
7.65	6.064	85299.58	14066.55	370.01101
7.70	6.078	85110.57	14003.05	370.01101

VI. RESULTS

Plotting the horizontal distance in the cylindrical pipe against a quotient of pressure divided by horizontal velocity a graph is obtained as shown below in graph 1. The analysis is done from a distance of 6.5m to avoid the hydrodynamic entrance region effect, where viscous shearing forces are felt. The part beyond an entrance region has velocity profile fully developed and remains unchanged with the temperature remaining constant.

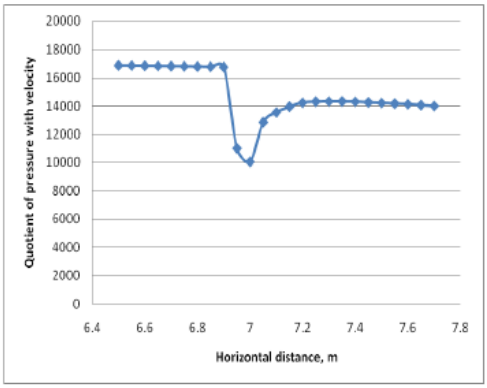

GRAPH 1: A QUOTIENT OF PRESSURE WITH HORIZONTAL VELOCITY COMPONENT AGAINST HORIZONTAL DISTANCE

This observation describes the variation of skin friction along the pipe in presence of a turbulator. An abrupt change of velocity and a drop in pressure are noted at the point where a DCR insert is placed on the pipe, which also generates the heat transfer enhancement. With the quotient considered to have stabilized at 14,000 then the coefficient of skin friction is determined on a range of Reynolds number as tabulated in table 2 below.

ISSN: 2319-5967
ISO 9001:2008 Certified
International Journal of Engineering Science and Innovative Technology (IJESIT)
Volume 7, Issue 3, May 2018

TABLE 2: VARIATION OF REYNOLDS NUMBER WITH COEFFICIENT OF SKIN FRICTION.

Reynolds number (Re)	Re ρ	Coefficient of Skin friction (C_f)
1000	957,900	0.02923
1500	1,436,850	0.01948
2000	1,915,800	0.01461
2500	2,394,750	0.01169
3000	2,873,700	0.00974
3500	3,352,650	0.00835

From equation 3 the coefficient of skin friction is determined and using values in table 1, which provide comparison of Reynolds number to skin friction to give the relationship shown in graph 2 below.

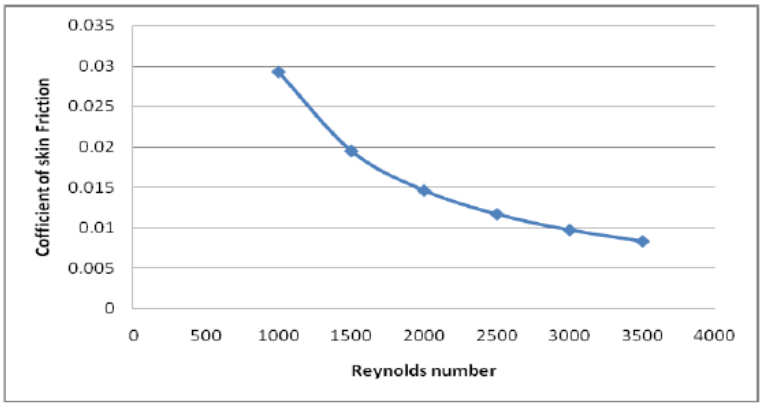

GRAPH 2: COEFFICIENT OF SKIN FRICTION AGAINST REYNOLDS NUMBER

The fluids coefficient of skin friction reduces with increase in Reynolds number or decreasing value of the quotient between fluid pressure to horizontal velocity component.

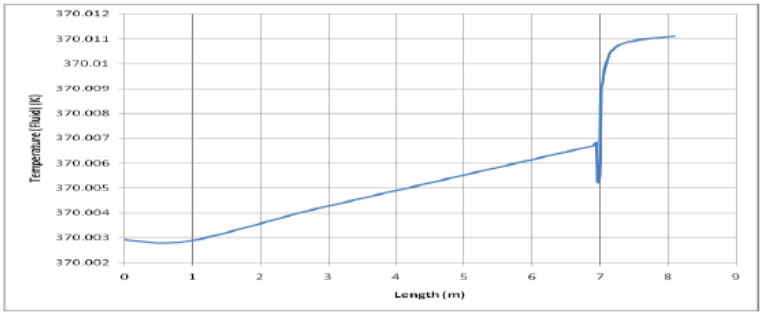

GRAPH 3: TEMPERATURE VARIATION ALONG THE CYLINDRICAL PIPE

ISSN: 2319-5967
ISO 9001:2008 Certified
International Journal of Engineering Science and Innovative Technology (IJESIT)
Volume 7, Issue 3, May 2018

Swirl flow created by placement of the DCR insert with slits in symmetrical positions helps in decreasing the boundary layer thickness of fluid flow and increases the residence time in the pipe. This increases the fluids internal friction leading to enhancement of heat transfer.

VII. RECOMMENDATION

Determining the coefficient of skin friction will enable establishment of which insert design in a cylindrical pipe will have the highest heat transfer enhancement with minimum energy required to have the fluid flow through the turbulator.

ACKNOWLEDGEMENT

The authors wish to thank Jomo Kenyatta University of Agriculture and Technology for an opportunity to do the research and Technical University of Mombasa for the financial support.

NOMECLATURE

ROMAN SYMBOL QUANTITY

A	Tube inner cross sectional area, m^2
a	acceleration, m/s^2
C_f	Skin friction
D	inner diameter of tube, m
d	inlet diameter of diverging conical insert, m
f	friction factor
F	Force, $kgms^{-2}$
$...k-1, k, k+1...$	Counters of discrete points
L	Axial pitch length, m
m	mass, kg
P	pressure, Pa (Nm^{-2})
Re	Reynolds number
r	radial distance in the tube , m.
T	temperature, K
u_z	axial fluid velocity, m/s

GREEK SYMBOLS QUANTITY

Δ	Small change
ρ	Fluid density, kg/m^3
π	Pi ≅ 3.1415926
τ	Shear stress
μ	Coefficient of dynamic fluid viscosity kg/ms

LIST OF ABBREVIATIONS

CRT	Circular ring turbulator
CFD	Computational fluid dynamics
DCR	Diverging conical ring

REFERENCES

[1] Avinash S., Dhiraj J., Madhura G., Vikrant P. and Sewatkar C.M., (2017) "Analysis of Heat Transfer in Pipe with Twisted Tape Inserts" Proceedings of the 2nd International Conference on Fluid Flow, Heat and Mass Transfer Ottawa, Ontario, Canada, pp. 143.

[2] Bhuiya, M. M. K., Azad, A. K., Chowdhury, M.S.U. and Saha. M., (2016). Heat transfer augmentation in a circular tube with perforated double counter twisted tape inserts. International Communications in Heat and Mass Transfer, 74, pp. 18-26.

ISSN: 2319-5967
ISO 9001:2008 Certified
International Journal of Engineering Science and Innovative Technology (IJESIT)
Volume 7, Issue 3, May 2018

[3] Hossain, S., Dev, U.K., Rahman K.A., (2015) The enhancement of heat transfer in a circular tube with insert and without insert by using finite element method. Journal of Procedia Engineering 105: 81 – 88.

[4] Jia, H., Z.C. Liu, Z. C., Liu, W., and Nakayama, A., (2014) "Convective heat transfer optimization based on minimum entransy dissipation in the circular tube", International Journal Heat Mass Transfer. 73 pp 124 -129.

[5] Karakaya, H. and Durmus, (2013) A. "Heat transfer and energy loss in conical spring turbulators", International Journal of Heat and Mass transfer, Volume 60, pp.756-762.

[6] Kongkaitpaiboon, V., Nanan, K., Eiamsa-ard, S., (2010) "Experimental investigation of heat transfer and turbulent flow friction in a tube fitted with perforated conical-rings", International Communications in Heat and Mass Transfer, 37, 560–567.

[7] Mugambi, E.K., Kinyanjui, M., and Humphrey, M., (2017) "Effect of slits in a diverging conical ring insert on heat transfer enhancement in a cylindrical tube". International Journal for Research in Applied Sciences and Engineering Technology. Volume 5, pp 1608- 1613.

[8] Promvonge, P. and Eiamsa-ard, S. (2006), "Experimental investigation of heat transfer and friction characteristics in a circular tube fitted with V-nozzle turbulators". International Communications in Heat and Mass Transfer 33, 591–600.

[9] Shivalingaswamy, B.P. and Narahari, G. A., (2014) "Numerical investigation of convective heat transfer and pressure loss in round tube fitted with conical ring turbulator", International Journal of Scientific and Research Publications, Volume 4, Issue 4.

AUTHOR BIOGRAPHY

Mr. Eric Mugambi Kinyua; M. Sc. Applied Mathematics, Jomo Kenyatta University of Agriculture and Technology, (2008). B. Science Education, Moi University (2002), both in Kenya. Publications: **1.** Mugambi, E.K.., Kinyanjui, M., and Humphrey, M., (2017) "Effect of slits in a diverging conical ring insert on heat transfer enhancement in a cylindrical tube". International Journal for Research in Applied Sciences and Engineering Technology. Volume 5, pp 1608- 1613; **2.** K. Kwanza., K.E Mugambi and M. Kinyanjui, Boundary layer thickness and frictional drag on submerged curved plate. Journal of advances and applications in fluid mechanics (2010); Vol. 7 pp 61-70. Academic staff at the Department of Mathematics & Physics, Technical University of Mombasa; mugambiek@tum.ac.ke

[2]Prof. Mathew Kinyanjui, Department of Pure & Applied Mathematics, Jomo Kenyatta University of Agriculture and Technology; Kenya. mathewkiny@yahoo.com

[3]Prof. Surindar Mohan Uppal, Department of Pure & Applied Mathematics, Jomo Kenyatta University of Agriculture and Technology; Kenya. smuppalprof@gmail.com